Prog. Oceanog. Vol. 17, pp. 1–59, 1986.
Printed in Great Britain.

0079–6611/86 $0.00+.50

Particulate Matter Distributions, Chemistry and Flux in the Panama Basin: Response to Environmental Forcing

JAMES K. B. BISHOP*, JEANNE C. STEPIEN* and PETER H. WIEBE**

*Lamont Doherty Geological Observatory of Columbia University, Palisades, New York 10964, U.S.A.
**Woods Hole Oceanographic Institution, Woods Hole, Massachusetts 02543, U.S.A.

ABSTRACT

Multidisciplinary studies of the particle cycle were carried out during two cruises in July-August and November-December 1979 at 5°N 82°W in the Panama Basin as part of the Sediment Trap Intercomparison Experiment (STIE) and Composition, Flux and Transfer Experiments (C-FATE). Measurements included: primary production; new production; hydrography; nutrient distributions; 12-kHz echo sounding; macrozooplankton biomass and group abundances; microzooplankton group abundances; vertical distributions, chemistry, and morphology of suspended and sinking particulate matter; and vertical particulate matter fluxes.

Comparisons were made among particle fluxes determined by several means. Size distributions of fecal matter and fecal pellets determined on samples from the Large Volume *in-situ* Filtration System (LVFS) were used in settling models to calculate vertical particle fluxes. These results were compared with fluxes estimated from measurements of new production, with fluxes determined by short-term deployments of sediment traps in the upper 300m, and with fluxes recorded by moored time-series traps at 1268m.

Previous C-FATE results had shown that the rates of primary production and new production are determined by the physical and chemical environment of the euphotic zone at this location. Results presented here indicate that new production and particle flux are in balance in the euphotic zone on the time scale of days. The data also demonstrate that particulate matter distributions, chemistry and fluxes in the water column extending from the euphotic zone to 1000m are closely related to rates of primary production and new production in the euphotic zone. Finally, the data show that the vertical particle flux gradient in the upper 1000m is determined by the instantaneous distributions, feeding activities, and migratory behaviour of zooplankton and fish present in the water column.

CONTENTS

1.	Introduction	2
2.	Methods	6
	2.1 Large Volume in situ Filtration	6
	2.2 Flux Models	11
	2.3 Zooplankton	17
	2.4 Other data	17
3.	Results and Discussion	20
	3.1 Hydrography of the water column	20
	3.2 Euphotic zone pigments, primary and new production	23
	3.3 Macrozooplankton and midwater fish distributions	25
	3.3.1 July-August data	25
	3.3.2 November-December data	28
	3.4 12-kHz scatterer distributions	28
	3.5 >53μm microzooplankton and phytoplankton abundances	32
	3.6 Particulate matter distributions and chemistry	33
	3.6.1 Organic matter percentages and element ratios	36
	3.7 Fecal matter and fecal pellet distributions	39
	3.8 Fecal matter and fecal pellet fluxes	43
	3.8.1 Temporal variability of particle flux at 530m	45
	3.9 Mass and chemical fluxes	46
	3.9.1 Organic carbon flux	48
	3.9.1.1 LVFS carbon flux and zooplankton	48
	3.9.1.2 LVFS carbon flux and new production	49
	3.9.1.3 LVFS carbon fluxes and sediment trap carbon fluxes	49
	3.9.2 Phosphorus	51
	3.9.3 Calcium	51
	3.9.3.1 LVFS calcium fluxes and sediment traps	52
	3.9.4 Biogenic silica	52
4.	Summary and Conclusions	53

1. INTRODUCTION

Particulate matter production, sinking and decomposition is a major process which causes non-conservative behaviour of many stable and radioactive chemical species in the ocean. The major source of particulate matter to the upper ocean is photosynthetic activity in the euphotic zone which is usually restricted to the upper 100m. The major agents of particle decomposition in the oceanic water column are bacteria, zooplankton, and nekton (invertebrates and fish). Furthermore, the sinking of fecal material at hundreds of meters per

day is a major mode of transport of chemical species from the euphotic zone to the deep ocean (FOWLER and KNAUER, 1986). Zooplankton and nekton resident in the deeper water column are responsible for the transformation, consumption and repackaging of particles (ANGEL, 1984), and therefore play a major role in determining the release sites of particle bound elements in the deep sea. Thus, the cycling of many chemical species is closely tied to biological activity in the water column.

The rates of particle formation and destruction are governed by processes which occur over a large range of time scales. For example, rates of particle formation by photosynthesis are closely linked to the physical and chemical environments of the euphotic zone. Events that affect production may be as short as tens of minutes (the passage of internal waves within the euphotic zone which causes modulation of light, or entrainment of nutrients into the euphotic zone due to internal wave breaking) or may be as long as months (seasonal upwelling). Factor of two changes in the euphotic zone particle load are possible over 1 to 2 days because of the short growth time scales of phytoplankton. In contrast to phytoplankton producers, the growth time scales of the particle consumers (zooplankton and fish) co-vary with organism size, and range from days to months (SHELDON, PRAKASH and SUTCLIFFE, 1972). Exceptions to this rule are some of the gelatinous zooplankton which have growth time scales as short as one day (ALLDREDGE, 1984). Because of the different growth time scales of particle producers and consumers, the efficiency and zones of particle recycling in the upper 1000m will be dependent on the instantaneous balance between rates of food production in the euphotic zone and the biomass distributions and activities of feeders in the oceanic water column. These considerations suggest that particulate matter flux at depth will vary temporally as well as spatially but not as a simple function of the primary productivity of overlying waters.

Time-series sediment trap observations below 1000m have provided an important first-order understanding of the temporal variability of particle flux to the deep sea (DEUSER and ROSS, 1980; HONJO, 1984; ITTEKKOT, DEGENS and HONJO, 1984). None of these studies included a simultaneous characterisation of water column hydrography or biological activities and had to rely on historical data for interpretations of temporal variations in flux. Only recently has the linkage of deep particle fluxes to mixed layer depth and temperature been described where both kinds of data were simultaneously determined (DEUSER, 1986).

Short-term studies of the particle cycle in upper water column using drifting sediment traps and large volume *in-situ* filtration have provided evidence that particle distributions and flux are closely related to the physical and chemical environment of the euphotic zone and that particle flux varies non-linearly with primary production (BISHOP, KETTEN and EDMOND, 1978; BISHOP, COLLIER, KETTEN and EDMOND, 1980; BETZER, SHOWERS, LAWS, WINN, DUTULLIO and KROOPNICK, 1984). These studies demonstrated that particle flux at a given depth is a greater fraction of primary production as primary production increases. On the other hand, KNAUER, MARTIN and KARL (1984) examined the relationship between particle flux and primary productivity at 9 VERTEX stations and concluded that no such relationship could be found. They suggested instead that particle flux should be closely related to new production, which

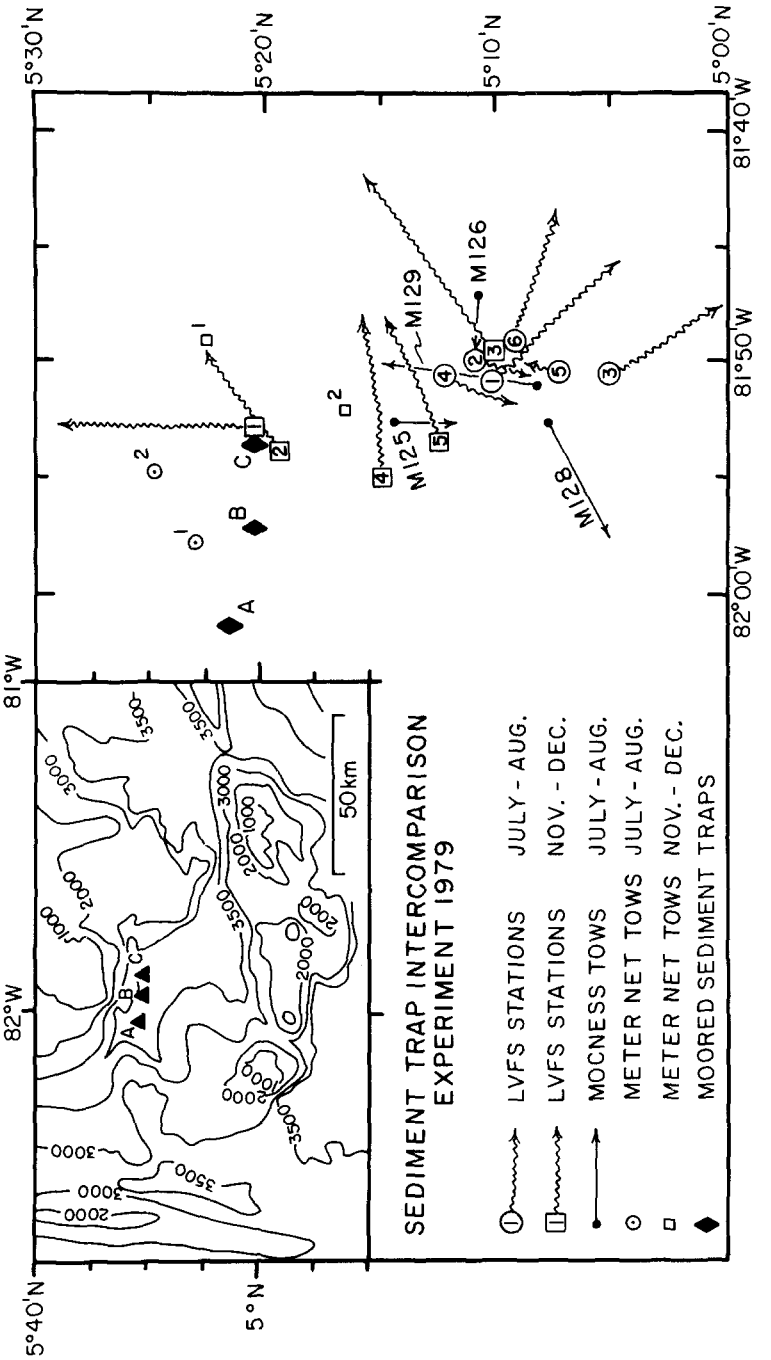

FIG. 1. Locations of Large Volume *in situ* Filtration System (LVFS) casts, Multiple Opening/Closing Net and Environmental Sensing System (MOCNESS) and meter net tows, and moored sediment trap locations. The arrows denote the beginning and ending points of LVFS and MOCNESS tows. Inset shows bottom topography at the site of the Sediment Trap Intercomparison Experiment.

is the fraction of primary production supported by nitrate ion entrained into the euphotic zone (DUGDALE and GOERING, 1967). We know of no published studies in which particle flux and new production have been measured in the same water column in order to test this hypothesis. One reason for the disagreement over the relationship between primary production and particle flux is that the few studies of particle flux in the upper 1000m have been conducted have been widely dispersed over different seasons and oceanographic environments. Another reason may be that the roles played by zooplankton and micronekton in the particle cycle have been ignored (ANGEL, 1984).

Although processes important to the sinking, decomposition and repackaging of particulate matter have been identified, few oceanic studies have been designed to learn either about the rates at which these processes operate or about factors which control them, especially in the upper kilometer of the ocean where large concentration gradients of dissolved non-conservative chemical species are found. Gaining a knowledge of particle dynamics will contribute to the understanding of the sources, reactions and sinks of these chemical species. It will also help provide constraints on models of ocean circulation by providing better source and sink terms for non-conservative dissolved species. Furthermore, a knowledge of the particle cycle will provide clues to the redistribution of many particle-reactive anthropogenically produced compounds in the ocean.

Since the particulate matter contributing to the vertical flux in the upper 1000m has a transit time of one week or less (FOWLER and KNAUER, 1986), it is possible to investigate directly the linkages between rates of particle formation in the euphotic zone and particle flux through the base of the euphotic zone during an oceanographic cruise. Furthermore, it should be possible to establish the dependence of vertical particle flux gradient on the activities and distributions of particle consumers in the water column.

An opportunity to conduct such investigations occurred during the Sediment Trap Intercomparison Experiment (STIE) which took place near 5°N 82°W in the Panama Basin between July and December 1979 (Fig.1). The Composition Flux and Transfer Experiments (C-FATE) occurred on the deployment (RV Knorr 73-17; July-August 1979) and recovery (RV Gilliss 7904/3; November-December 1979) cruises of STIE. C-FATE was designed to complement STIE by measuring water column primary production, hydrography, nutrient distributions, nephelometry, and zooplankton distributions during the two cruises. New production measurements were made by E. Renger and R. Eppley as part of the STIE during the July-August cruise and were used by BISHOP and MARRA (1984) to model new production during the November-December cruise.

The site of the STIE/C-FATE experiment was in a narrow basin extending to nearly 4000m depth at the base of the Coiba Ridge (Fig.1). Topography as shallow as 300m was found approximately 15km to the north and 25km to the south. Sills at depths of 3000 and 3500m close the trough to the west and east, respectively. A 3km thick nepheloid layer extended from the bottom of the trough to 900m indicating significant lateral inputs of particulate matter from the walls of the trough (GARDNER, BISHOP and BISCAYE, 1984).

FORSBERGH (1969) provides the only available summary of the climatology and biology of the Panama Bight (defined as the area of the equatorial Pacific between 1° and 9°N and east of 81°W) which lies to the east of the STIE/C-FATE location. In the Panama Bight, upwelling and shallowest mixed layer conditions occur between January and March. Coincident with these conditions are highest primary production rates and chlorophyll concentrations. Zooplankton populations lag behind the phytoplankton, and double between January and March. They increase by another 50% by June, thereafter they decline to minimum levels in November and December. Fish harvest in the Bight generally parallels the zooplankton abundance patterns.

BISHOP and MARRA (1984) have shown that the seasonal trends of primary production in the Panama Bight and STIE area are similar. We therefore expected the temporal changes of zooplankton and fish biomass in the STIE area would follow the trend established for the Panama Bight.

The focus of this paper is to present an integrated study of the cycling of biogenic chemical elements in the upper 1000m using STIE/C-FATE data. In the sections below we will describe the hydrography (Section 3.1), chlorophyll distributions (Section 3.2), and primary productivity of the STIE water column. The distributions of macrozooplankton, fish, and microzooplankton (all major particle consumers) are described in Sections 3.3, 3.4 and 3.5 respectively. Large volume *in-situ* Filtration System (LVFS) data are used to describe particulate matter chemistry (Section 3.6), abundances of fecal material (Section 3.7), and calculated vertical fluxes (Sections 3.8 and 3.9). Comparisons are made between calculated vertical particle fluxes and surface-tethered sediment traps deployed in the upper 100m and also with time-series sediment trap collections at 1268m (Section 3.9). By extending the intercomparison of particle distributions and fluxes to include biological and physical data, we will show: (1) that the physical and chemical environment of the euphotic zone determines both the rate of particle production and the particle flux through the base of the euphotic zone; and (2) that the distributions of particle consumers in the water column determine the vertical gradient of particle concentration and flux.

2. METHODS

2.1 *Large Volume in-situ Filtration*

The LVFS is capable of filtering *in-situ* up to 20,000l of seawater through a filter series consisting of acid-cleaned 53µm Nitex mesh and two identical acid cleaned 1µm Mead 935-BJ glass fibre filters. These three filter samples are operationally described as the >53µm, 1-53µm and <1µm size fractions (BISHOP and EDMOND, 1976). Since the particle collection efficiency of the glass fibre filter drops sharply below 1µm, the <1µm fraction is non-quantitative. Up to 4 such size-fractionated samples may be collected serially during a LVFS cast and a three cast profile of the upper 1500m can be obtained in approximately 2 days

of station time. The methodology of sample collection, treatment and analysis of LVFS samples has been described by BISHOP, EDMOND, KETTEN, BACON and SILKER (1977) and by BISHOP *et al.*(1978, 1980).

Recent (1981) calibrations of the LVFS flowmeter revealed mathematical error in the calibration reported by BISHOP and EDMOND (1976). All LVFS data on particle concentrations and fluxes published up to and including 1980 should be multiplied by a constant factor of 1.2 to correct for this error. *Data from these publications discussed in this paper have been corrected already.*

The LVFS was used in an identical configuration to that described by BISHOP *et al.* (1980) with the exception of the filterholders, which were modified by the addition of a 30cm diameter, 60cm tall PVC cylinder to the top baffle plate of each filter holder. This addition was intended to enhance the retention of particles on the 53µm Nitex filters in conditions of high turbulence.

During the STIE/C-FATE experiment, a total of 44 samples of particulate matter were obtained from the upper 1300m during 11 casts of the LVFS (Table 1, Fig.1). The telemetering of flow meter data failed on the first and third LVFS casts during the November cruise. Volumes filtered for the affected samples were estimated from total volume filtered for the four samples of each cast and apportioned according to filtration time.

During a deep LVFS cast on each cruise, one filter set, exposed at depth but not used, was used for blank purposes. Six samples were collected from 530m over a 24 hour period during the July-August cruise to study the diel variability of particle distributions and fluxes.

The resulting samples have been analysed for dry weight and for the elements, Na, K, Mg, Sr, Ca, Si, C, N and P (Table 2). The Na data have been used to correct results for Mg, K, Ca and Sr in order to remove contributions from contamination by residual sea salt on the filters. The >53µm organic carbon concentration was estimated from the difference between dry weight and the sum of inorganic constituents. The 1-53µm Si concentration was estimated by separate Niskin sampling and filtration of 2-10 l samples through 0.4µm Nuclepore filters followed by Si analysis (BISHOP *et al.*, 1977). High and variable major element blanks were found in the glass fiber filters used during the July-August cruise. For this reason no 1-53µm Mg and K data will be reported. The filter blank problem was completely eliminated in subsequent sampling by adopting microquartz fiber filters instead of the glass fibre filters (BISHOP, SCHUPACK, SHERRELL and CONTE, 1985).

LVFS prefilters were also analysed for fecal pellet and fecal matter abundances. Fecal pellets can be classified into elliptical, spherical, and tubular shape categories (BISHOP *et al.* 1980). Elliptical pellets had rounded ends and ranged in length from 50-500µm with length/width ratios ranging from 2-5. Spherical pellets were nearly spherical in shape. Tubular pellets (Fig.2) were less dense (i.e. more optically transparent) than the others. These ranged in length from several hundred µm to nearly 4mm, and their widths ranged from

TABLE 1: SUMMARY OF LVFS SAMPLES

JULY-AUGUST 1979

cast	samp.	Z	Z*	°C	Salinity	m^3	factor	viscosity	local start	time stop
1	P001	100	83	14.80	34.921	10.843	34.46	0.0122	0058	0328
1	P002	200		12.70	34.891	13.270	32.98	0.0127	0358	0658
1	P003	350		9.60	34.712	14.670	31.22	0.0133	0722	1022
1	P004	500		7.90	34.636	14.064	34.64	0.0149	1046	1346
2	P005	530		7.60	34.626	14.014	31.92	0.0149	2244	0144
2	P006DB	530		"	"	**.385		"	2204	0629
2	P007	530		"	"	13.675	32.65	"	0147	0447
2	P008SP	530		"	"	34.093		"	0449	0549
3	P009	530		7.60	34.626	11.035	37.43	0.0149	1229	1459
3	P010	530		"	"	11.557	32.13	"	1503	1733
3	P011	530		"	"	11.756	31.42	"	1735	2005
3	P012	530		"	"	12.574	29.87	"	2006	2236
4	P013	12	9	26.70	32.284	1.668	33.42	0.0092	0212	0242
4	P014	25	18	25.70	32.797	1.715	31.12	0.0097	0250	0320
4	P015	32	34	19.40	34.639	1.603	31.27	0.0104	0330	0400
4	P016	55	58	16.10	34.899	3.803	31.87	0.0117	0411	0526
5	P017	12	10	26.60	32.340	1.613	31.62	0.0092	0025	0055
5	P018	32	43	17.60	34.809	1.757	30.46	0.0104	0105	0135
5	P019	50	50	16.70	34.869	4.764	34.70	0.0117	0145	0315
5	P020	75	91	14.60	34.921	7.129	33.76	0.0122	0326	0526
6	P021	720		5.80	34.585	15.047	32.70	0.0157	1003	1403
6	P022	910		4.90	34.585	16.146	31.97	0.0161	1430	1830
6	P023	1100		4.40	34.592	13.705	33.70	0.0166	1904	2234
6	P024	1260		3.50	34.607	13.365	31.77	0.0169	2327	0257

NOVEMBER-DECEMBER 1979

cast	samp.	Z	Z*	°C	Salinity	m^3	factor	viscosity	local start	time stop
1	P031	100	130	14.60	34.950	10.445	34.34	0.0122	2004	2304
1	P032	200		13.70	34.930	*15.690	34.04	0.0126	2321	0221
1	P033	320		11.60	34.930	*15.690	35.44	0.0134	0243	0543
1	P034	425		9.80	34.750	*15.690	32.33	0.0141	0600	0900
2	P035	530		7.87	34.636	14.300	34.22	0.0149	2050	2342
2	P036	673		6.62	34.601	15.905	31.03	0.0155	0026	0326
2	P037	800		5.92	34.587	18.759	33.87	0.0159	0349	0719
2	P038	1000		4.69	34.586	17.544	29.42	0.0163	0743	1113
3	P039	290		13.01	34.890	*15.690	32.13	0.0131	1731	2031
3	P040	290		"	"	*15.690	28.10	"	2032	2332
3	P041	290		"	"	*15.320	33.03	"	2333	0220
3	P042DB	290		"	"	**.475		"	1731	0220
4	P043	25	25	26.70	31.400	1.918	32.65	0.0092	1123	1153
4	P044	40	40	26.50	31.800	2.141	31.57	0.0092	1319	1349
4	P045	55	50	21.00	34.600	2.939	31.57	0.0106	1421	1506
4	P046	77	76	17.10	34.810	5.705	30.74	0.0114	1542	1742
5	P047	100	103	15.10	34.980	8.689	31.77	0.0122	1948	2148
5	P050SP	100	103	"	"	17.209		"	2306	2351
5	P049SP	100	103	"	"	11.737		"	0034	0134
5	P048	100	103	"	"	7.525	33.03	"	0215	0345

KNORR 73-17

cast-1	2 Aug 1979	5°10.0' N 81°50.6' W	5°04.8' N 81°45.5' W
cast-2	3- 4 Aug 1979	5°10.7' N 81°49.7' W	5°09.2' N 81°50.5' W
cast-3	4 Aug 1979	5°05.2' N 81°50.6' W	5°00.4' N 81°47.7' W
cast-4	5 Aug 1979	5°12.3' N 81°50.5' W	5°09.1' N 81°51.6' W
cast-5	6 Aug 1979	5°07.5' N 81°49.8' W	5°08.5' N 81°49.9' W
cast-6	6- 7 Aug 1979	5°09.4' N 81°48.9' W	5°07.7' N 81°43.3' W

GILLISS 7904/3

cast-1	23-24 Nov 1979	5°20.8' N 81°51.1' W	5°29.0' N 81°51.5' W
cast-2	24-25 Nov 1979	5°19.3' N 81°53.7' W	5°22.9' N 81°44.4' W
cast-3	25-26 Nov 1979	5°10.0' N 81°50.0' W	5°15.7' N 81°41.9' W
cast-4	26 Nov 1979	5°15.0' N 81°55.0' W	5°13.9' N 81°52.8' W
cast-5	26-27 Nov 1979	5°13.9' N 81°52.0' W	5°16.4' N 81°48.1' W

Z* = depth based on mean temperature profile and temperature of sample as determined by XBT (Knorr) or shallow hydrocast (Gilliss); Salinity = 10^{-3}; local time = time interval of sampling; m^3 = volume of water filtered; factor = 1/fraction of prefilter analyzed for fecal material; viscosity = kinematic viscosity (poise); SP = > 53 µm samples collected at constant flow rate; * = flow meter telemetry was bad. volume estimated based on total flow volume during the cast and elapsed time; ** = there was a leak in the sample manifold valve. Volume filtered through this sample was estimated by C/N/P analysis of the samples and concentrations of particulate C/N/P at the same depth; P006DB dipped blank; P008SP 9.47 l s^{-1}; P050SP 6.37 l s^{-1}; P049SP 3.26 l s^{-1}; P042DB dipped blank

TABLE 2: PARTICULATE MATTER CHEMISTRY (nmol kg^{-1})

JULY-AUGUST 1979

Samp	Z	Z*	Temp	Dry weight			C_{org}			N		P			Ca		Si	Mg	K	Sr	%Org	
#				< 1	1-53	> 53	< 1	1-53	> 53	< 1	1-53	< 1	1-53	> 53	1-53	> 53	> 53	> 53	> 53	> 53	1-53	>53
13	12	9	26.70	14.6	98.8	39.73	486	1517	836	33.3	213.7	2.50	11.48	9.869	68.0	41.43	110.38	1.825	8.893	15.190	61	63
17	12	10	26.60	14.2	85.4	40.71	473	1427	943	83.3	215.8	4.06	11.10	4.913	35.1	39.57	103.06	1.938	2.442	6.771	67	69
14	25	18	25.70	15.1	87.4	37.16	503	1442	816	94.0	218.8	? 0.04	11.50	7.397	71.0	39.70	104.03	2.087	4.280	7.773	67	66
15	32	34	19.40	16.0	56.4	56.05	532	1473	1558	93.5	217.9	5.10	11.34	6.476	80.8	28.48	84.54	0.795	3.590	2.940	107	83
18	32	43	17.60	10.4	74.9	15.05	345	900	195	58.1	133.1	3.01	7.58	1.562	28.2	23.73	93.40	0.351	2.853	1.591	50	39
19	50	50	16.70	4.8	25.8	30.35	162	543	752	25.7	79.2	1.75	4.69	3.787	18.0	21.36	79.17	0.984	2.936	0.637	82	74
16	55	58	16.10	6.1	36.3	22.49	202	584	446	34.9	87.1	2.03	4.51	3.584	21.9	19.69	98.24	1.374	4.025	1.517	65	59
1	100	83	14.80	1.0	17.2	8.69	35	238	207	10.5	37.2	0.27	1.72	1.008	13.7	5.72	26.71	0.580	0.272	0.235	47	71
20	75	91	14.60	2.1	16.0	9.91	69	274	178	13.1	39.0	0.89	1.77	1.281	15.8	13.45	44.88	0.513	1.088	0.395	64	54
2	200	200	12.70	0.8	13.9	2.94	26	226	56	5.6	28.3	0.23	1.40	0.228	16.2	3.27	13.09	0.350	0.472	0.077	54	57
3	350	350	9.60	0.4	14.6	2.99	13	194	68	2.4	23.0	0.09	1.23	0.126	15.0	2.22	10.46	0.278	0.028	0.013	43	68
4	500	500	7.90	0.8	18.1	4.12	26	202	101	2.8	23.7	0.13	1.12	0.094	17.0	2.65	11.87	0.408	0.091	0.039	38	73
5	530	530	7.60	0.2	13.7	4.27	6	177	120	1.2	20.7	0.03	1.05	0.101	16.9	1.56	6.89	0.247	0.139	0.074	40	85
7	530	530	7.60			3.83			100	1.7	19.2			0.106		2.07	8.89	0.379	0.088	0.063		78
9	530	530	7.60			3.59			80	1.9	24.7			0.276		3.64	11.83	0.816	0.116	0.086		66
10	530	530	7.60	0.4	21.4	3.53	12	211	81	1.7	23.9	0.02	1.36	0.196	7.9	2.77	11.69	0.402	0.102	0.075	31	69
11	530	530	7.60			2.34			45	2.1	25.1			0.162		2.68	9.98	0.654	0.518	0.103		58
12	530	530	7.60	0.3	18.2	2.77	10	209	60	1.6	24.3	-0.03	1.33	0.146	18.0	2.58	10.02	-0.131	0.116	0.104	36	65
21	720	720	5.80	0.3	12.4	3.74	10	184	92	1.3	22.5	0.13	1.21	0.178	15.5	3.08	9.48	0.612	0.065	-0.001	47	74
22	910	910	4.90	0.2	12.5	2.39	6	177	49	1.1	21.2	0.11	1.07	0.109	17.8	3.12	8.64	0.290	0.147	-0.001	44	62
23	1100	1100	4.40	0.6	13.5	2.60	19	173	60	1.8	20.0	0.04	1.05	0.110	15.5	2.64	7.67	0.348	0.106	0.017	43	69
24	1260	1260	3.50	0.3	19.4	2.56	12	177	59	2.7	21.0	0.09	1.14	0.123	19.5	2.42	7.92	0.409	0.059	0.001	29	69

NOVEMBER-DECEMBER 1979

Samp	Z	Z*	Temp	Dry weight			C_{org}			N		P			Ca		Si	Mg	K	Sr	%Org	
#				< 1	1-53	> 53	< 1	1-53	> 53	< 1	1-53	< 1	1-53	> 53	1-53	> 53	> 53	> 53	> 53	> 53	1-53	>53
43	25	25	26.70	9.6	95.7	11.59	319	1192	289	47.5	177.3	1.18	8.21	2.678	46.1	10.58	20.70	1.372	1.720	2.309	47	75
44	40	40	26.50	14.1	69.4	13.67	471	1502	349	63.5	209.2	2.47	9.28	2.981	65.4	11.40	23.88	1.153	1.493	2.095	85	77
45	55	50	21.00	10.0	77.6	15.35	333	1249	342	52.9	185.9	2.18	7.36	1.800	63.3	13.12	51.83	0.840	1.749	0.819	61	67
46	77	76	17.10	4.4	22.5	8.73	148	658	178	26.7	102.2	1.26	4.03	0.893	41.0	8.79	34.91	0.685	0.587	0.290	107	61
47	100	103	15.10	2.4	21.6	4.98	79	373	111	12.5	61.0	0.60	2.17	0.813	32.7	4.48	16.67	0.503	0.184	0.241	63	67
48	100	103	15.10	1.8	32.4	5.57	62	418	121	10.6	61.4	0.84	2.71	0.561	34.9	4.65	20.19	1.099	0.095	0.123	44	65
31	100	130	14.60	1.5	23.2	5.61	50	342	122	8.0	53.8	0.33	2.61	0.421	31.9	5.93	19.20	0.284	0.300	0.232	51	65
32	200	200	13.70	0.9	13.2	2.67	31	218	63	3.6	30.9	0.14	1.19	0.128	19.4	2.32	7.53	0.388	0.002	0.074	57	71
39	290	290	13.01	0.6	17.9	1.55	19	206	23	3.2	27.5	0.16	1.32	0.160	16.6	2.68	8.23	0.338	0.095	0.065	38	45
40	290	290	13.01	0.6	12.6	2.31	19	193	50	3.4	25.9	0.31	1.35	0.166	16.1	2.47	7.69	0.283	0.104	0.049	50	66
41	290	290	13.01	0.3	15.9	3.11	11	194	82	2.4	26.1	0.23	1.15	0.275	13.1	1.86	6.51	0.252	0.068	0.052	39	79
33	320	320	11.60	0.4	13.0	2.57	12	175	60	1.9	26.0	0.12	1.04	0.196	14.1	2.45	7.52	0.417	0.055	0.044	43	70
34	425	425	9.80	0.9	17.7	2.36	28	188	58	4.6	22.6	0.08	1.03	0.286	16.8	1.92	5.97	0.459	0.011	0.041	37	74
35	530	530	7.87	0.4	25.7	3.84	14	183	111	1.9	25.5	0.12	1.71	0.332	18.8	1.62	5.08	0.489	0.025	0.022	23	86
36	673	673	6.62	0.9	14.3	2.84	31	170	69	3.3	22.3	0.11	1.12	0.162	13.6	2.01	7.82	0.561	0.059	0.053	42	73
37	800	800	5.92	0.6	15.6	1.77	20	128	42	2.3	17.2	0.17	0.87	0.052	11.7	1.27	5.28	0.239	0.035	0.038	29	72
38	1000	1000	4.69	0.4	18.6	2.80	14	138	81	2.3	20.3	0.14	1.11	0.049	12.1	0.89	4.05	0.413	0.082	0.023	24	87

Samp = Sample #; Z = depth (m); Z* = depth mased on mean temperature profile and sea water water temperature determined at the time of sampling.; Temp = degrees Celcius; < 1 = less than 1 µm size fraction; 1-53 = 1-53 µm size fraction; > 53 = > 53 µm size fraction; Dry weight = µg kg^{-1}; C_{org} = Particulate Organic Carbon; N = Particulate Nitrogen; P = Particulate Phosphorus; Ca = Particulate Calcium; Si = Particulate Biogenic Silicon; Mg = Magnesium; K = Potassium; Sr = Strontium; %Org = Organic matter % of dry weight; ? = questionable data.

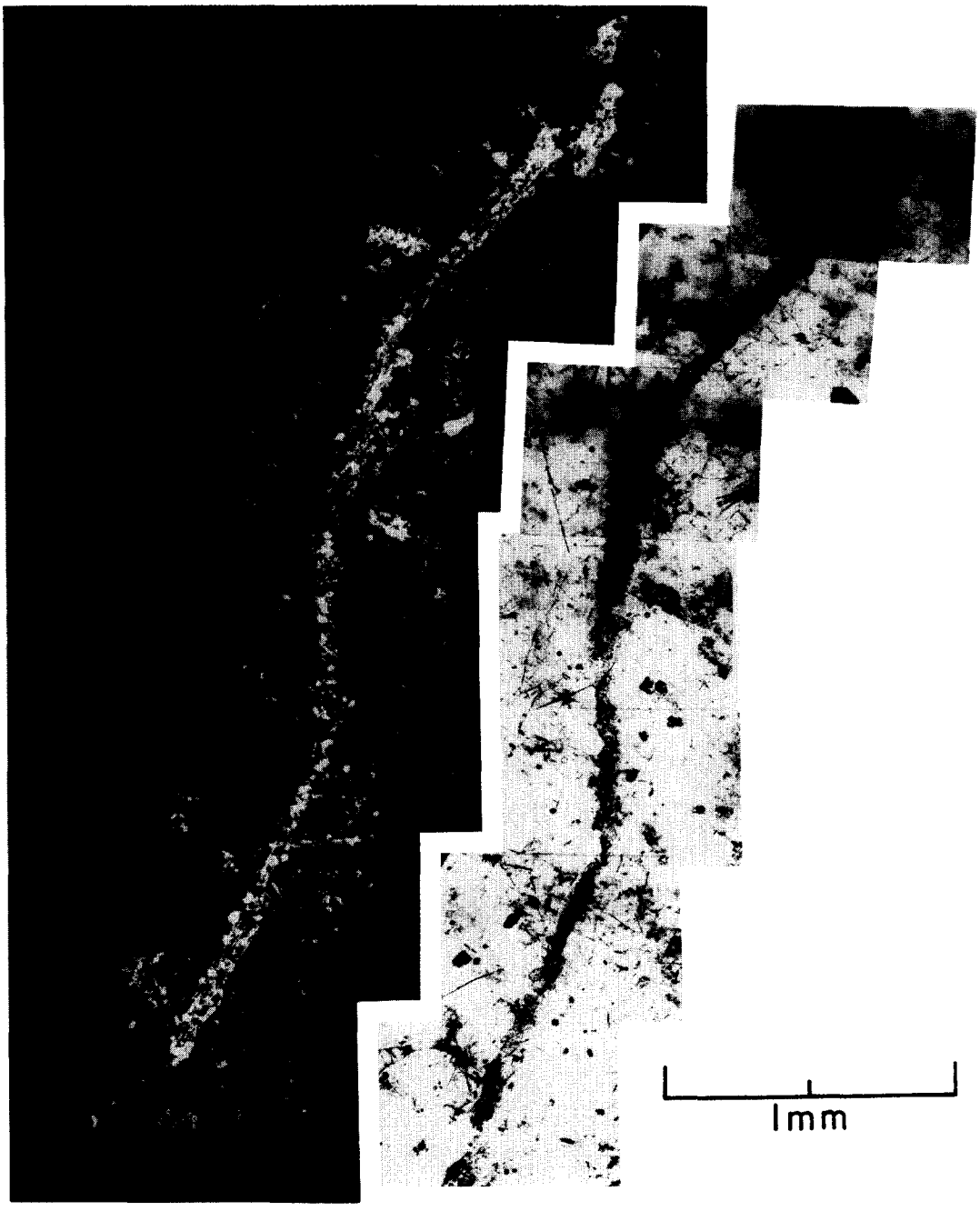

FIG.2. Polarised and unpolarised transmitted light photograph mosaic, of a long tubular fecal pellet typical of those found in near surface waters during the July-August cruise.

25μm to approximately 200μm. Most fecal pellets occurred individually in the samples.

Subcategories of fecal pellet classification included characterisation of particle raggedness optical density and birefringence. These sub-categories were used to assess respectively pellet degradation and thus its potential for breakup during sedimentation, particle density and calcium carbonate content.

Fecal matter (BISHOP *et al.* 1980) is a class of macroscopic aggregates which have irregular symmetry, range in size from 50μm to 1cm and contain the same kinds of particles as found in fecal pellets. This class of particles is a subset of the large macroscopic particles observed by cameras (HONJO, DOHERTY, AGRAWAL and ASPER, 1984) and from submersibles (ALLDREDGE and YOUNGBLUTH, 1985) described collectively as "marine snow".

Experiments to determine the efficiency of recovery of >1mm fecal pellets and fecal matter by the LVFS as a function of flow rate indicated that it has a recovery efficiency of >90% for these particle classes (BISHOP, 1982). Since smaller fecal pellets are more cohesive, it is assumed that the LVFS is an efficient sampler for all classes of fecal material.

LVFS samples were enumerated for the two classes of fecal material and for phytoplankton and microzooplankton groups in three steps. Two subsamples of each 53μm Nitex filter were prepared for light microscopy using a phenol/toluene wash treatment (BISHOP *et al.*, 1977). The first subsample, representing approximately 1/60 of the sample, was counted at 250 x for organism distributions (Table 3) and for >50μm long fecal pellets and fecal matter. The second subsample, comprising 1/30 of the sample, was enumerated for >100μm fecal pellets only. The third step was to count the whole 53μm Nitex filter for abundances of >1mm long material in the tubular fecal pellet and fecal matter categories. Size distributions of fecal pellets and fecal matter from the three analyses were merged to provide a single data set describing the abundances of these particles in the water column (Table 4); these were used in flux calculations.

2.2 *Flux Models*

Two empirically derived settling models were used to calculate the fecal pellet and fecal matter fluxes described in Section 3.8 (Table 5). The relationship of KOMAR, MORSE, SMALL and FOWLER (1981) was used to calculate fecal pellet fluxes. This model applies to the complete range of fecal pellet sizes encountered on our samples:

$$Ws = 0.0790/\eta * \Delta\rho * g * d^2 * (d/w)^{-1.664} \text{ cm s}^{-1} \quad (1)$$

where Ws is the settling velocity of the particle, η is sea water viscosity, $\Delta\rho$ is the density contrast of the particle with sea water, g is acceleration due to gravity, d is particle length, and w is particle width. Based on microscopic analysis of the different fecal pellet classes, $\Delta\rho$ was assigned a value of 0.3g cm^{-3} for elliptical and spherical pellets, 0.2g cm^{-3} for tubular pellets and 0.1g cm^{-3} for thin tubular pellets. These assumed densities, based

TABLE 3: ABUNDANCES OF > 53 μm PHYTOPLANKTON AND MICROZOOPLANKTON (# liter^{-1})

JULY-AUGUST 1979

Samp	Z	Z*	Temp	Dino	Silic	Cent	Penn	Stich	Nass	Spum	Phaeo	Acant	Tint	Foram	Ptero	Cop-W	Cop-P	N/S	P/N+S
13	12	9	26.70	5.42	23.4	113.1	78.9	3.37	8.03	1.74	0.11	38.67	1.48	4.23	0.42	0.08	0.27	4.61	0.01
17	12	10	26.60	3.96	17.8	32.1	5.2	3.50	5.96	1.25	0.00	14.96	0.75	1.70	0.11	0.14	0.75	4.77	0.00
14	25	18	25.70	8.80	17.5	89.8	62.4	2.87	8.80	1.49	0.11	29.38	2.69	3.71	0.55	0.44	0.87	5.90	0.01
15	32	34	19.40	1.50	50.9	45.8	15.0	0.23	10.04	1.62	0.15	4.31	1.23	2.14	0.04	0.31	0.62	6.21	0.02
18	32	43	17.60	0.21	33.5	41.0	13.3	0.38	5.99	3.32	0.38	4.29	0.10	0.62	0.07	0.10	0.17	1.80	0.06
19	50	50	16.70	0.27	13.1	31.1	5.6	0.23	6.97	0.77	0.61	0.88	0.19	0.94	0.13	0.33	0.37	9.10	0.09
16	55	58	16.10	0.28	15.3	44.7	21.2	1.05	7.39	0.56	0.67	2.11	0.14	1.37	0.05	0.05	0.28	13.14	0.09
1	100	83	14.80	0.01	3.1	6.7	5.2	0.81	7.25	0.40	0.76	0.50	0.01	0.17	0.06	0.02	0.07	18.24	0.10
20	75	91	14.60	0.08	2.5	9.7	2.0	0.19	4.54	0.35	0.46	0.59	0.09	1.29	0.02	0.04	0.11	12.95	0.10
2	200	200	12.70	0.12	1.7	1.9	1.2	0.78	5.70	0.46	0.36	0.29	0.08	0.15	0.07	0.02	0.09	12.39	0.06
3	350	350	9.60	0.09	3.6	5.8	4.3	0.05	3.49	0.13	0.12	0.21	0.11	0.04	0.02	0.00	0.17	27.07	0.04
4	500	500	7.90	0.16	1.3	3.5	2.6	0.04	4.45	0.26	0.17	0.15	0.12	0.06	0.00	0.00	0.20	17.16	0.04
5	530	530	7.60	0.08	1.4	0.9	1.2	0.09	1.88	0.29	0.14	0.09	0.07	0.06	0.00	0.01	0.04	6.55	0.07
7	530	530	7.60	0.03	1.1	1.8	1.5	0.07	2.33	0.21	0.23	0.05	0.07	0.07	0.01	0.00	0.07	11.25	0.10
9	530	530	7.60	0.02	2.4	2.5	1.4	0.10	4.44	0.23	0.27	0.19	0.13	0.02	0.01	0.00	0.06	19.40	0.06
10	530	530	7.60	0.01	1.5	1.9	1.7	0.14	2.72	0.24	0.25	0.05	0.11	0.05	0.03	0.00	0.08	11.50	0.09
11	530	530	7.60	0.02	1.6	1.7	1.6	0.11	3.16	0.26	0.27	0.07	0.17	0.02	0.01	0.00	0.09	12.04	0.09
12	530	530	7.60	0.13	1.0	2.5	1.7	0.08	4.22	0.30	0.38	0.15	0.19	0.05	0.00	0.01	0.19	14.27	0.09
21	725	720	5.80	0.05	0.6	0.6	0.6	0.18	2.50	0.23	0.91	0.07	0.12	0.02	0.01	0.01	0.09	10.72	0.36
22	930	910	4.90	0.10	1.6	2.1	1.9	0.15	2.55	0.19	0.52	0.05	0.12	0.02	0.00	0.01	0.07	13.30	0.20
23	1100	1100	4.40	0.09	1.7	2.5	1.8	0.24	3.84	0.40	0.92	0.08	0.13	0.06	0.01	0.01	0.12	9.70	0.24
24	1300	1260	3.50	0.08	1.6	2.1	1.8	0.14	2.63	0.19	0.64	0.04	0.05	0.01	0.00	0.00	0.08	13.63	0.24

NOVEMBER-DECEMBER 1979

Samp	Z	Z*	Temp	Dino	Silic	Cent	Penn	Stich	Nass	Spum	Phaeo	Acant	Tint	Foram	Ptero	Cop-W	Cop-P	N/S	P/N+S
43	25	25	26.70	9.14	21.0	8.0	13.3	12.51	4.52	1.29	0.07	19.67	8.15	4.50	0.07	0.00	0.59	3.51	0.01
44	40	40	26.50	5.14	27.7	8.1	15.2	8.19	5.02	1.63	0.06	18.16	5.59	5.32	0.00	0.39	1.78	3.07	0.01
45	55	50	21.00	1.04	78.3	51.0	44.0	3.80	20.72	2.90	0.22	9.12	3.26	3.85	0.04	0.24	0.54	7.14	0.01
46	77	76	17.10	0.17	18.0	10.3	10.4	0.80	13.83	1.37	0.19	1.60	1.14	1.39	0.01	0.03	0.24	10.09	0.01
47	100	103	15.10	0.28	23.4	11.6	11.6	0.73	8.53	1.00	0.24	1.73	0.38	0.33	0.01	0.05	0.36	8.54	0.03
48	100	103	15.10	0.44	11.0	4.9	6.0	2.15	3.95	1.39	0.57	2.79	0.74		0.03	0.02	0.49	2.83	0.14
31	100	130	14.60	0.17	2.6	2.6	2.7	0.98	2.43	0.78	0.11	0.24	0.17	0.08	0.02	0.01	0.24	3.12	0.04
**32	200	200	13.70	0.04	1.2	1.3	1.0	0.34	1.29	0.34	0.08	0.03	0.09	0.04	0.00	0.00	0.07	3.76	0.06
39	290	290	13.01	0.04	2.0	1.8	1.9	0.96	4.96	?4.17	0.10	0.36	0.13		0.00	0.00	0.11	?1.19	0.02
40	290	290	13.01	0.06	2.6	2.8	3.4	0.78	3.92	0.72	0.08	0.23	0.16		0.00	0.00	0.09	5.44	0.02
41	290	290	13.01	0.02	2.5	2.1	2.5	0.54	3.72	0.67	0.07	0.23	0.09		0.00	0.00	0.08	5.59	0.02
33	320	320	11.60	0.09	1.9	1.5	0.6	0.68	6.03	0.72	0.13	0.32	0.10	0.02	0.02	0.04	0.10	8.42	0.02
34	425	425	9.80	0.06	6.8	0.9	0.6	0.00	3.43	0.27	0.06	0.06	0.11	0.01	0.01	0.00	0.03	12.81	0.02
35	530	530	7.87	0.02	0.7	0.4	0.4	0.02	1.12	0.11	0.09	0.00	0.05	0.00	0.01	0.00	0.02	10.52	0.08
36	673	673	6.62	0.06	3.0	1.2	1.0	0.14	3.08	0.34	0.22	0.01	0.11		0.00	0.00	0.04	9.01	0.07
37	800	800	5.92	0.03	1.9	0.9	2.0	0.14	1.78	0.24	0.38	0.01	0.10		0.00	0.00	0.04	7.43	0.22
38	1000	1000	4.69	0.03	1.3	0.8	1.0	0.14	1.41	0.20	0.34	0.00	0.08		0.00	0.00	0.05	6.89	0.24

Samp = Sample #; Z = depth (m); Z* = depth based on mean temperature profile; Temp = degrees Celcius; Dino = Dinoflagellates; Silic = Silicoflagellates; Cent = Centrate Diatoms; Penn = Pennate Diatoms; Stich = Sticholonche; Nass = Nassellaria; Spum = Spumellaria; Phaeo = Phaeodaria; Acant = Acantharia; Tint = Tintinnids; Foram = Live Foraminifera; Ptero = Pteropods; Cop-W = Whole Copepods; Cop-P = Part Copepods; N/S = Nassellaria / Spumellaria ratio; P/N+S = Phaeodaria / Nassellaria+Spumellaria ratio ** - Organism counts for smaller classes of material may be underestimated; ? - questionable data.

TABLE 4: ABUNDANCE AND VOLUME CONCENTRATIONS OF FECAL MATERIAL

JULY-AUGUST 1979

Samp	Z	Z*	°C	Birefringent pellets # m^{-3} EL	SP	TU	Non birefringent pellets # m^{-3} EL	SP	TU	Total pellets # m^{-3}	Fecal Matter # m^{-3}	Birefringent pellets µm^3 ml^{-1} EL	SP	TU	Non birefringent pellets µm^3 ml^{-1} EL	SP	TU	Total pellets µm^3 ml^{-1}	Fecal Matter µm^3 ml^{-1}
13	12	9	26.70	865	844	831	65	350	0	2955	17331	414	323	3185	13	31	0	3967	54644
17	12	10	26.60	837	616	2501	72	180	0	4206	14703	172	87	23521	9	20	0	23809	38732
14	25	18	25.70	655	547	2182	61	219	12	3676	9650	377	118	16736	10	16	1	17258	40225
15	32	34	19.40	530	449	1712	77	307	13	3087	8271	323	72	9607	4	31	1	10038	27334
18	32	43	17.60	744	274	1242	241	131	0	2632	13227	180	48	12509	20	11	0	12767	34456
19	50	50	16.70	329	231	693	75	35	0	1364	5496	53	34	10028	18	35	0	10168	35290
16	55	58	16.10	307	142	827	37	84	0	1397	5653	111	62	4212	9	12	0	4407	29225
1	100	83	14.80	908	229	152	121	134	25	1568	7679	231	51	116	10	9	3	421	18721
20	75	91	14.60	544	96	189	67	48	0	944	4712	287	21	2484	30	15	0	2838	18511
2	200	200	12.70	376	74	16	23	11	0	500	2331	68	28	28	3	2	0	130	8242
3	350	350	9.60	550	181	68	35	28	0	861	2720	87	28	42	4	3	0	164	8852
4	500	500	7.90	584	60	69	28	74	0	814	2734	108	22	89	3	9	0	232	7715
5	530	530	7.60	614	108	61	63	24	0	871	1673	152	55	169	14	3	0	393	3060
7	530	530	7.60	653	223	70	20	53	0	1020	1823	182	28	36	2	4	0	253	4428
9	530	530	7.60	1498	367	186	139	92	9	2290	1498	327	37	78	29	9	4	483	6256
10	530	530	7.60	739	317	88	19	33	0	1197	918	144	26	66	3	3	0	242	4476
11	530	530	7.60	1013	219	84	20	53	0	1389	2060	233	24	180	5	4	0	446	4988
12	530	530	7.60	508	86	77	14	38	0	724	2467	159	6	256	4	4	0	430	6843
21	720	720	5.80	459	154	69	19	36	0	738	1817	177	45	74	3	3	0	302	4477
22	910	910	4.90	322	79	58	4	27	1	491	2005	101	14	84	1	2	0	202	3667
23	1100	1100	4.40	305	184	42	24	42	5	602	1484	151	51	129	5	2	0	339	5742
24	1260	1260	3.50	261	87	56	16	29	0	449	1677	67	10	90	1	2	0	171	2847

NOVEMBER-DECEMBER 1979

Samp	Z	Z*	°C	Birefringent pellets # m^{-3} EL	SP	TU	Non birefringent pellets # m^{-3} EL	SP	TU	Total pellets # m^{-3}	Fecal Matter # m^{-3}	Birefringent pellets µm^3 ml^{-1} EL	SP	TU	Non birefringent pellets µm^3 ml^{-1} EL	SP	TU	Total pellets µm^3 ml^{-1}	Fecal Matter µm^3 ml^{-1}
43	25	25	26.70	112	66	161	33	33	11	417	5468	34	4	448	4	3	2	495	7154
44	40	40	26.50	199	40	250	0	30	0	519	3155	91	13	604	0	1	0	709	4497
45	55	50	21.00	305	225	161	20	109	7	828	4817	107	21	246	1	19	0	395	5391
46	77	76	17.10	163	74	155	49	42	11	493	1903	28	30	319	5	3	0	385	4171
47	100	103	15.10	267	105	51	41	68	0	532	3090	47	27	201	3	3	0	282	4619
48	100	103	15.10	411	101	125	47	67	0	751	3866	68	14	222	4	6	0	313	6107
31	100	130	14.60	312	96	74	23	47	2	554	2672	48	17	103	4	7	0	179	10169
32	200	200	13.70	135	14	26	6	4	0	184	694	36	3	46	3	1	0	88	2042
39	290	290	13.01	76	42	32	3	29	0	181	571	17	11	51	0	6	0	85	1156
40	290	290	13.01	104	41	21	8	12	0	186	646	64	41	125	1	5	0	236	1796
41	290	290	13.01	137	63	14	5	22	0	242	654	47	24	96	0	3	0	170	1467
33	320	320	11.60	245	46	36	13	23	0	364	1128	32	8	146	2	1	0	189	4565
34	425	425	9.80	167	20	41	11	12	1	251	845	23	2	69	3	1	0	98	1425
35	530	530	7.87	67	6	11	13	0	0	97	584	13	2	56	3	0	0	73	3167
36	673	673	6.62	180	18	18	3	0	0	219	654	48	15	118	1	0	0	181	1379
37	800	800	5.92	137	18	26	0	11	0	192	628	48	7	205	0	1	0	261	1026
38	1000	1000	4.69	98	29	13	1	6	0	147	461	27	6	88	0	1	0	123	722

Samp - Sample #; Z = depth (m); Z* - depth of sample based on mean temperature profile.; EL - > 53 µm Elliptical Fecal Pellet; SP - > 53 µm Spherical Fecal Pellet; TU - > 53 µm Tubular Fecal Pellet

on the transparency of the different groups of pellets, are consistent with those published by KOMAR *et al.* (1981).

Fecal matter fluxes were calculated using the empirical settling velocity relationship of BISHOP *et al.*(1978, 1980):

$$Ws = 0.098/\eta * \Delta\rho * g * h * d * e^{-7.38d} cm\ s^{-1} \quad (2)$$
$$h = 0.052d + 0.0045cm$$

All terms are the same as in Equation 1 with the addition of h for particle thickness and d which is diameter of a disk having the same crossectional area as the particle. $\Delta\rho$ of fecal matter was assigned a value of 0.1g cm^{-1} based on measurements of particle density by BISHOP *et al* (1978).

Recent studies have identified and characterised settling rates of particles which because of their shape and morphology would be included in the fecal matter classification. ROBISON and BAILEY (1981) measured settling rates of 1-5mm sized fecal matter from 6 species of midwater fish in 5-27°C water. Their data for 5-10°C water showed settling rates ranging from 0.2 to 1.3cm s^{-1}, whereas at warmer temperatures they ranged from 0.3 to 3.1cm s^{-1}, demonstrating the fundamental importance of water viscosity in determining settling rates of these particles. According to equation 2, 1-5mm sized fecal matter sinks at between 0.25 - 0.5cm s^{-1} through 7°C water. Thus, the midwater fish fecal matter studied by ROBISON and BAILEY (1981) sank faster than predicted by Equation 2. BRULAND and SILVER (1981) measured 0.5-3cm s^{-1} sinking rates for salp fecal material. These rates also exceed those predicted by Equation 2. In the same paper, however, they reported settling rates of doliolid fecal material which were half those predicted by Equation 2. SILVER and ALLDREDGE (1981) measured 0.06-0.12cm s^{-1} sinking velocities for marine snow, which are also much slower than predicted by Equation 2. However, this later result is expected since the particles classified as fecal matter have higher than average densities and are only a component of the marine snow populations in the water column (BISHOP *et al.*, 1977, 1980). Typical marine snow aggregates are nearly transparent in transmitted light, whereas fecal matter is optically dense.

Many groups of gelatinous and non-gelatinous zooplankton, and nekton besides the few groups described above are likely contributors to the fecal matter class of particles. Because the predictions of fecal matter sinking velocities derived from Equation 2 are intermediate between the observed rates for doliolid fecal material and those for salp and midwater fish fecal material, and because Equation 2 was derived empirically from settling experiments with particles of this class, we conclude that Equation 2 provides reasonable mean estimates of fecal matter settling velocities.

Elemental fluxes for organic carbon, phosphorus, biogenic Si and Ca (Table 6) were calculated using the compositional data for the >53μm fraction corrected for contributions of organisms to Si and Ca (BISHOP *et al.*, 1980). The magnitude of error of each of these steps is difficult to assess but the aim of STIE was to compare calculated particle fluxes with fluxes determined by sediment traps.

TABLE 5:NUMBER** AND MASS FLUXES OF FECAL MATERIAL

JULY-AUGUST 1979

Samp	Z	Z*	°C	Birefringent pellets # m^2d^{-1} EL	SP	TU	Non birefringent pellets # m^2d^{-1} EL	SP	TU	Total pellets # m^2d^{-1}	Fecal Matter mg m^2d^{-1}	Birefringent pellets mg m^2d^{-1} EL	SP	TU	Non birefringent pellets mg m^2d^{-1} EL	SP	TU
13	12	9	26.70	71.6	74.2	116.1	4.7	9.0	0.0	275.6	1215.7	21.7	51.2	767.8	0.3	0.5	0.0
17	12	10	26.60	50.9	20.6	680.6	3.9	5.1	0.0	761.2	807.1	5.7	2.4	2583.3	0.1	0.4	0.0
14	25	18	25.70	67.1	30.7	499.1	3.3	4.0	0.3	604.5	800.0	29.0	5.1	1201.2	0.2	0.2	0.0
15	32	34	19.40	49.2	21.1	273.7	2.1	7.8	0.2	354.0	466.9	20.1	2.3	1419.2	0.0	0.6	0.0
18	32	43	17.60	36.6	6.0	320.4	7.8	3.4	0.0	374.3	612.3	8.0	3.5	1613.8	0.2	0.1	0.0
19	50	50	16.70	14.1	6.2	197.6	4.4	4.3		226.7	318.2	1.0	1.1	1342.7	0.5	5.5	
16	55	58	16.10	21.4	9.6	117.7	2.1	1.8	0.0	152.5	346.4	3.7	6.7	373.8	0.2	0.5	0.0
20	75	91	14.60	33.7	3.6	40.6	4.7	2.4	0.0	84.9	200.4	77.0	1.1	422.2	3.3	1.4	0.0
1	100	83	14.80	41.9	6.2	4.4	2.9	1.2	0.5	57.1	262.1	21.6	5.1	7.5	0.1	0.1	0.0
2	200	200	12.70	14.7	3.9	0.6	0.7	0.4	0.0	20.2	81.7	2.1	2.9	3.7	0.1	0.1	0.0
3	350	350	9.60	18.7	4.4	1.5	1.1	0.6	0.0	26.3	97.3	2.0	2.0	3.8	0.1	0.0	0.0
4	500	500	7.90	19.0	2.7	2.0	0.9	1.4	0.0	25.9	81.9	2.2	1.7	9.0	0.0	0.3	0.0
5	530	530	7.60	25.0	4.7	2.7	2.6	0.4	0.0	35.3	42.5	3.7	9.8	30.5	0.3	0.1	0.0
7	530	530	7.60	28.2	5.7	1.6	0.5	0.4	0.0	36.4	52.9	5.4	0.4	1.9	0.0	0.1	0.0
9	530	530	7.60	53.5	5.9	3.1	5.3	0.9	0.3	68.9	84.5	11.4	0.5	4.9	0.6	0.3	0.0
10	530	530	7.60	24.3	2.9	1.5	0.5	0.3	0.0	29.5	28.0	3.3	0.3	7.9	0.0	0.0	0.0
11	530	530	7.60	38.4	4.3	3.2	1.0	0.4	0.0	47.4	61.9	5.8	0.3	18.8	0.1	0.0	0.0
12	530	530	7.60	23.5	0.3	4.5	0.8	0.6	0.0	29.6	82.3	4.0	0.1	45.0	0.1	0.0	0.0
21	720	720	5.80	21.1	5.2	1.6	0.7	0.2	0.0	28.8	55.8	12.9	3.6	8.0	0.0	0.0	0.0
22	910	910	4.90	13.4	2.1	1.7	0.2	0.2	0.0	17.7	57.3	5.2	0.5	8.2	0.0	0.0	0.0
23	1100	1100	4.40	16.8	5.3	3.0	0.8	0.3	0.0	26.2	56.1	8.3	3.9	7.2	0.1	0.0	0.0
24	1260	1260	3.50	9.4	1.2	1.5	0.2	0.4	0.0	12.7	44.7	2.5	0.3	9.7	0.0	0.0	0.0

NOVEMBER-DECEMBER 1979

Samp	Z	Z*	°C	Birefringent pellets # m^2d^{-1} EL	SP	TU	Non birefringent pellets # m^2d^{-1} EL	SP	TU	Total pellets # m^2d^{-1}	Fecal Matter mg m^2d^{-1}	Birefringent pellets mg m^2d^{-1} EL	SP	TU	Non birefringent pellets mg m^2d^{-1} EL	SP	TU
43	25	25	26.70	6.9	0.0	15.4	0.9	1.4	0.3	25.0	248.1	1.0	0.0	68.1	0.0	0.0	0.0
44	40	40	26.50	16.5	4.5	20.5	0.0	0.0	0.0	41.5	172.3	6.6	0.5	73.2	0.0	0.0	0.0
45	55	50	21.00	20.2	3.9	9.9	0.4	3.2	0.1	37.6	192.8	6.0	0.4	25.3	0.0	1.1	0.0
46	77	76	17.10	6.6	4.9	10.7	1.4	0.4	0.1	24.1	70.7	0.5	3.1	37.3	0.1	0.0	0.0
47	100	103	15.10	10.4	4.5	5.0	1.1	0.0	0.0	21.1	93.7	1.1	1.7	22.8	0.0	0.0	0.0
48	100	103	15.10	15.1	1.9	6.6	0.8	1.2	0.0	25.6	133.9	1.3	0.5	22.7	0.1	0.1	0.0
31	100	130	14.60	10.6	2.0	3.6	0.9	1.5	0.0	18.7	86.2	0.8	1.4	10.2	0.0	0.1	0.0
32	200	200	13.70	6.3	0.6	1.1	0.4	0.2	0.0	8.6	27.0	1.2	0.1	6.2	0.2	0.1	0.0
39	290	290	13.01	3.0	1.6	1.3	0.1	1.4	0.0	7.3	18.3	0.3	0.5	6.3	0.0	0.1	0.0
40	290	290	13.01	7.1	4.3	2.9	0.3	0.8	0.0	15.4	26.8	9.7	8.3	12.3	0.0	0.4	0.0
41	290	290	13.01	7.1	2.5	2.0	0.0	0.4	0.0	12.0	22.1	3.4	4.3	10.0	0.0	0.1	0.0
33	320	320	11.60	6.7	1.3	2.6	0.3	0.0	0.0	10.9	38.2	0.9	0.2	21.0	0.0	0.0	0.0
34	425	425	9.80	4.9	0.2	1.6	0.5	0.0	0.0	7.2	25.5	0.4	0.0	6.8	0.1	0.0	0.0
35	530	530	7.87	2.3	0.2	0.9	0.4	0.0	0.0	3.9	17.4	0.2	0.1	6.7	0.0	0.0	0.0
36	673	673	6.62	7.1	1.1	2.2	0.1	0.0	0.0	10.4	17.7	1.2	1.8	14.3	0.0	0.0	0.0
37	800	800	5.92	5.0	1.1	2.9	0.0	0.1	0.0	9.2	18.7	5.7	0.3	21.0	0.0	0.0	0.0
38	1000	1000	4.69	3.8	0.6	1.1	0.0	0.2	0.0	5.7	12.4	1.1	0.2	23.0	0.0	0.0	0.0

** = Number fluxes in 1000 's; Samp - Sample #; Z = depth (m); Z* - depth of sample based on mean temperature profile.; EL - > 53 µm Elliptical Fecal Pellet; SP - > 53 µm Spherical Fecal Pellet; TU - > 53 µm Tubular Fecal Pellet

TABLE 6: MASS AND CHEMICAL FLUXES OF FECAL MATERIAL

JULY-AUGUST 1979

Samp	Z	Z*	°C	DW	FP	FM	FP+FM	FM/FP+FM	C_{ORG}	P	Si	Si**	$CaCO_3$	$CaCO_3$**
				μg kg^{-1}	mg m^{-2}d^{-1}			ratio	mmol m^{-2}d^{-1}		mmol m^{-2}d^{-1}		mmol m^{-2}d^{-1}	
13	12	9	26.70	6.313	842	1550	2392	0.648	50.25	0.5935	8.21	7.70	3.08	3.44
17	12	10	26.60	8.130	2592	1230	3822	0.322	88.45	0.4607	10.76	10.50	4.13	4.30
14	25	18	25.70	6.944	1236	986	2222	0.444	48.73	0.4419	7.01	6.57	2.67	2.98
15	32	34	19.40	4.656	1442	812	2254	0.360	62.60	0.2602	3.61	3.44	1.22	1.33
18	32	43	17.60	5.984	1626	1110	2736	0.406	35.39	0.2835	17.54	17.13	4.45	4.73
19	50	50	16.70	5.384	1351	1000	2351	0.425	58.17	0.2930	6.23	6.04	1.68	1.81
16	55	58	16.10	3.716	385	782	1167	0.670	23.09	0.1858	5.26	5.13	1.05	1.15
20	75	91	14.60	2.416	505	585	1090	0.537	19.59	0.1407	5.02	4.90	1.50	1.59
1	100	83	14.80	1.968	34	513	547	0.937	13.02	0.0634	1.71	1.70	0.37	0.38
2	200	200	12.70	0.864	9	256	265	0.966	5.05	0.0205	1.19	1.04	0.30	0.41
3	350	350	9.60	0.928	8	246	254	0.969	5.75	0.0107	0.89	0.82	0.19	0.24
4	500	500	7.90	0.832	13	183	196	0.933	4.78	0.0045	0.57	0.52	0.13	0.16
5	530	530	7.60	0.404	44	80	124	0.642	3.50	0.0029	0.20	0.19	0.05	0.06
7	530	530	7.60	0.512	8	109	117	0.933	3.04	0.0032	0.28	0.26	0.06	0.07
9	530	530	7.60	0.913	18	164	182	0.903	4.02	0.0139	0.61	0.55	0.19	0.23
10	530	530	7.60	0.511	11	124	135	0.916	3.09	0.0075	0.46	0.44	0.11	0.12
11	530	530	7.60	0.609	25	119	144	0.826	2.78	0.0100	0.63	0.59	0.17	0.20
12	530	530	7.60	0.783	49	145	194	0.747	4.18	0.0102	0.72	0.64	0.18	0.24
21	720	720	5.80	0.527	25	91	116	0.786	2.84	0.0055	0.29	0.27	0.09	0.11
22	910	910	4.90	0.416	14	66	80	0.826	1.64	0.0036	0.29	0.26	0.10	0.13
23	1100	1100	4.40	0.659	20	107	127	0.846	2.91	0.0054	0.37	0.28	0.13	0.19
24	1260	1260	3.50	0.326	12	47	59	0.792	1.37	0.0029	0.19	0.16	0.06	0.07

NOVEMBER-DECEMBER 1979

Samp	Z	Z*	°C	DW	FP	FM	FP+FM	FM/FP+FM	C_{ORG}	P	Si	Si**	$CaCO_3$	$CaCO_3$**
				μg kg^{-1}	mg m^{-2}d^{-1}			ratio	mmol m^{-2}d^{-1}		mmol m^{-2}d^{-1}		mmol m^{-2}d^{-1}	
43	25	25	26.70	0.810	69	221	290	0.762	7.22	0.0670	0.61	0.35	0.31	0.49
44	40	40	26.50	0.593	80	89	169	0.527	4.33	0.0370	0.34	0.25	0.16	0.22
45	55	50	21.00	0.629	33	106	139	0.764	3.09	0.0163	0.48	0.39	0.12	0.19
46	77	76	17.10	0.490	41	130	171	0.760	3.49	0.0175	0.69	0.62	0.17	0.22
47	100	103	15.10	0.524	26	89	115	0.775	2.54	0.0186	0.39	0.31	0.11	0.16
48	100	103	15.10	0.675	25	134	159	0.845	3.43	0.0046	0.57	0.39	0.13	0.12
31	100	130	14.60	1.061	13	124	137	0.907	2.96	0.0102	0.47	0.46	0.15	0.16
32	200	200	13.70	0.224	8	58	66	0.882	1.55	0.0031	0.19	0.18	0.06	0.06
39	290	290	13.01	0.134	7	31	38	0.810	0.57	0.0040	0.21	0.06	0.07	0.17
40	290	290	13.01	0.235	31	41	72	0.570	1.56	0.0051	0.24	0.18	0.08	0.12
41	290	290	13.01	0.185	18	36	54	0.671	1.43	0.0048	0.12	0.09	0.03	0.05
33	320	320	11.60	0.498	22	94	116	0.809	2.70	0.0089	0.34	0.20	0.11	0.22
34	425	425	9.80	0.162	7	32	39	0.818	0.97	0.0048	0.10	0.08	0.03	0.05
35	530	530	7.87	0.334	7	25	32	0.781	0.93	0.0028	0.04	0.04	0.01	0.01
36	673	673	6.62	0.179	17	33	50	0.657	1.24	0.0029	0.14	0.13	0.04	0.05
37	800	800	5.92	0.159	27	16	43	0.370	1.02	0.0013	0.13	0.12	0.03	0.04
38	1000	1000	4.69	0.098	24	13	37	0.353	1.08	0.0007	0.06	0.05	0.01	0.01

Samp - Sample number; °C - Temperature determined by XBT (Knorr) or hydrocast (Gilliss); DW - Dry weight of fecal pellets and fecal matter; FP - fecal pellet flux; FM - fecal matter flux; FP+FM - fecal material flux; FM/FP+FM - fecal matter / fecal material flux ratio; C_{ORG} - Organic carbon flux; P - Phosphorus flux; Si - Biogenic silicon flux; $CaCO_3$ - Calcium carbonate flux; * - Depth based on mean temperature profile; ** - Si and Ca fluxes corrected for Si and Ca bound in organisms.

2.3 *Zooplankton*

Zooplankton samples were collected during the July-August cruise using the Multiple Opening/Closing Net and Environmental Sensing System (MOCNESS; WIEBE, BURT, BOYD and MORTON, 1976; Table 7). The MOCNESS was equipped with nine $1m^2$ 333μm mesh nets and collected eight depth stratified samples per tow. MOCNESS sampling was not possible in November, and zooplankton samples from the upper 200m were collected also using oblique hauls of a 333μm mesh 1m diameter ring net during both cruises (see page 376 in SVERDRUP, JOHNSON, and FLEMING, 1942).

Major taxonomic groups of zooplankton were enumerated from MOCNESS tows 125, 126, 128 and 129 because of their close proximity in time to LVFS sampling (Table 8). Similar analysis of a pair of ring net tows from each cruise was also done to compare zooplankton data between cruises. All MOCNESS samples were measured for wet displacement volume 4-6 weeks after collection. Conversion of wet displacement volume to carbon biomass was estimated using the regression relationship of WIEBE, BOYD and COX, (1975).

The comparison of >53μm copepod counts from LVFS samples with those determined by the MOCNESS allows a test of the extent to which actively swimming organisms are captured by the LVFS during sampling. Contamination of samples with living organisms is a problem particularly affecting shallow sediment trap sampling as evidenced by the fact that "swimmers" contribute substantially to the material recovered by poisoned traps (see eg., KNAUER, MARTIN, and BRULAND, 1979; FELLOWS, KARL and KNAUER, 1981; KARL and KNAUER, 1984). Copepod abundances determined by LVFS sampling were integrated and then averaged over the upper 100m and were compared to MOCNESS data from the same depth interval. LVFS data showed copepod abundances averaging $156m^{-3}$ in the 0-100m interval whereas MOCNESS data (Table 8) gave abundances of $404m^{-3}$. Compared to the MOCNESS, the LVFS undersampled by at least 60%, since some individual copepods are small enough to be extruded through the 333μm mesh used in the MOCNESS. This undersampling is not surprising given the fact that tow speeds of the MOCNESS ($100cm\ s^{-1}$) exceed the maximum LVFS flow velocities ($1.7cm\ s^{-1}$) substantially, so that animals which cannot swim fast enough to avoid the MOCNESS might easily avoid capture by the LVFS. This provides direct evidence that swimming organisms actively avoid capture by the LVFS during sampling. Thus, one advantage of the LVFS over shallow sediment traps is the substantial reduction in contamination by living organisms in the collected samples.

2.4 *Other data*

Methods for the determination of ^{14}C productivity, chlorophyll, and phaeopigments are described by MARRA *et al.* (in press). Twelve-kHz echo sounding records of the upper 750m were taken continuously during all LVFS casts to provide a record of migratory scatterers. The 12-kHz data were also used to monitor LVFS depth during deployment.

Nephelometer data (an optical measure of suspended particulate matter concentrations, BISCAYE and EITTRIEM, 1977) were collected during both LVFS casts and deep hydrocasts on the July-August cruise and have been described by GARDNER *et al.* (1984). The data obtained during

TABLE 7: MOCNESS AND METER NET SAMPLING SUMMARY

JULY-AUGUST 1979

Tow		depth range m	Date	local time start	stop	Latitude Longitude start	Latitude Longitude finish
MOC-1-119	2	0 - 200	28-Jul-79	1535	1600	5o22.3'N 82o02.0'W	5o20.3'N 82o02.0'W
MOC-1-120	2	0 - 200	29-Jul-79	0129	0157	5o28.3'N 82o00.1'W	5o26.6'N 82o02.7'W
TOW-1	* 1 ++	0 - 200	29-Jul-79	1545		5o23.2'N 81o57.7'W	
TOW-2	* 1 ++	0 - 200	29-Jul-79	2109		5o24.9'N 81o54.6'W	
TOW-3	* ++	0 - 200	30-Jul-79	1400		5o21.3'N 81o54.2'W	
TOW-4	* ++	0 - 200	30-Jul-79	2003		5o17.4'N 81o51.2'W	
TOW-6	* ++	0 - 200	31-Jul-79	1326		5o17.0'N 81o52.1'W	
MOC-1-121	2	0 - 200	31-Jul-79	2322	0053	5o18.4'N 81o52.7'W	5o15.0'N 81o48.5'W
MOC-1-122	2	0 - 1000	1-Aug-79	1239	1410	5o18.2'N 81o49.9'W	5o18.9'N 81o55.9'W
TOW-7	* ++	0 - 200	1-Aug-79	1507		5o18.9'N 81o55.9'W	
MOC-1-123	2	0 - 1000	1-Aug-79	2255	0018	5o13.3'N 81o48.8'W	5o10.0'N 81o50.6'W
MOC-1-124	2	0 - 200	2-Aug-79	1510	1536	5o04.8'N 81o45.5'W	5o04.5'N 81o48.0'W
MOC-1-125	* 1 2	0 - 100	3-Aug-79	1453	1527	5o14.4'N 81o52.5'W	5o12.7'N 81o52.7'W
MOC-1-126	* 1 2 +	0 - 100	3-Aug-79	2034	2132	5o10.8'N 81o46.9'W	5o11.0'N 81o49.3'W
MOC-1-127	2 +	0 - 200	4-Aug-79	1044	1126	5o07.7'N 81o49.8'W	5o05.2'N 81o50.6'W
MOC-1-128	* 1 2 +	0 - 1000	5-Aug-79	1040	1218	5o07.5'N 81o52.6'W	5o05.2'N 81o57.9'W
MOC-1-129	* 1 2	0 - 1000	5-Aug-79	2110	2240	5o08.1'N 81o50.9'W	5o15.1'N 81o50.0'W
MOC-1-130	2	0 - 2000	7-Aug-79	1430	1658	5o16.8'N 81o53.1'W	5o15.9'N 82o01.5'W
MOC-1-131	2 +	0 - 2000	7-Aug-79	2216	0052	5o18.4'N 81o45.3'W	5o18.1'N 81o38.0'W

NOVEMBER-DECEMBER 1979

Tow		depth range m	Date	local time start	stop	Latitude Longitude start	Latitude Longitude finish
PT- 1	* 1 ++	0 - 193	24-Nov-79	1819		5o22.6'N 81o49.4'W	
PT- 2	* 1	0 - 232	25-Nov-79	1612		5o16.5'N 81o51.8'W	
PT- 3	++	0 - 200	26-Nov-79	0353		5o15.7'N 81o41.9'W	
PT- 4	*	0 - 199	26-Nov-79	1240		5o14.0'N 81o55.5'W	
PT- 5	*	0 - 217	26-Nov-79	2228		5o14.0'N 81o52.5'W	
PT- 6		0 - 200	27-Nov-79	1107		5o17.2'N 81o51.5'W	
PT- 7		0 - 200	27-Nov-79	2340		5o18.4'N 81o55.3'W	
PT- 8	++	0 - 200	28-Nov-79	0013		5o17.5'N 81o55.4'W	
PT- 9	*	0 - 208	30-Nov-79	1312		5o22.1'N 81o57.9'W	
PT-10	*	0 - 200	30-Nov-79	2230		5o21.8'N 81o55.9'W	
PT-11		0 - 200	1-Dec-79	2350		5o20.5'N 81o46.5'W	
PT-12		0 - 200	2-Dec-79	1226		5o19.0'N 81o54.6'W	
PT-13	++	0 - 200	3-Dec-79	0031		5o17.1'N 81o50.6'W	

PT and TOW - oblique meter net hauls; MOCNESS - depth stratified samples from 8 discrete depth intervals; * - enumeration of copepods; 1 - enumeration of major taxonomic groups; 2 - displacement volumes (MARRA, WIEBE, STEPIEN and BISHOP; in press); + - enumeration of Foraminifera (FAIRBANKS, SVERDLOVE, WIEBE and BÉ; 1982); ++- enumeration of Foraminifera (BÉ, BISHOP, SVERDLOVE and GARDNER; 1985)

TABLE 8: > 333 um ZOOPLANKTON ABUNDANCES (# m^{-3})

Z	Int	Carbon	Cop	Larv	Chaet	Ost	Euph	Ptero	Siph	Amphi	Gast	Polyc	Fish L	Salp	Cru L	Cru O	Moll	Fish	Other
								MOC-1-125 3 AUGUST 1979 Day											
6	12.5	1182	731.2	18.200	55.900	24.700	11.200	3.700	9.300	4.200	3.300	0.470	1.400	7.400	6.100	0.470	3.700	-	0.470
19	12.5	900	465.7	18.200	35.100	10.400	5.700	3.300	6.000	5.100	2.700	0.890	0.670	6.000	2.700	1.800	0.440	-	1.300
31	12.5	1046	729.4	7.700	46.700	9.000	6.500	4.100	11.800	7.900	0.270	0.270	1.100	6.600	1.900	0.550	1.100	-	1.100
44	12.5	1438	431.4	4.900	31.500	21.400	8.600	0.210	7.100	5.600	0.430	1.500	1.700	3.600	0.640	0.640	1.100	-	1.500
56	12.5	957	157.1	1.400	10.800	23.000	10.200	0.860	3.500	2.200	0.760	1.800	3.300	0.540	0.430	-	0.220	-	0.760
69	12.5	453	92.0	0.150	3.000	15.500	5.700	0.520	2.700	1.600	1.300	0.370	2.400	1.500	0.290	0.520	0.580	-	0.300
81	12.5	588	73.1	-	2.000	16.000	4.500	0.290	2.300	1.200	0.950	0.880	1.900	0.440	0.070	-	0.290	-	0.950
94	12.5	505	43.7	0.160	1.900	8.600	2.800	0.380	1.600	0.470	1.200	0.200	0.050	0.160	0.018	0.018	0.180	-	0.520
								MOC-1-126 3 AUGUST 1979 Night											
6	12.5	1232	485.9	20.900	43.800	26.200	35.700	9.100	11.200	5.400	3.700	1.800	-	3.600	4.600	0.660	0.970	-	1.500
19	12.5	1081	326.8	2.300	48.500	0.690	2.600	5.200	9.900	1.200	0.690	0.870	0.690	2.400	0.520	1.900	0.520	0.011	0.520
31	12.5	2064	540.0	-	23.700	4.700	9.500	2.900	1.100	5.100	2.900	0.730	2.900	2.200	1.500	1.500	0.360	0.035	2.900
44	12.5	2827	533.5	0.600	12.900	64.300	24.900	2.200	0.400	8.400	3.000	0.600	6.400	3.200	3.200	0.200	0.400	0.051	3.800
56	12.5	694	106.6	0.320	3.500	20.500	3.700	1.200	0.320	2.100	0.400	0.560	2.500	0.560	1.600	-	-	0.018	0.720
69	12.5	850	61.3	0.340	2.400	14.000	3.200	0.680	0.490	1.000	0.340	0.190	1.800	0.150	0.190	0.110	0.038	-	0.160
81	12.5	399	50.4	0.014	1.500	12.700	2.100	0.060	0.520	0.940	0.220	0.130	0.280	0.080	-	0.140	0.028	0.007	0.320
94	12.5	435	25.1	-	0.750	8.900	1.600	-	0.270	0.350	0.025	0.220	0.050	0.050	-	0.500	0.025	0.007	0.350
								MOC-1-128 5 AUGUST 1979 Day											
50	100.0	917	448.7	29.400	39.100	22.900	10.000	4.200	4.500	3.900	7.100	5.500	2.100	2.500	1.000	0.500	1.600	-	1.500
150	100.0	256	46.1	-	2.000	12.900	1.300	3.500	2.300	0.370	0.037	0.320	0.037	0.130	-	0.056	0.180	0.004	0.920
250	100.0	352	39.6	-	1.000	4.600	1.000	0.450	0.180	0.150	-	0.090	-	0.044	-	0.044	-	-	0.260
350	100.0	463	42.4	0.019	0.270	0.910	1.400	0.019	-	-	-	0.160	-	0.019	-	0.019	0.019	-	0.490
475	150.0	348	21.4	-	0.270	0.590	0.260	0.035	-	0.027	-	0.190	0.120	0.050	0.009	0.080	0.027	0.092	0.110
625	150.0	121	2.8	0.006	0.290	0.540	0.012	0.006	-	0.030	-	0.180	0.048	0.042	0.012	0.050	0.012	0.030	0.036
775	150.0	101	5.2	0.006	0.280	0.590	0.013	0.006	-	0.050	-	0.180	0.003	0.380	-	0.012	0.003	0.016	0.062
925	150.0	89	1.6	-	0.200	0.150	-	-	-	0.025	-	0.050	-	0.390	0.008	0.017	0.004	0.004	0.021
								MOC-1-129 5 AUGUST 1979 Night											
50	100.0	1366	561.2	25.900	42.800	17.900	8.600	16.300	8.300	7.400	4.500	5.100	3.800	1.600	1.900	0.320	1.900	0.084	3.200
150	100.0	89	27.8	0.045	1.700	4.300	0.720	-	0.140	0.500	-	0.090	0.045	0.045	-	-	0.045	-	0.270
250	100.0	183	33.5	-	1.100	3.700	0.032	0.032	0.130	-	-	0.380	-	-	-	-	-	-	0.250
350	100.0	272	34.0	0.036	0.360	2.100	-	-	-	-	0.036	0.430	-	-	-	0.036	-	-	0.320
475	150.0	133	13.5	-	0.240	0.390	-	-	-	-	-	0.130	0.060	0.037	-	0.012	-	-	0.060
650	200.0	84	3.7	-	0.410	0.810	-	-	0.008	0.060	-	0.140	0.046	0.170	0.100	0.030	-	0.034	0.015
800	100.0	136	4.4	0.009	0.410	0.390	-	-	-	0.026	-	0.034	-	0.260	-	-	-	0.026	0.040
925	150.0	91	3.4	0.007	0.360	0.330	-	0.020	-	0.044	0.020	0.090	0.003	0.510	0.017	0.010	0.017	0.010	0.051

Z = mid depth of MOCNESS sample (m); int = depth interval (m); Carbon = Zooplankton carbon (nmol kg^{-1}) from Wiebe et al. (1975); Cop = copepods; Larv = larvaceans; Chaet = chaetognaths; Ost = ostracods; Euph = euphausiids; Ptero = pteropods; Siph = siphonophores; Amph = amphipods; Gast = gastropods; Fish = fish; Fish L = fish larvae; Polyc = polychaets; Salp = salps and doliolids; Cru L = crustacean larvae; Cru O = other crustaceans including shrimp, mysids, Lucifer, and isopods; Moll = other mollusks - including heteropods, gymnosomes, cephalopod larvae, and bivalve larvae; Other = includes medusae, trocophores, schyhozoans, fish eggs and unidentified groups; "-" = not present in sample; blank = not analyzed.

LVFS casts have been regressed against total suspended particulate matter (SPM) dry weight (Table 2) to produce the first shallow water calibration reported for the nephelometer:

$$SPM = 6.8\ e^{1.65*LOG(E/ED)} \qquad \mu g\ kg^{-1} \qquad (3)$$

$$R^2 = 0.94$$

where E/ED is the ratio of scattered to direct light intensities recorded by photographic film in the instrument. No nephelometer data were obtained during the November-December cruise.

3. RESULTS AND DISCUSSION

In the sections that follow we will present STIE/C-FATE data from the July-August and November-December cruises.

3.1 *Hydrography of the water column*

The vertical distributions of hydrographic and nutrient properties in the euphotic zone play an important role in determining the rates of particle formation during photosynthesis. During both cruises, the euphotic zone (defined by the 1% light level) was 70m thick and could be divided into two major layers (Fig.3) based on thermal structure (BISHOP and MARRA, 1984). The upper mixed layer was approximately 18m deep during the July-August cruise and approximately 35m deep during the November-December cruise. It was warm, had low salinity, and was depleted in nutrient elements. The lower layer of the euphotic zone contained the upper thermocline where levels of nutrient elements sharply increased. Maxima of 0.3 and 0.7 $\mu mol\ kg^{-1}$ ammonia and nitrite concentrations respectively were found a few meters below the base of the mixed layer and highest salinities observed were near 70m at the base of the lower layer.

The distributions of temperature and salinity in the entire water column reveal three layers in addition to the two described above (Fig.4). A weakly developed thermostad (T = 12-14°C and S = 34.85-34.92 x 10^{-3}) was evident between 100 and 250m both in XBT profiles (not shown) and could also be seen in the water column profiles of silica concentrations (Fig.4). The fourth and fifth layers were respectively a broad salinity minimum between 700-800m (T = 6°C, S = 34.58 x 10^{-3}) and a region of nearly constant properties below 3000m.

The low salinity of the surface mixed layer is largely due to the excess of runoff over evaporation in the Panama Bight (FORSBERGH, 1969). The shallow salinity maximum is believed to be a relict feature of the equatorial undercurrent which has been identified at 0°N, 84°W (STEVENSON and TAFT, 1971) and is thought to have a southern origin in Subtropical Surface Water. The mid-depth salinity minimum is derived from the Antarctic Intermediate Water mass (WYRTKI, 1966). The waters of the thermostad are also thought to have a southern

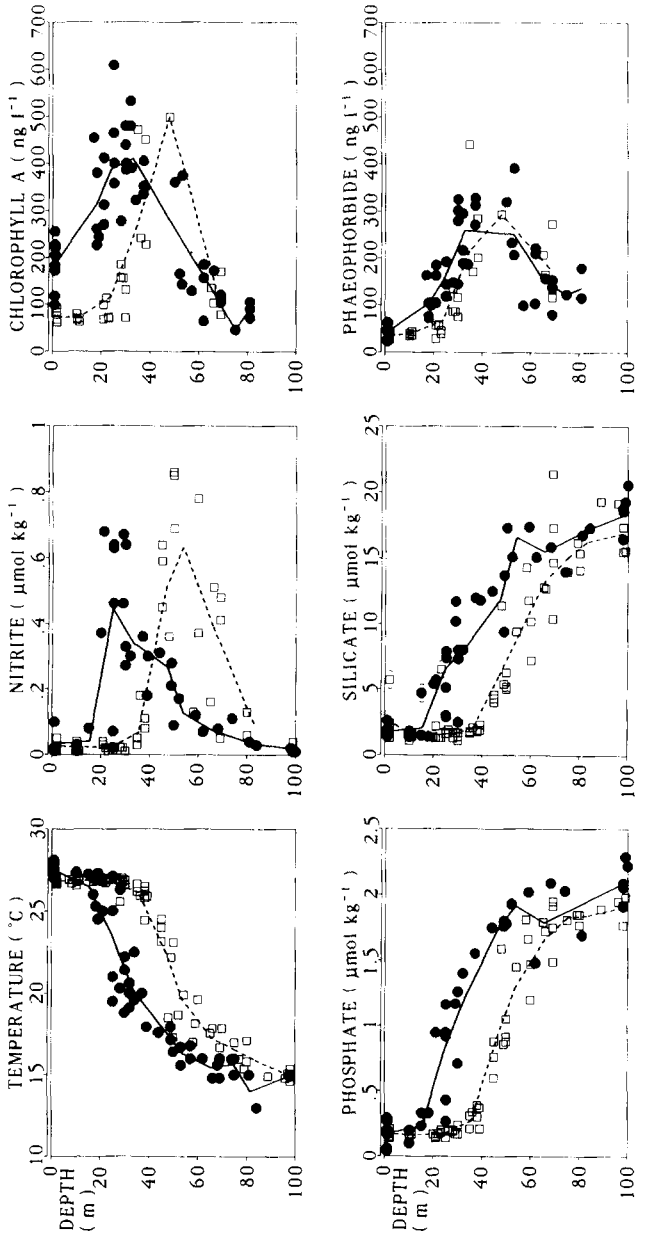

FIG.3. Distributions of temperature, phosphate, silicate, nitrite, chlorophyll and phaeopigments in the upper 100m during the July-August and November-December STIE/C-FATE cruises. The distributions of nutrient elements and chlorophyll were closely related to temperature whereas the distributions of phaeopigments showed almost no relationship with temperature. Mixed layer depth averaged 18m during the July August cruise and 35m during the November cruise. Mean primary production for the July-August and November-December periods was 286 and 174 mg C $m^{-2}d^{-1}$, respectively. Mean particle flux through the base of the 70m thick euphotic zone, calculated based on new production estimates, was 138 and 59 mg C $m^{-2}d^{-1}$ for the two cruises, respectively (BISHOP and MARRA, 1984).

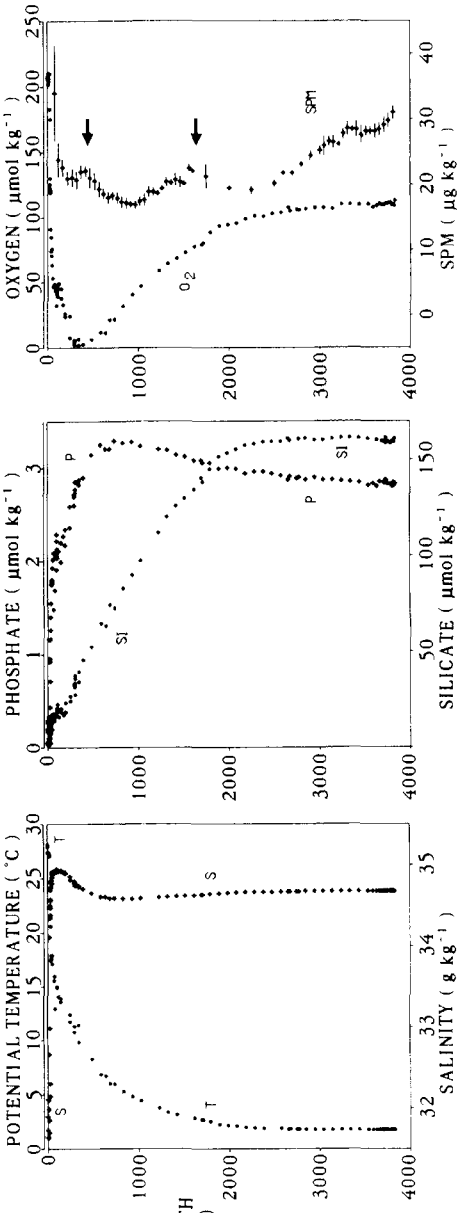

FIG. 4. Distributions of potential temperature (T), salinity (S), phosphate (P), silicate (Si), oxygen (O_2) and optically-determined suspended particulate matter (SPM) concentration in the 3800m deep water column during the July-August cruise. Error bars represent (1 S.D.) of SPM as determined from nephelometer profiles. Two subsurface SPM maxima (indicated by arrows) were found centered at 450m and 1500m. Both maxima are probably caused by plumes of material resuspended from nearby topography.

origin and have been traced to the Tasman Sea north of New Zealand (TSUCHIYA, 1981).

Comparison of isotherm depths found during the July-August and November-December cruises with historical data for the upper 100m (ROBINSON, 1973) showed that temperatures at 30 and 60m were colder by 2-3°C than the historical mean during July-August but had recovered to mean values by the November-December cruise. The abnormally cold values in July-August were probably related to the equatorial upwelling event contemporaneously observed at 153°W by WYRTKI and ELDIN (1982).

The phosphate concentration profile was typical for the eastern equatorial Pacific. Concentrations increased ten-fold from <0.2µmol kg^{-1} in the mixed layer to 2µmol kg^{-1} at 70m. Concentrations increased slowly to a broad maximum of 3.2µmol kg^{-1} between 500m and 800m and decreased to 2.8µmol kg^{-1} in deeper waters. Silica also increased ten-fold between the surface and 70m. Silica concentrations were nearly constant at 20µmol kg^{-1} between 100m and 250m in the thermostad and increased to 155µmol kg^{-1} below 3000m. Dissolved oxygen decreased strongly from surface values of 210µmol kg^{-1} to 40µmol kg^{-1} at 100m. Oxygen concentrations continued to decrease to very low but measurable values (2-5µmol kg^{-1}) in the layer between 250m and 400m but subsequently increased with depths to levels greater than 100µmol kg^{-1} below 2000m.

Nephelometer data were used to calculate the mean suspended particulate matter (SPM) profile in July-August. The optically determined SPM values decreased from near surface values of approximately 100µg kg^{-1} (not shown in the figure) to a broad minimum of 17µg kg^{-1} at 900m and then increased to near bottom values of >30µg kg^{-1}. Two 22µg kg^{-1} secondary maxima were observed in the SPM profile and may have been caused by lateral transport of resuspended sediments from nearby topography (Fig.1). The first at 400-500m, located below the oxygen minimum zone, coincided with the daytime depths of migratory organisms and so may be the result of biological activity. The second maximum near 1500m occurred at a depth where a step was observed in the dissolved oxygen profile.

3.2 *Euphotic zone pigments, primary and new production*

The chlorophyll maximum (Fig.3) and productivity maximum (MARRA *et al.*, in press) was located 5-10m deeper than the base of the mixed layer. Consistent with differences in mixed layer depths, the highest chlorophyll concentrations were found between 20-30m and between 35-50m during the July-August and November-December cruises, respectively. Integrated chlorophyl concentration in the euphotic zone was 20mg m^{-2} during July-August and 15mg m^{-2} during the November-December cruise. Although the integrated chlorophyll levels decreased by only 25% between cruises, the increase in mixed layer depth between July-August and November-December resulted in a 40% reduction of primary production during the latter cruise. Similarly new production was estimated to be 60% lower (BISHOP and MARRA, 1984; Table 9).

Phaeopigment concentration distributions, in contrast to those of chlorophyll, showed little difference between the two cruises. These pigments were mostly composed of phaeophorbide,

a chlorophyll degradation product produced during the digestion of phytoplankton by zooplankton (WELSCHMEYER and LORENZEN, 1985). On both cruises, phaeopigments showed a broad peak at 30-50m and had integrated euphotic zone values of approximately 11mg m^{-2}.

3.3 *Macrozooplankton and midwater fish distributions*

Zooplankton are important contributors to and modifiers of the particles found in the > 53μm fraction sampled by the LVFS and derive their energy from carbon originally fixed by phytoplankton. Once started on the way to the bottom within fecal material, most particles must undergo multiple processing (KARL and KNAUER, 1984) before reaching the sediments.

3.3.1 *July-August data.* Distributions of >333μm zooplankton biomass (expressed as zooplankton carbon) derived from MOCNESS tows (Fig.5) show that the upper 2000m may be divided into several major zones. The first zone was coincident with the 70m deep euphotic zone and contained most zooplankton biomass. Maxima of 1200 (day) and 2400 (night) nmol C kg^{-1} were found in the 25-50m depth interval. This zone also coincided with the maximum chlorophyll concentrations and the highest rates of primary production. The 100-500m zone was dominated during daylight hours by migratory species which swam up into the euphotic zone to feed at night. Hence biomass in this zone fluctuated between 400 (day) and 200 (night) nmol C kg^{-1}. The observed increases in zooplankton biomass in the upper zone at night can be entirely explained by this upward migration of zooplankton from the deeper zone. A third zone extended below 600m, where there was little day versus night variability in zooplankton carbon concentrations. Biomass decreased from 150nmol C kg^{-1} at 600m to 100nmol C kg^{-1} by 1000m. Concentrations dropped sharply to between 10 and 50nmol C kg^{-1} by 2000m.

The vertical distributions of major groups of zooplankton (Figs.6 and 7) further enhance the picture of biological zonation of the water column. The five most numerically dominant groups of organisms were copepods, chaetognaths, ostracods, larvaceans, and euphausiids (Table 8). All of these groups showed strong concentration gradients in the upper 100m with a strong bias to the upper 50m where most primary production occurred (MARRA *et al*, in press). Many groups showed maximal abundances at night in the 37-50m interval. Euphausiids were the only group of the five exhibiting significant day-night differences due to their daily migrations between 500m and the surface. On the other hand, larvaceans were almost exclusively limited to the upper 100m and showed little tendency to migrate.

Next in abundance were siphonophores, pteropods, salps, amphipods, and polychaetes. The siphonophores and pteropods migrated diurnally over the upper 200 and upper 300m respectively. Both groups had highest nighttime concentrations in the upper 25m. Salps consistently preferred the upper 50m and showed little evidence of migration. Amphipod distributions were correlated with those of salps (Amphipod abundance = 1.0 (salp) + 0.6, R^2 = 0.60 n=32), consistent with their frequent association with salps (MADIN and HARBISON, 1977).

Fish larvae were next in abundance in the upper 100m and showed little evidence of diurnal migration. They showed a secondary layer between 400m and 750m centred on 500m. A number

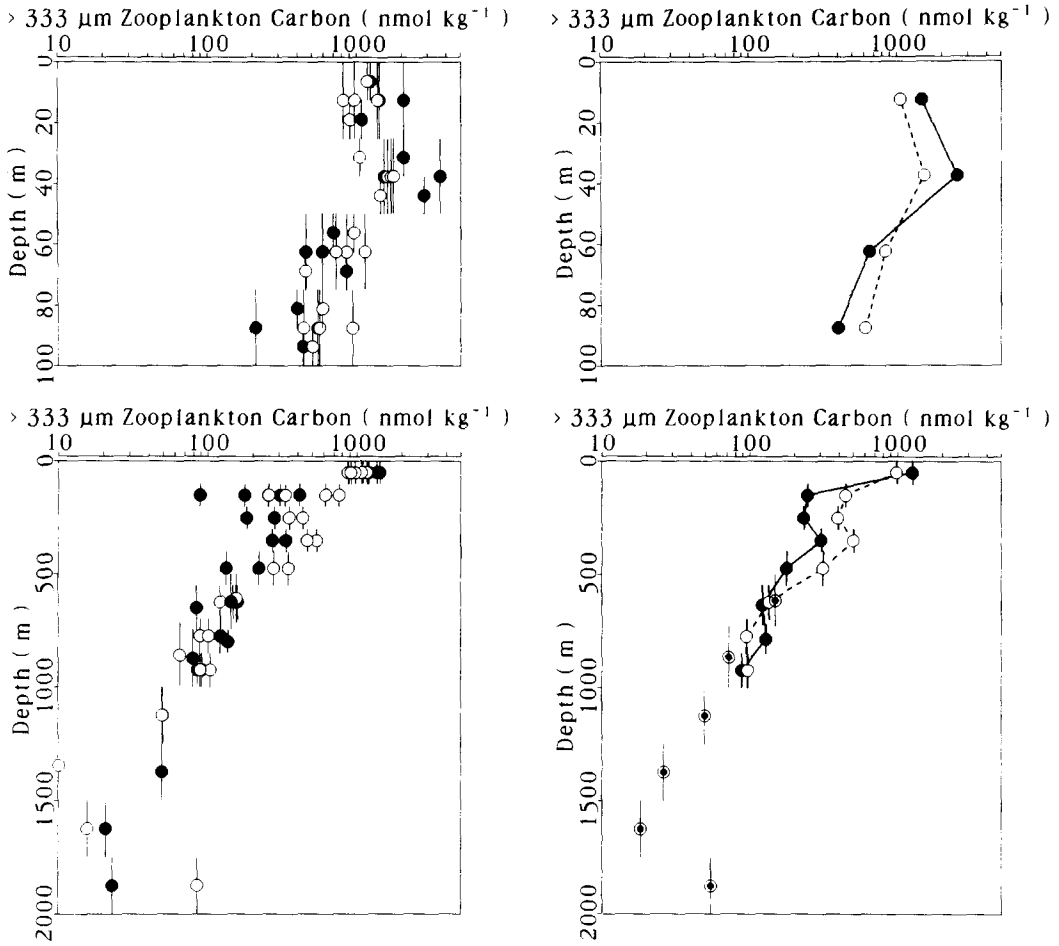

FIG.5. Left, distributions of >333µm zooplankton carbon from day (O) and night (●) MOCNESS tows during the July-August cruise. Right, averages of all day and night MOCNESS data are connected by dashed and solid lines respectively. Vertical bars represent the depth interval averaged by each MOCNESS sample. Day and night data from the 0-2000m MOCNESS tows were averaged below 500m since there was little evidence of diurnal variability below this depth. The additional biomass in the surface 50m at night was made up of migrating organisms from the 50-500m interval. Log scales are used to facilitate the representation of the data.

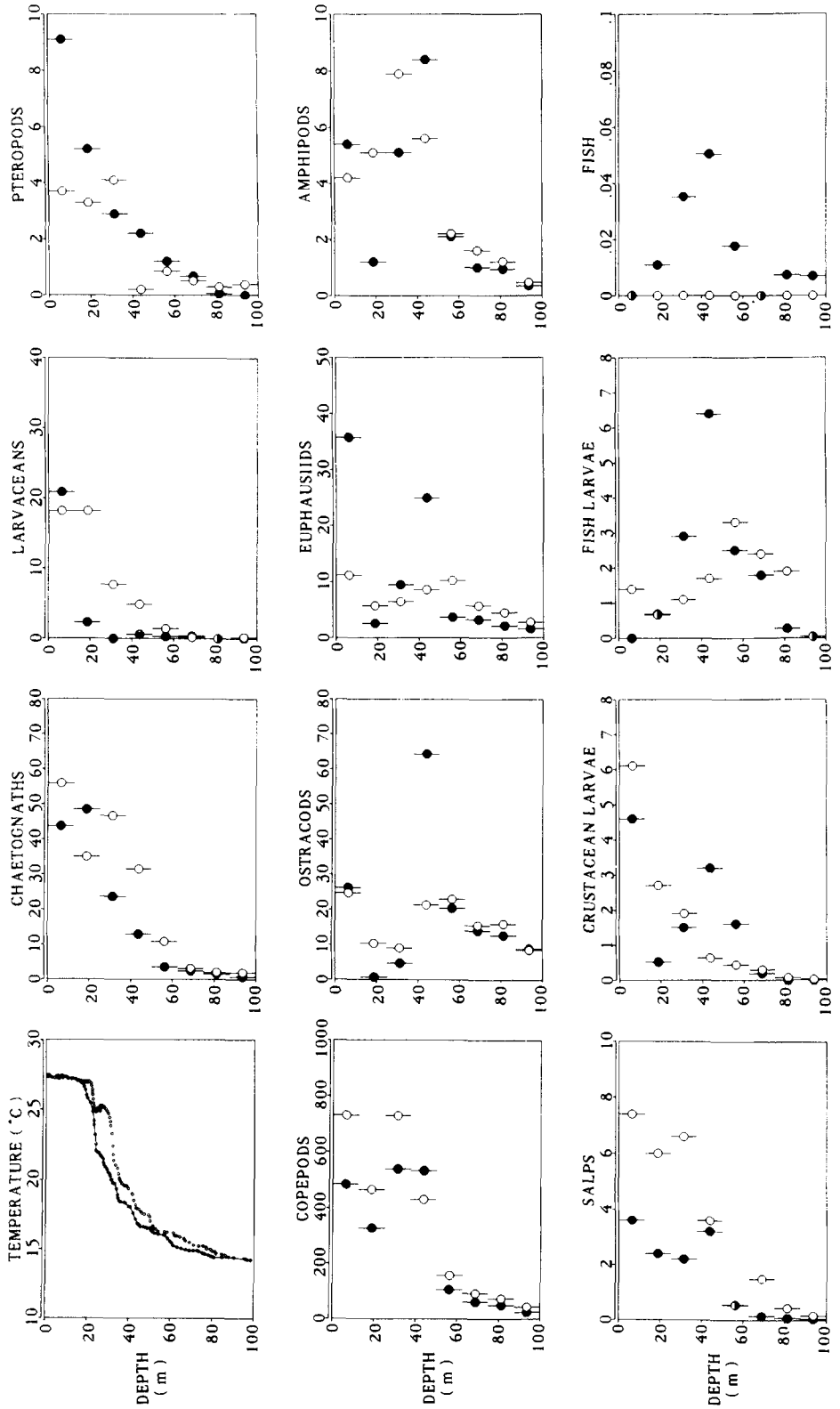

FIG. 6. Day (○) versus night (●) distributions of major zooplankton groups (#m-3) in the upper 100m on 3 August 1979 from MOCNESS tows 1-125 (day) and 1-126 (night) during the July-August cruise. Shown for comparison are the temperature profiles made at the same time of sample collection. Many zooplankton groups had maximum night time abundances in the 37.5-50m depth interval.

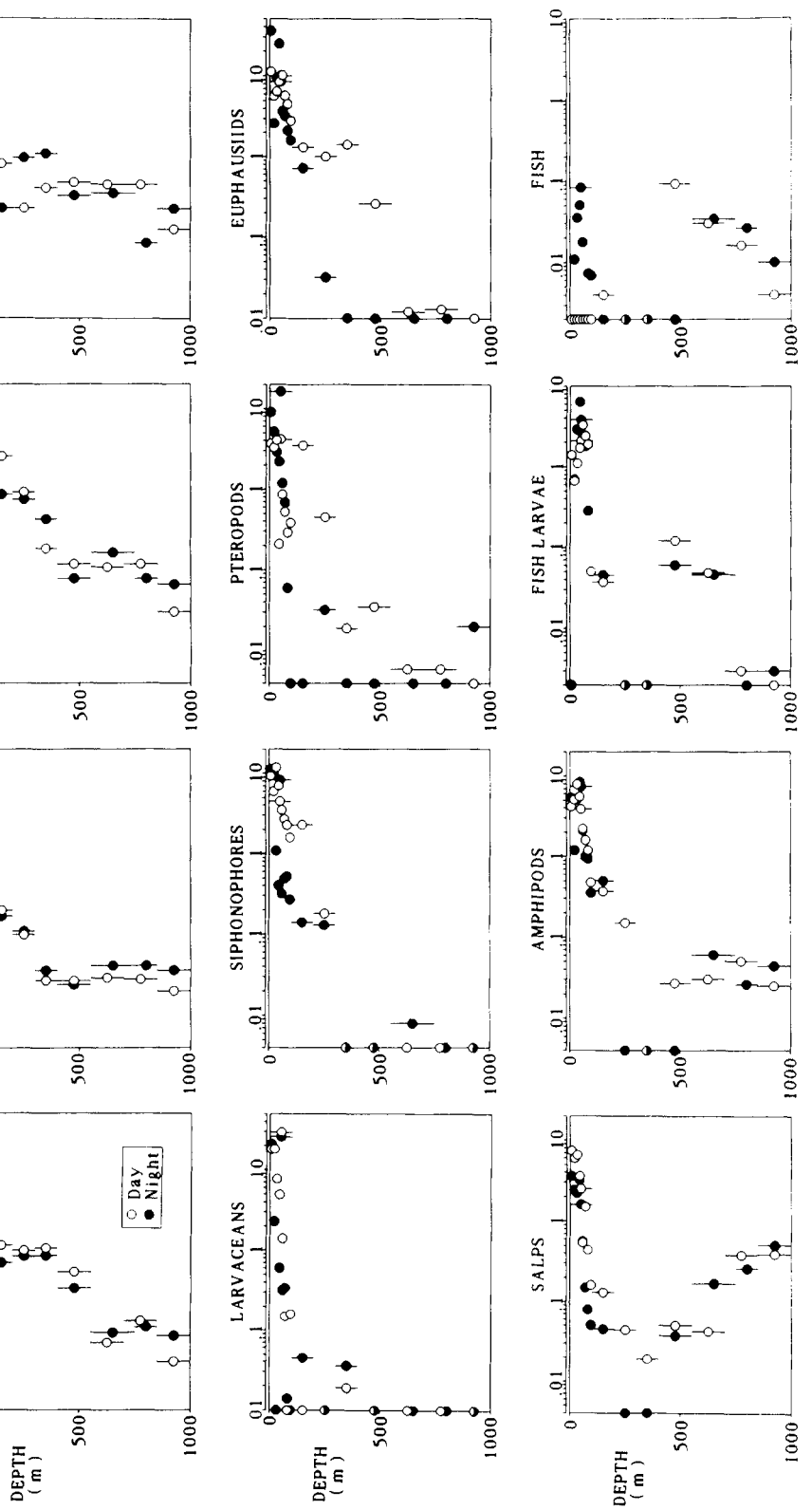

FIG.7. Day (○) versus night (●) abundance profiles ($\#m^{-3}$) of major zooplankton groups in the upper 1000m on 5 August 1979 from MOCNESS tows 1-128 (day) and 1-129 (night). All data are plotted on log scales.

of midwater fish species (which were probably undersampled by the MOCNESS) migrated from 500-600m to the upper 100m. Highest migrator abundances were observed at night in the 25-50m interval (MOC-1-120 and 121) and between 37.5m and 50m (MOC-1-125). The migratory fish, although numerically small, contributed equally with euphausiids to the day versus night biomass differences in the 400-550m depth interval. No species of midwater fish appeared to migrate from 600m.

Other zooplankton groups sampled included medusae, scyphozoans, heteropods, gymnosomes, mysids, isopods, decapods, mollusc larvae, crustacean larvae and fish eggs, but were not present in all samples and, when they did occur, were only present in small numbers (Table 8)

The oxygen minimum zone between 250m and 400m (Fig.4) appeared to exclude some groups but not others. No adult or larval fish were sampled in the oxygen minimum zone, nor were any salps or amphipods. On the other hand, the distribution of copepods, chaetognaths, ostracods polychaetes, pteropods and euphausiids appeared unaffected by the low oxygen waters.

3.3.2 *November-December data.* An intercomparison of the zooplankton population differences between the two cruises was based on average abundances for the 0-200m depth interval sampled by meter net tows (Table 9). Without exception, all >333μm zooplankton groups declined by at least 60% relative to abundances observed during the July-August cruise. This decline is also consistent with the 60% seasonal decrease of zooplankton biomass in the Panama Bight observed by FORSBERGH (1969).

The least change was observed for copepods, chaetognaths, ostracods, euphausiids and salps (losses of 64-75%). Pteropods, midwater fish, and larvaceans declined in abundance by 92%, 93% and 95% respectively from their July-August values. These differences will be important in Sections 3.7 and 3.8 where we describe inter-cruise differences in fecal pellet and fecal matter abundances and flux in the water column.

The decline observed for midwater fish seems extreme in the context of the low seasonal variability observed by BLACKBURN, LAURS, OWEN and ZEITZSCHEL (1970) for micronekton fish in this region. This may be due to the inadequacy of the meter net as a collector for these fishes. However, the absence of large scatterers on the 12 kHz records in November (below) supports the notion that some decline took place.

3.4 *12kHz scatterer distributions*

Twelve kilohertz echo sounding records were used during both cruises to investigate semi-quantitatively the distributions of animals unsampled by the MOCNESS and the meter net but yet which may have been responsible for some of the production of fecal material sampled by the LVFS (Figs.8 and 9). Sound-scattering data collected from the upper 75m during one nighttime LVFS cast on the 6th August (Fig.8) showed many intense patches of scattering in the upper 20m which persisted from the start of sampling near midnight until 0300h, but fewer occurred after 0300h. No such patches were observed during the November-December

TABLE 9: MEAN BIOLOGICAL PROPERTIES OF THE UPPER WATER COLUMN

		1 JULY-AUG	2 NOV-DEC	ratio 2:1
	EUPHOTIC ZONE 0-70 m			
[1]	primary production (mg C m-2d-1)	286.	174.	0.60
[1]	new production "	138.	59.	0.42
[2]	chlorophyll (mg m-2)	19.8	14.5	0.73
[2]	phaeophorbide "	12.1	10.7	0.88
>53 um PHYTOPLANKTON (numbers l-1)				
[3]	dinoflagellates	2.88	5.44	1.889
[3]	silicoflagellates	24.51	36.00	1.469
[3]	centrate diatoms	57.63	18.89	0.328
[3]	pennate diatoms	30.68	20.91	0.682
>53 um ZOOPLANKTON (numbers l-1)				
[3]	sticholonche	1.52	8.29	5.45
[3]	tintinnids	0.98	5.71	5.83
[3]	Foraminifera	2.13	4.14	1.94
[3]	nassellaria	7.88	9.64	1.22
[3]	Spumellaria	1.44	1.76	1.22
[3]	Phaeodaria	0.327	0.117	0.358
[3]	Acantharia	13.04	14.81	1.136
[3]	pteropods	0.197	0.042	0.213
[3]	copepods	0.206	0.133	0.646
	0-200 m ZONE			
> 333 um ZOOPLANKTON (numbers m-3)				
[4]	copepods	180.9	65.7	0.36
[4]	larvaceans	15.5	0.77	0.05
[4]	chaetognaths	14.7	3.42	0.24
[4]	ostracods	12.1	3.02	0.25
[5]	Foraminifera	7.3	1.30	0.18
[4]	euphausiids	4.5	1.18	0.27
[4]	pteropods	3.7	0.3	0.08
[4]	siphonophores	3.1	0.59	0.19
[4]	amphipods	2.2	0.76	0.36
[4]	gastropods	2.1	0.2	0.10
[4]	polychaetes	2.0	0.38	0.20
[4]	fish larvae	1.3	0.29	0.23
[4]	salps	1.1	0.31	0.27
[4]	other	3.2	0.7	0.22
[4]	mid-water fish*	0.025	0.0015	0.06

[1] - BISHOP and MARRA (1984); [2] - This paper; [3] - This paper, Table 3; [4] - This paper; [5] - BE, BISHOP, SVERDLOVE and GARDNER (1985); * - mid-water fish are probably undersampled by the MOCNESS and meter nets.

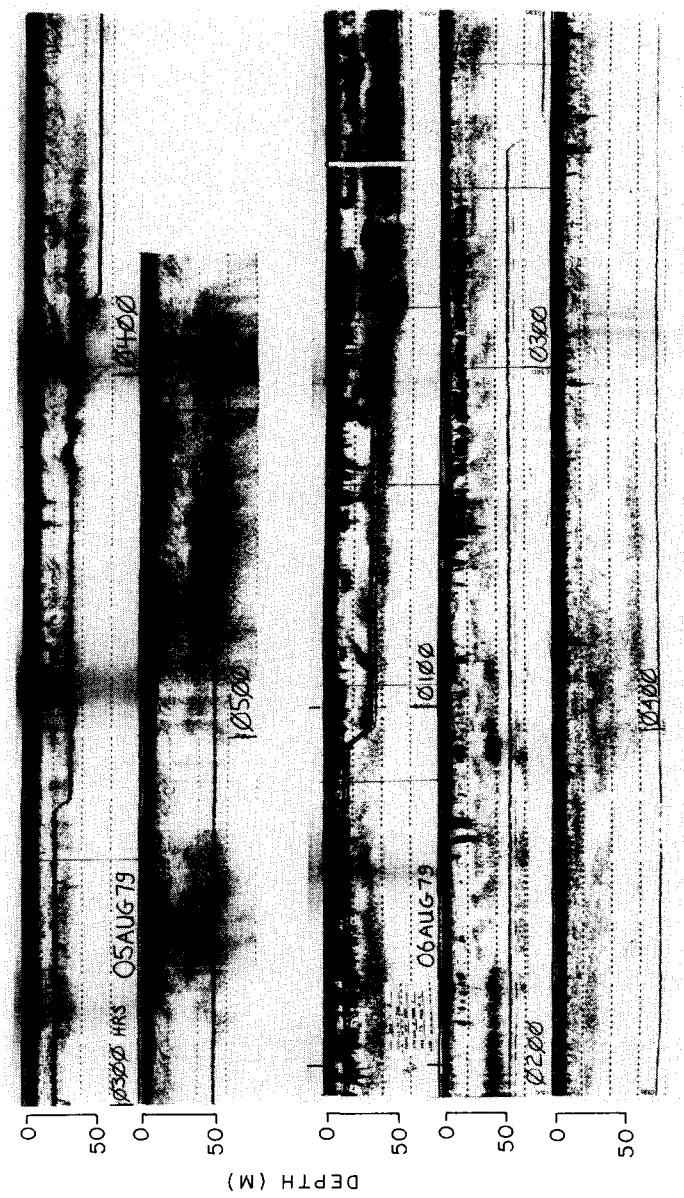

FIG.8. 12kHz echo sounder records of the upper 75m during the nights of August 5 and 6, 1979. We observed intense patches of scatterers near midnight on August 6. The horizontal lines show reflection from the LVFS during the two night casts The LVFS sample from 12m on August 6, when the patchy scatterers were abundant, was loaded heavily with long tubular fecal pellets of the type shown in Fig.2, suggesting that the scatterers or their prey were the source of this material. The 12m sample from the previous night, when scatterers were absent, showed relatively few long tubular pellets. Apart from the patchy scatterers, the scattering maximum appeared to be concentrated in the vicinity of the chlorophyll maximum at 35m.

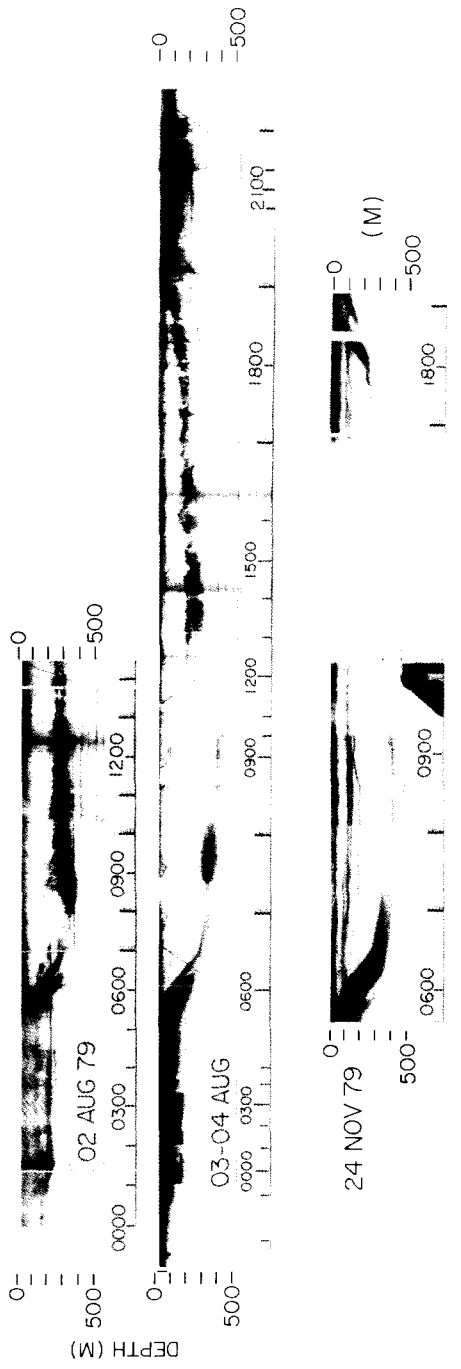

FIG.9. 0-750m records of 12kHz sound scattering during the July-August and November-December cruises. The comparison of the two records suggests that the diel migrators during July-August were dominated by species which were highly mobile compared to those present during the November-December cruise.

cruise. Apart from these patches, most scattering (on both occasions where complete records were obtained) during the July-August cruise occurred at night between 20m and 50m and was generally most intense in the vicinity of the chlorophyll maximum. Strongest scattering occurred deeper during the November-December cruise centred at 50m, which was again close to the depth of the chlorophyll maximum.

Distributions of 12 kHz sound scattering in the 0-750m interval during both cruises (Fig.9) showed that the scatterers were undertaking diel migrations. At first light they migrated down from the upper 100m to depths ranging from 200m to 500m, and returned to the surface layer at dusk. Otherwise the characteristics and behaviour of scatterers changed markedly between the two sets of observations. During July-August scattering layers migrating to the surface in late afternoon showed great vertical variability over short horizontal distances and time, consistent with the population being dominated by one or more species of high mobility. For example, between 1500h and 1900h on both July 29 and 31 (not shown) scattering layer depths were observed to change by 100m within 2-3 minutes on several occasions. In contrast in November-December no short-term changes in scattering layer depth exceeded 20m and those which did occur were gentle undulations at periods of 15-20 minutes. Comparable 12-kHz data collected at 1°N 86°W in July 1976 showed scattering patterns similar to those observed in November-December but of weaker scattering intensity (BISHOP *et al* 1980).

As a subscript we note that large pelagic fish, such as tunas, were very abundant in July-August but less so in November-December.

3.5 *>53μm Microzooplankton and phytoplankton abundances*

Microzooplankton are important consumers of primary produced carbon and, therefore, also greatly influence particle distributions and fluxes (WELSCHMEYER and LORENZEN, 1985). Microzooplankton group abundances, as determined on >53μm LVFS filters (Table 3), were integrated over the 0-70m euphotic zone using depths normalised to the mean temperature profile and sample temperatures determined by XBTs shot during each cast. This normalisation was done to reduce variability due to internal waves. The integrated standing stocks were then divided by the 70m euphotic zone depth to yield mean euphotic zone microzooplankton concentrations (Table 9).

Unlike the macrozooplankton and the 12-kHz scatterers described above, most microzooplankton groups *increased* during the November-December period compared to July-August values. Sticholonche and tintinnids increased by over 500%; Foraminifera in the >53-<333μm fraction doubled; radiolarians in the Spumellaria and Massellaria groups increased by 25%; and Acantharia increased by 15%. Only Phaeodaria and juvenile pteropods decreased, following the macrozooplankton trends.

The Foraminifera were interesting in that abundances of >333μm individuals decreased by 82% between the two cruises but smaller individuals increased in abundance. BÉ, BISHOP, SVERDLOVE and GARDNER (1985) concluded that not only were Foraminifera in the >333μm fraction

more abundant in July-August but also most were in a state of reproductive maturity as a consequence of an elevated food supply at that time. The higher populations of smaller Foraminifera in November and December is attributed to lower mortality due to predation in this season as discussed below.

We hypothesise that the more numerous macrozooplankton grazers and fish present during the July-August cruise had suppressed the populations of microzooplankton through predation. The subsequent decline of macrozooplankton between the two cruises through either migration or advection out of the STIE area or enhanced mortality caused by predation by higher organisms, would have allowed the faster growing populations of microzooplankton to attain higher abundances by November-time.

Limited evidence to support the above hypothesis comes from the comparison of abundances of >53µm microzooplankton and phytoplankton abundances in two LVFS samples collected from 12m on successive nights during the July-August cruise. On the first night (sample 13, Table 3), >53µm organism abundances were double (excluding Phaeodaria and pennate diatoms which were greater than 15 times higher) those on the second night (sample 17). Sample 13 was taken when few 12kHz scatterers were present (5 August, 0212-0242hrs) whereas sample 17 was taken when abundant 12kHz scatterers were present (6 August, 0025-0055hrs, Fig.8). A link between reduced microzooplankton concentrations and the presence of 12kHz scatterers is also indicated by the seven-fold increase in long tubular fecal pellet volume concentrations (Table 4, Section 3.7 below) in sample 17 compared to sample 13. While spatial patchiness cannot be ruled out as a cause for these observations, they are consistent with the idea that the feeding activities of macrozooplankton and nekton were important factors in regulating the >53µm phytoplankton and microzooplankton populations during the July-August cruise.

3.6 *Particulate matter distributions and chemistry*

The above discussion has focused on the distributions of particle producers and consumers in the water column. Now we examine profiles of 1-53µm and >53µm sized particulate matter and how they may be governed by these organisms. The smaller particle size class has long settling or residence times in the water column relative to the material in the >53µm fraction (McCAVE, 1975). However, exchange between the two size classes can occur through both repackaging and disintegration in the water column.

Particulate dry weight, organic carbon, biogenic silica, calcium and phosphorus (Figs.10 and 11) occurred in greater concentrations throughout the upper 1000m during July-August when primary production was higher, than during November-December. This was especially true for the >53µm fraction for which concentrations in the euphotic zone in July-August were double those in November-December.

Besides this temporal difference, concentration ranges over the upper 1000m were much greater for particles in the >53µm fraction compared to the 1-53µm fraction. For example,

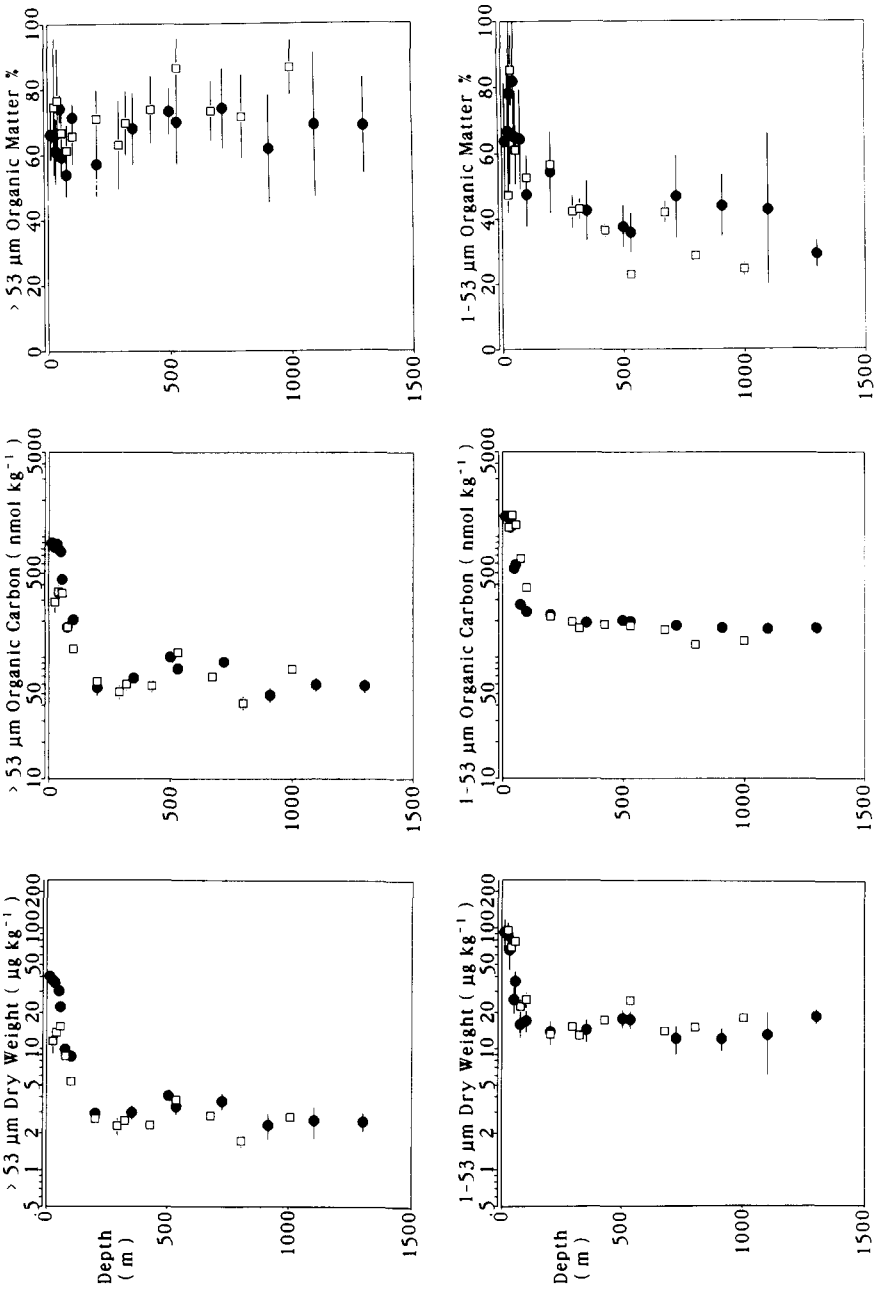

FIG. 10 Distributions of >53µm and 1-53µm particulate dry weight, organic carbon, and percentage of particulate dry weight composed of organic matter determined by LVFS sampling during the July-August (●) and November-December (□) cruises.

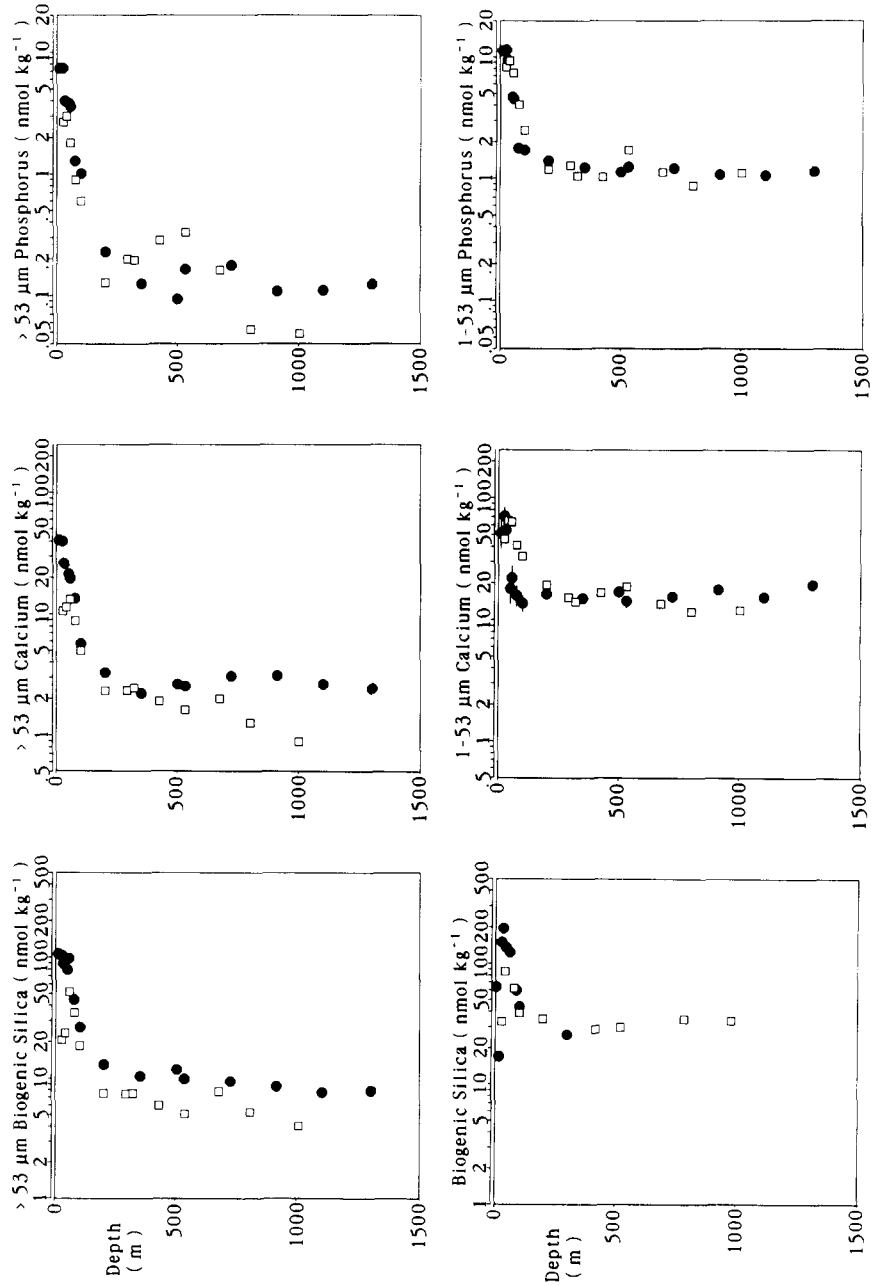

FIG.11. Profiles of >53µm and 1-53µm biogenic silica, calcium and phosphorus during the July-August (●) and November-December (□) cruises. Biogenic silica data (shown in the lower part of the figure) was determined from Niskin bottle samples filtered through 0.4µm Nuclepore filters. Most elements in the 1-53µm size fraction exhibited lower vertical concentration gradients in the upper 200m during November-December than in July-August. This was attributed to a probable reduction in the efficiency of downward transport of particles from the 0-200m zone in November-December when there appeared to be an increase in microzooplankton grazing relative to macrozooplankton grazing.

July-August >53μm dry weight decreased 20-fold between 12 and 200m whereas 1-53μm concentrations dropped only by 6-fold over the same depth interval. The greatest vertical concentration gradient of >53μm particles coincided with the zone of greatest zooplankton biomass. Thus, the differences in the profiles of the 1-53μm and >53μm size fractions are probably due to the larger particles being more available and so, more efficiently utilised by the coprophagous zooplankton and fish. If fragmentation of large particles occurs during feeding, it would add particles to the smaller size class and so reduce the vertical concentration gradients of small particles; conversely, any scavenging of small particles by, for example, discarded mucus feeding webs would have the opposite effect.

SHELDON *et al.* (1972) investigated the partitioning and size distributions of carbon in particulate and living pools. They showed that there was more living carbon compared to particulate carbon in many parts of the ocean, especially in the upper several hundred metres. To examine if this is true of the macrozooplankton (particle consumers) versus >53μm particles (the sinking fraction), we compared >333μm zooplankton biomass (Fig.5) to >53μm organic carbon (Fig.10) from the July-August cruise. In the upper 50m at night, zooplankton biomass exceeded the >53μm particulate carbon by factors of 2-4. Between 200m and 500m, the ratio of swimming to >53μm carbon ranged from 3:1 (night) to 10:1 (day). This ratio decreased below 500m to 2:1 at 1000m and further to 1:1 by 1300m. Even when compared to total particulate carbon (<1μm) the macrozooplankton carbon to particulate carbon ratio exceeded unity between 200m and 500m. These ratios are underestimates since not all animal biomass was sampled by the MOCNESS.

An interesting feature of the 1-53μm fraction element distributions during the two cruises was that lower vertical concentration gradients were found for most elements in the upper 100m during the November-December cruise than during the July-August cruise. This difference was most extreme for 1-53μm calcium which was predominantly of coccolithophorid origin (see e.g. BISHOP *et al*, 1977; HONJO, 1982). In July-August calcium concentrations in the 1-53μm fraction dropped from 80nmol kg^{-1} at 32m to 20nmol kg^{-1} at 50m but then remained below 20nmol kg^{-1} throughout the 50-1300m depth interval. In November-December the concentrations only decreased from 65nmol kg^{-1} at 40m to 41nmol kg^{-1} at 77m and continued to decrease to 30nmol kg^{-1} at 100m, and down to 20nmol kg^{-1} at 200m. These lower calcium concentration gradients in November-December are interpreted to result from the reduction in macrozooplankton and fish feeding activity (see Section 3.5) leading to a lower efficiency of small particle export within sinking fecal material from the upper 100m.

3.6.1 *Organic Matter percentages and Element ratios.* The ratio of organic matter to dry weight in >53μm fraction remained nearly constant at 60-70% between the surface and 1300m. In contrast, the 1-53μm organic percentages decreased with depth from 45-85% in the upper 100m to 25-40% below 1000m. Generally higher organic percentages were found in the 1-53μm fraction in July compared with November (Fig.10).

The only comparable data from sediment traps deployed in the same depth interval are those reported by MARTIN and KNAUER (1983). Their traps deployed in the upper 2000m showed organic

matter percentages ranging from 60-80% in the upper 200m decreasing to 30-40% near 1000m. These data follow more the depth trends of the 1-53µm fraction than of the >53µm fraction.

Oxidation of particulate organic carbon (C_{org}) and dissolution of calcium carbonate contribute to the dissolved inorganic carbon pool in the ocean. In the >53µm fraction, most particulate calcium occurs as calcium carbonate and calcium carbonate is the dominant contributor to particulate inorganic carbon (BISHOP *et al.*, 1978). The changes in the ratio of C_{org} to Ca in the >53µm fraction as a function of depth indicates the relative release rates of these two particulate carbon species to the water column.

The >53µm C_{org}/Ca ratios ranged between 13:1 and 35:1 in the euphotic zone (Fig.12) with the most extreme limits being found in the July-August samples. Between 200 and 1000m, >53µm ratios averaged 30:1 on both cruises. The nearly constant C_{org}/Ca ratio in the >53µm fraction over the upper 1000m indicates that there is no differential regeneration of organic and inorganic carbon in the STIE/C-FATE water column. The 1-53µm fraction had C_{org}/Ca ratios ranging from 20:1 to 30:1 in the euphotic zone, and decreasing with depth to a ratio of 10:1 by 1000m. This decrease is consistent with a preferential loss of organic carbon from small particles.

The >53µm Si/Ca ratios are a measure of the relative dominance of siliceous to carbonate organisms as sources of particulate matter and of the relative dissolution behaviour of these two elements. Ratios were lowest in the euphotic zone indicating either a preference of calcareous organisms (e.g. Foraminifera) for the near-surface waters or the occurrence of preferential dissolution of carbonate below the euphotic zone.

Phosphorus to carbon ratios in the 1-53 and >53µm fractions were very similar in the euphotic zone but strongly diverged from one another in deeper waters. In the euphotic zone, the >53µm C_{org}/P ratio was 125:1 in July-August and 138:1 in November-December, but this ratio increased rapidly to >500:1 in deeper waters during both cruises. BISHOP *et al.* (1980) reported that >53µm C_{org}/P averaged 200:1 in the euphotic zone and >500:1 in deeper samples. Values as high as 1000:1 were found in all three data sets. In contrast, the 1-53µm fraction showed a much lower range of variation in the upper 1000m. Euphotic zone values were 127:1 in July-August and 160:1 in November-December and during both cruises were 160:1 below 200m. BISHOP *et al.* (1980) observed C_{org}/P ratios averaging 195:1 in the euphotic zone and 240:1 below 200m. Thus, all three LVFS profiles from the Panama Basin showed there to be relatively close correspondence between the C_{org}/P ratios of the >53µm and 1-53µm material in the euphotic zone, but that a strong divergence in the ratios of these two fractions occurred below 100m. Lowest euphotic zone values were observed during the July-August cruise when water column primary production was highest.

Phosphorus is more easily released than carbon from organic particles (KNAUER *et al.* 1979; COLLIER and EDMOND, 1984). Our evidence suggests that in spite of its short residence time in the upper 1000m, the >53µm fraction is extensively reworked by biological processes, which explains the observed loss of particulate phosphorus relative to carbon. The data

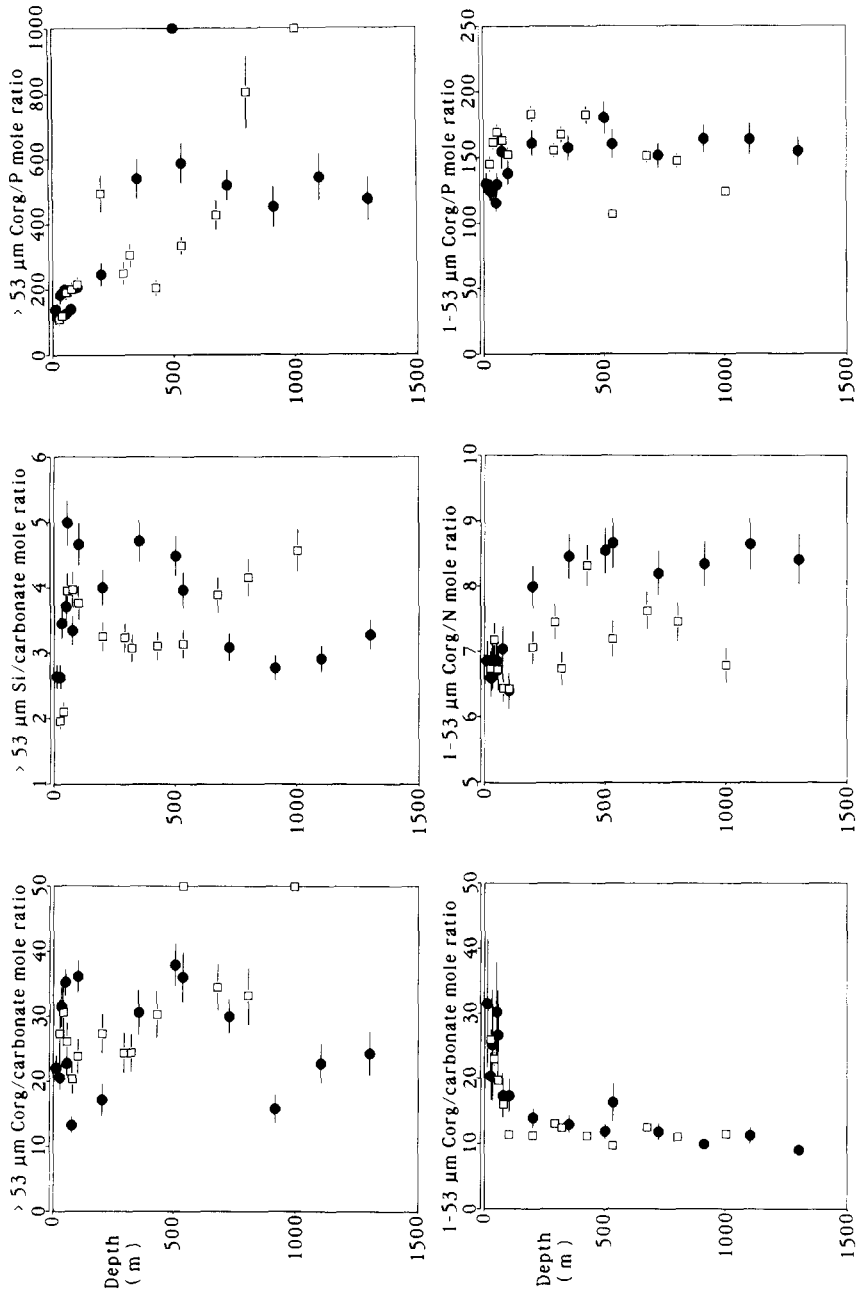

FIG.12. Profiles of the ratios of organic carbon (C_{org}) to calcium carbonate and C_{org}/P ratio in both >53µm and 1-53µm fractions; biogenic silica to calcium carbonate >53µm; and C_{org}/N 1-53µm. Calcium carbonate was estimated from calcium analysis in the samples. The >53µm C_{org}/carbonate ratios indicate that there is no preferential release of either organic or inorganic carbon with increasing depth. On the other hand, >53µm C_{org}/P ratios indicate that there is a rapid loss of phosphorus from sinking material, especially in the upper 200m. The 20% changes in the distributions of 1-53µm C_{org}/N which occurred between July-August and November-December can be explained by the 1-53µm particles turning over on a time scale of months.

for the 1-53μm fraction cannot be explained in this way. Because of their small size, these particles have longer setting residence times in the water column, increasing the opportunity for phosphorus loss to surrounding waters. The small dynamic range in C_{org}/P ratio for this size fraction can only be explained if (1) bacteria with low C_{org}/P ratio contribute significantly to the 1-53μm fraction (e.g. BISHOP *et al*., 1977); (2) there is a refractory phosphorus particle phase present in the small size fraction or (3) the release of P relative to carbon from small particles is less than from large particles at depths below the euphotic zone.

The 1-53μm C_{org}/N ratios in July-August averaged 6.8 in the euphotic zone and ranged between 8 and 8.7 below 200m. In November-December, the similar C_{org}/N ratios again averaged 6.9 in the euphotic zone but remained near this value in deeper samples. The 20% decrease in 1-53μm C_{org}/N below 200m between the July-August and November-December cruises indicates that small particles in the upper 1500m can turnover on time scales of months, possibly as a result of the period of higher primary productivity and particle flux which occurred between the two cruises (BISHOP and MARRA, 1984). Changes in the bacteria abundances in the 1-53μm fraction or horizontal advection may have also caused these changes. Increased bacteria during November-December as a cause for the lower C_{org}/N appears to be ruled out since the C_{org}/P ratios would also be expected to be lower in the same samples. The time scale of several months for turnover of small particles is much faster than the residence time of several years based on particle settling rates (assuming 10μm particles with density contrast ($\Delta\rho$) = 0.5g cm^{-1}; Equation 2 in BISHOP *et al*., 1977).

3.7 *Fecal matter and fecal pellet distributions*

We have discussed above the impact that biota have on particles in the water column. Now we look at how the distributions of fecal material in the water column can be used to understand the distributions and activities of particle consumers. With few exceptions, higher abundances of fecal material were found throughout the water column during July-August than in November-December (Fig.13).

Fecal matter, as opposed to fecal pellets, was by far the most important contributor to the total volume of fecal material. As noted in Section 2.2, these large macroscopic aggregates are a subset of particles usually described as marine snow. Unlike typical marine snow particles which are usually nearly transparent to transmitted light, fecal matter is optically dense. SMETACEK (1985) suggested that diatoms may be a source of large aggregates. Microscopic analysis of our samples suggests that diatoms do not play a major role in the formation of this class of particles in Panama Basin waters. Furthermore, a centrate diatom maximum found at 500m (BISHOP *et al*. 1980) where diatoms were 100 times more concentrated than in surfce waters, was not coincident with a maximum in fecal matter abundance. Fecal matter appears to be produced by zooplankton and nekton.

Fecal matter volumes during the July-August cruise were the highest ever observed and ranged from 50,000μm^3 ml^{-1} in the shallowest sample at 12m to 3000μm^3 ml^{-1} at 1300m in a smoothly

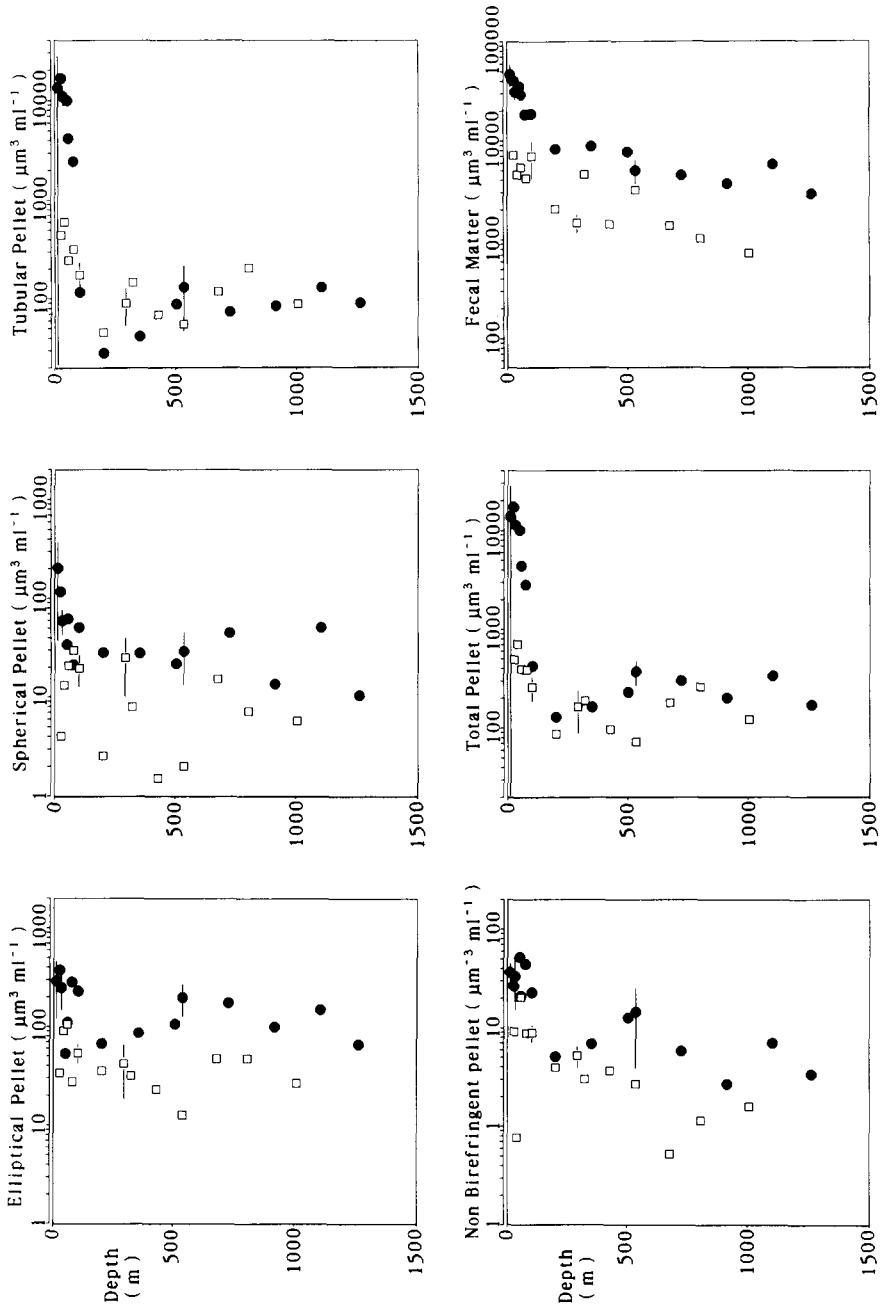

FIG.13. Particle volume distributions of major classes of fecal material determined in LVFS samples from the July-August (●) and November-December (□) cruises. All data are plotted on log scales covering a 2000-fold range. Horizontal bars indicate the standard deviation of independently collected samples from the same depth.

decreasing profile. Volume distributions in November-December ranged from 7000μm^3 ml^{-1} in the shallowest sample at 25m, to less than 1000μm^3 ml^{-1} by 1000m. The six-fold decrease in mean fecal matter concentration in the euphotic zone between July-August and November-December matched the general decrease in macrozooplankton abundances observed between these two periods. No single zooplankton group could be identified as the primary source of fecal matter. Larvaceans and pteropods do not appear to be a major source of fecal matter because the declines of their populations of over an order of magnitude between cruises greatly exceeded that of fecal matter concentrations.

Tubular fecal pellets exhibited very high volume concentrations in the July-August surface waters, decreasing 500-fold from a mean of 15,000μm^3 ml^{-1} in the layer <25m to a minimum of 28μm^3 ml^{-1} at 200m. Below 200m, concentrations increased again 4-fold to a maximum at 500m and from there on down remain unchanged. Note that the 500m maximum corresponded to the deepest limit of migration by zooplankton and midwater fish, and therefore its presence may be related to the activities of these migrators.

The November-December tubular pellet profile showed a maximum of 600μm^3 ml^{-1} in the euphotic zone at 40m (a 25-fold decrease from July-August values) and decreased 6-fold to 100μm^3 ml^{-1} values at >100m which were then comparable to those observed during the July-August period. Once again, the lowest volume concentration of this material occurred at 200m, repeating the pattern found in the July-August data. For comparison, the highest tubular pellet volume concentration observed by BISHOP *et al.* (1980) was 200μm^3 ml^{-1} at 60m with a strong decrease to between 2 and 5μm^3 ml^{-1} at 1000m. Thus this particle class may differ in concentration by many orders of magnitude in the upper 1000m of the Panama Basin.

There are several groups of zooplankton which, based on abundance and vertical distribution, may have produced the long tubular fecal pellets. Copepods, although very abundant, produce elliptical or spherical pellets and so are ruled out, as are larvaceans (ALLDREDGE, 1984). During the July-August cruise euphausiids, pteropods, chaetognaths, siphonophores, and crustacean larvae exhibited highest abundances in the upper 25m at night and therefore may have produced the pellets (Fig.6). Euphausiids, although clearly a source of long tubular pellets (FOWLER and SMALL, 1972) were not abundant enough to produce the quantity of these particles found in the surface waters in July-August. A similar argument may be used to eliminate chaetognaths. The pteropods and crustacean larvae do not appear to be numerous enough to explain the abundances and number fluxes (Table 5) of this particle class. Siphonophores and other gelatinous organisms (although potentially undersampled by the nets) are not known to produce these kinds of particles.

The 12kHz echo sounder observations (Section 3.4, Fig.8) during the shallow LVFS casts provide additional clues to the origin of the long tubular fecal pellets. Intense but patchy scattering (most likely due to schools of fish) was observed in the 0-20m interval during the July-August cruise. As noted above (Section 3.5), there was a positive association between the presence of 12kHz scatterers and the enhanced abundances of long tubular fecal pellets in the two LVFS samples from 12m taken on successive nights. We suspect that the

bulk of the pellets were produced either by the 12kHz scatterers or by the scatterers' prey. The 25-fold decrease in euphotic zone loadings of tubular pellets between the July-August and November-December cruises also was consistent with the 12kHz data which showed little evidence for the shallow patchy scatterers in November-December. Euphausiids may have been the dominant producers of these particles at this time. Thus we conclude that most of the long tubular pellets found in abundance in near surface waters during the July-August cruise were produced by organisms associated with 12kHz scattering and which were probably not sampled by our nets.

Birefringent elliptical fecal pellets produced by copepods (SMALL, FOWLER and UNLU, 1979) had least variation in concentration in the water column during both the July-August and November-December cruises. Although there were only two shallow LVFS casts in July-August, there appeared to be a bimodal distribution in this fecal pellet class in the upper 100m (Table 4). BISHOP *et al.* (1980) reported a similar bimodal distribution to the southwest. In this case, the pellet minimum at approximately 50m corresponded to a subsurface maximum in copepod abundance. This zone was also occupied by maximum nighttime populations of ostracods, euphasiids, fish larvae, amphipods, mid-water fish and crustacean larvae (MOC-1-126, Fig.6) suggesting that detritovores in these groups may have been consuming proportionately more fecal pellets at this depth. Deeper in the water column, elliptical pellet volumes decreased to a minimum of $70\mu m^3\ ml^{-1}$ at 200m, increased to approximately $200\mu m^3\ ml^{-1}$ by 1300m. Once again, the maximum at 500m corresponded to the deepest limit of migratory zooplankton. November-December elliptical pellet volumes ranged from the $100\mu m^3\ ml^{-1}$ maximum at 40m and 55m in the euphotic zone to $30\mu m^3\ ml^{-1}$ at 1000m. The three-fold decrease in elliptical pellet abundances in the shallow euphotic zone between July-August and November-December cruises paralleled the abundance differences found for copepods in the upper 200m over the same period (Table 9).

Spherical birefringent pellets during the July-August cruise had highest concentrations of $320\mu m^3\ ml^{-1}$ at 12m and decreased through the euphotic zone to levels between 20 and 50 $\mu m^3\ ml^{-1}$. These pellets are larger than the spherical minipellets described by GOWING and SILVER (1985) and may have been produced by small cyclopoid copepods. Data from deeper down showed little trend below 200m and concentrations ranged between 10 and $30\mu m^3\ ml^{-1}$. During November-December, a maximum of $30\mu m^3\ ml^{-1}$ was found just below the euphotic zone at 77m which was only a tenth of the maximum concentrations in July-August. From deeper down, the concentration data varied between 2 and $41\mu m^3\ ml^{-1}$ with no discernible trend.

In July-August non-birefringent pellets in all categories had volume concentrations averaging $40\mu m^3\ ml^{-1}$ in surface waters, which declined to a minimum of $5\mu m^3\ ml^{-1}$ at 200m, and showed a secondary maximum of $10\text{-}15\mu m^3\ ml^{-1}$ at 500m, below which there was a decrease to $3\mu m^3\ ml^{-1}$ by 1300m. In November-December volume concentrations decreased from $10\mu m^3\ ml^{-1}$ in surface waters to approximately $1\mu m^3\ ml^{-1}$ by 1000m, in an almost identical profile to that observed by BISHOP *et al.*(1980).

3.8 *Fecal matter and fecal pellet fluxes*

The sinking of fecal pellets and fecal matter is a major transport mechanism for chemical elements in the water column. Vertical fluxes (Fig.14) were calculated using the settling models of KOMAR *et al.*(1981) and BISHOP *et al.* (1980) in conjunction with the measured size distributions of these particle classes (Section 2.2). As in the particle volume profiles (Fig.13), these estimated fluxes of fecal matter and fecal pellets throughout the upper 1300m were generally higher in July-August than in November-December.

Foraminifera are also important contributors to the vertical transport of elements. However, BÉ *et al.*(1985) have shown that foraminiferan fluxes varied by over two orders of magnitude during the July-August cruise. Because of this variability, we will only briefly refer to variability of foraminiferan fluxes at 530m later.

We assume that fluxes of fecal material in the water column may be combined to form a single profile. This assumption is reasonable given the fact that fecal material production is related to feeding activity which must go on daily. A series of samples was collected over 24 hours at 530m to test the validity of this assumption. Combining samples in this way to describe foraminiferan fluxes in the water column would not be reasonable since the production of empty foraminiferan shells is due to time-variable reproductive processes.

ALLDREDGE (personal communication) has suggested that heavy fecal material may accumulate in the mixed layer due to turbulence and shear at the base of the mixed layer. Such processes may cause these particles to be reentrained into the mixed layer and so prevent them from settling into the thermocline. During the July-August cruise, there was evidence for shear at the base of the mixed layer and therefore the July-August distributions of fecal material may be affected by the physical processes. We do not believe that reentrainment processes dominated the distributions of fecal material in our samples because no class of fecal material was unusually concentrated in the mixed layer relative to the upper thermocline as would be consistent with her suggestion. Therefore, we conclude that biological processes and sinking dominated in controlling the distribution of these particles in the water column.

Fecal matter was the dominant contributor to the vertical flux of the seven types of fecal material (Fig.14). The two fecal matter profiles were almost identical in shape, but November-December fluxes were five times lower than in July-August. This decreased flux followed both the trends established for zooplankton group abundances and for new production (BISHOP and MARRA, 1984; Table 9).

However, the July-August tubular pellet flux profile was substantially different in shape from the fecal matter flux profiles just described. Tubular pellet flux averaged 1500mg $m^{-2}d^{-1}$ above 50m but fell sharply to 10mg $m^{-2}d^{-1}$ by 100m. The settling velocity of this material is calculated to be approximately 30m hr^{-1} (Equation 1) so the residence time of this material in the upper 100m can only be several hours. The almost total absence

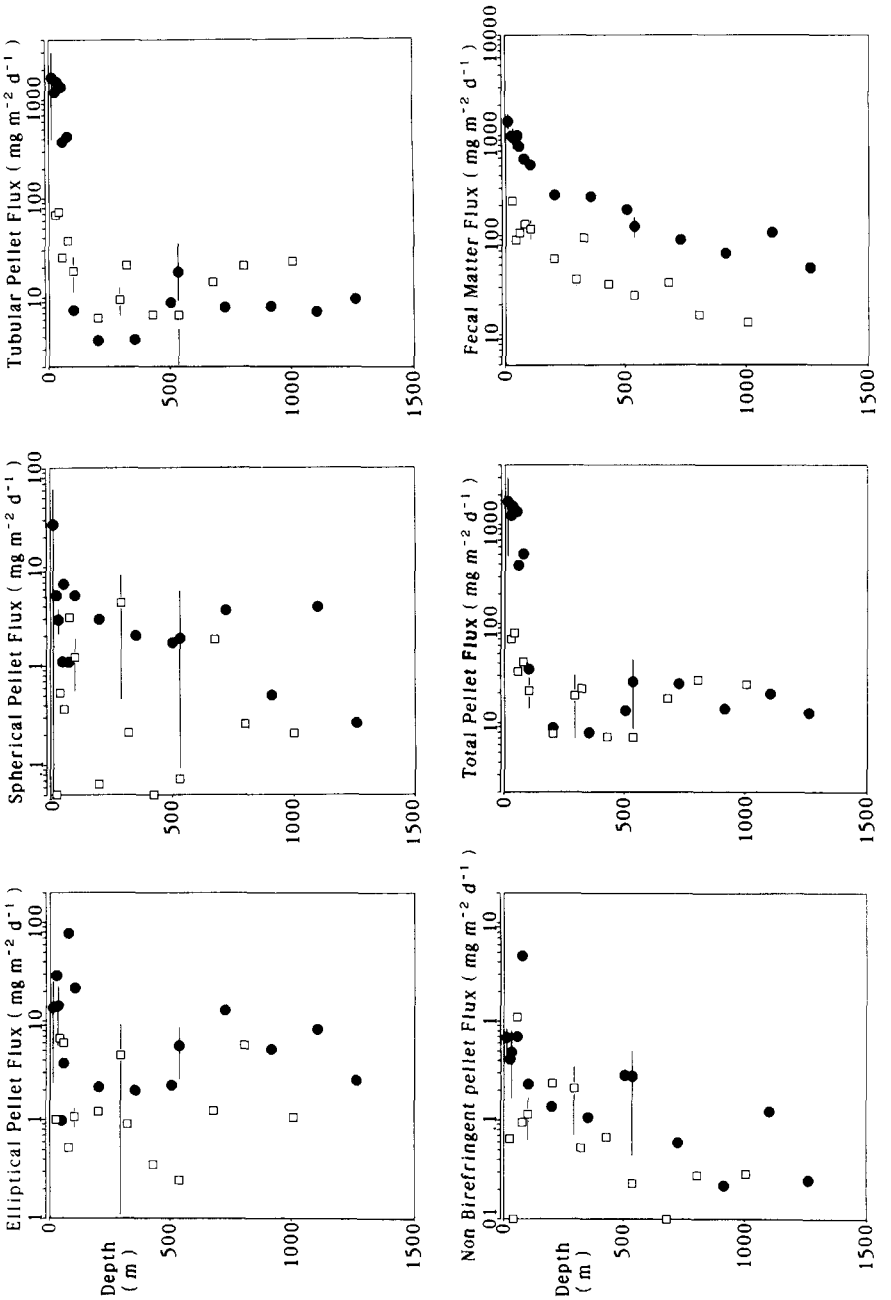

FIG.14. Calculated mass fluxes for major classes of fecal material. Vertical particle flux during both cruises was dominated by fecal matter, tubular fecal pellets, and elliptical fecal pellets. Most classes of fecal material showed a decreased flux in November-December relative to July-August. The declines were probably linked to the declines in both zooplankton group abundances and new production.

of tubular pellets below 100m provides direct evidence for active coprophagy in the top 100m, especially as there was no increase in fragments of this material with depth which rules out particle breakup being responsible for its disappearance.

July-August tubular pellet fluxes continued to decrease to a minimum between 200m and 350m (also the oxygen minimum zone) but increased five-fold to a maximum at 530m, further evidence for the link between this type of fecal material and diel migrators (Section 3.7). Fluxes decreased two fold below 700m. In November-December the tubular pellet fluxes decreased by a factor of two across the euphotic zone from 70mg $m^{-2}d^{-1}$ above 40m down to 40mg $m^{-2}d^{-1}$ at 77m. Fluxes in deeper water averaged 14mg $m^{-2}d^{-1}$ (range 6-23mg $m^{-2}d^{-1}$).

Fluxes of birefringent elliptical fecal pellets in July-August showed a bimodal distribution in the upper 100m, decreased to a minimum between 200m and 350m, increased to a maximum by 700m and thereafter decreased slowly in deeper samples. In November-December their fluxes were generally lower throughout the water column.

Spherical pellet fluxes were only a few percent of total mass flux. There was little difference between cruises. Non-birefringent elliptical and spherical pellet fluxes contributed insignificantly to total flux during both the July-August and November-December cruises.

3.8.1 *Temporal variability of particle flux at 530m*. Temporal variability of fluxes of fecal matter and fecal pellet classes was determined at 530m during the July-August cruise over a 24 hour period (Fig.15). This depth corresponded to the deepest limit of euphausiid migration as well as to the zone occupied by migratory midwater fish during the day. The sample from 500m, collected 2 days earlier, was also included to provide some check for temporal consistency. Fecal matter was the most important contributor to flux and showed lowest values near midnight and a factor of two increase by midday. It is not clear that the diel cycle in this data set is significant because of the small number of observations. On the other hand, tubular fecal pellets exhibited a clearly defined diel variation of flux ranging over an order of magnitude with highest values near midnight and lowest values in the early morning. Elliptical fecal pellets showed no discernible trend over the sampling period nor did the fluxes of foraminiferan shells. The single sample from 500m, collected two days earlier showed good agreement with the temporal trends of fecal matter and tubular pellet flux established by the six 530m samples. This suggested that the variation observed was temporal and was not due to the collection of samples at slightly different locations (Fig.1).

ANGEL (1984) suggested that migratory animals might feed in the upper 70m at night, and defecate after they have descended to deeper depths, thus short circuiting particle sedimentation over their migration interval. The long tubular pellet class exhibited diel variation and if this variation at 530m was caused by such a process, then the perturbation in flux due to migratory inputs was approximately 20% of the total fecal material transport through that depth.

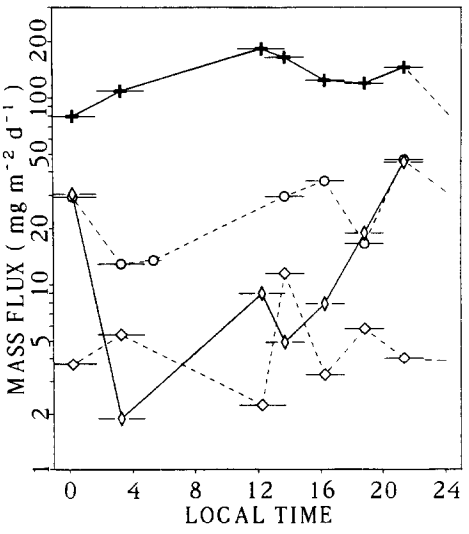

FIG.15. Temporal variability of flux of fecal matter (⊕), tubular fecal pellets (◊), elliptical fecal pellets (◇), and Foraminifera (0) at 530m during the July-August cruise. Horizontal bars denote the time period of sampling. Fecal matter exhibited a midday peak in calculated flux, whereas tubular fecal pellets showed highest fluxes at night. Little diurnal variation was found for elliptical fecal pellets or for Foraminifera at this depth. Flux data from sample 4, collected 2 days earlier from 500m, were included in the plot to test for temporal consistency in the data and showed reasonable agreement with trends for fecal matter and tubular fecal pellets established by other samples.

The phasing of the diel cycle of tubular fecal pellet flux suggests that the bulk of this material was produced at depths shallower than 530m.

3.9 *Mass and chemical fluxes*

Mass fluxes carried by fecal material were calculated by summing the mass fluxes of fecal pellets and fecal matter. This total has been used to compute chemical fluxes by multiplying the mass flux by molar contributions of organic carbon, phosphorus, biogenic silica, and calcium to >53μm dry weight (Fig.16). The contributions of organisms to >53μm Si and Ca have been subtracted prior to the estimation of the molar contributions of these elements to >53μm dry weight (BISHOP *et al.* 1977).

Calculated fecal material mass fluxes in July-August decreased from 3000mg $m^{-2}d^{-1}$ at 12m to 200mg $m^{-2}d^{-1}$ by 200m, showed little change to 500m and then decreased slowly to below 100mg $m^{-2}d^{-1}$ at 800m. In November-December the mass fluxes were only 300mg $m^{-2}d^{-1}$ near the surface, dropped sharply to below 100mg $m^{-2}d^{-1}$ at 150m, and then more slowly to 30mg $m^{-2}d^{-1}$ by 1000m. Fecal matter was the dominant contributor to particle flux compared to fecal pellets everywhere in the water column except in near surface waters during the July-August cruise and in waters deeper than 800m during November-December where tubular fecal pellets were important contributors to flux.

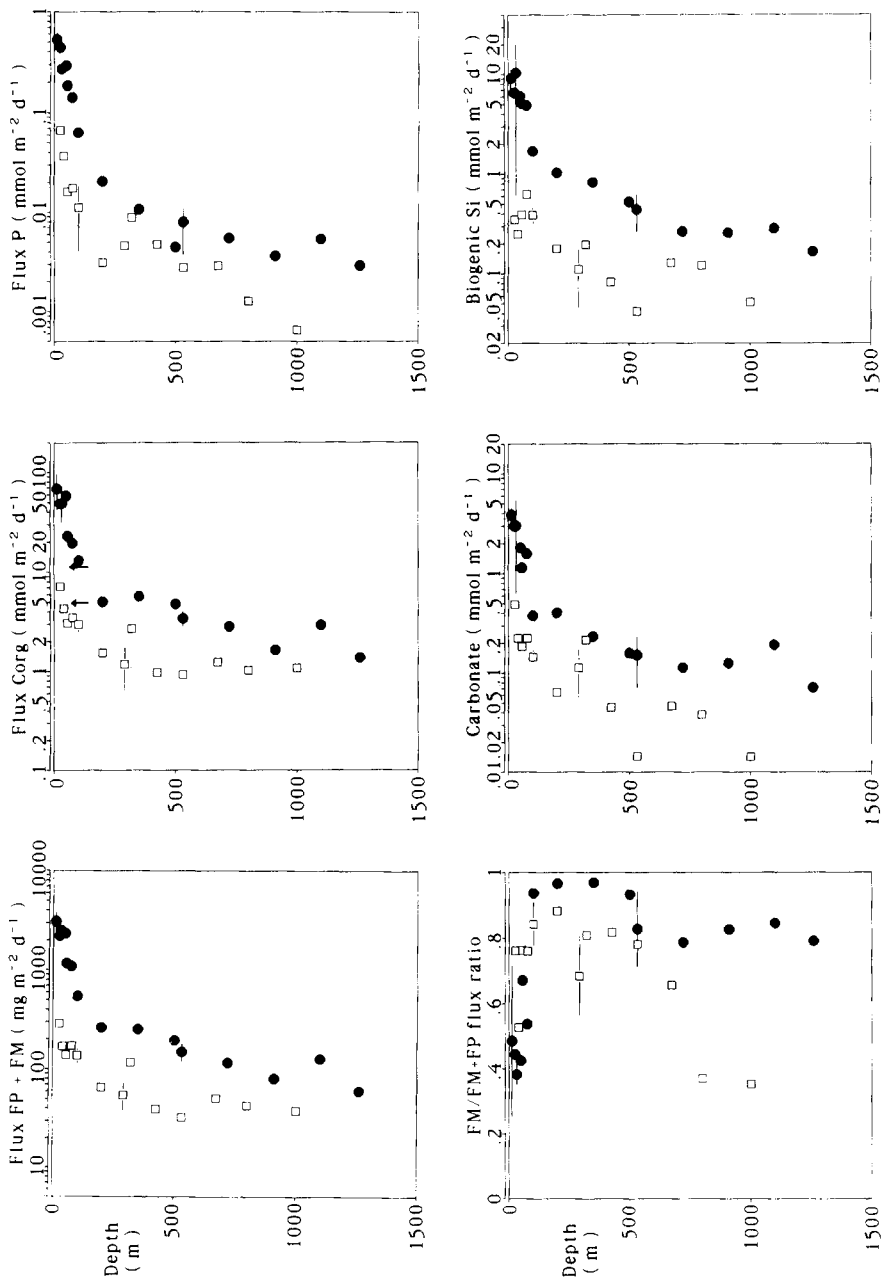

FIG.16. Vertical distributions of fecal material flux, the ratio of fecal matter flux total fecal material flux, and of C_{org}, P, carbonate, and biogenic silicon fluxes during the July-August (●, and November-December (□) cruises. The vertical arrows in the C_{org} flux diagram denote estimates of carbon flux through 70m based on new production (Table 9, Bishop and Marra, 1984) and show good agreement between flux estimated by the two methods at that depth. The sharp decrease in carbonate flux carried by fecal material can only be explained by biologically mediated dissolution of calcium carbonate in the guts of particle consumers.

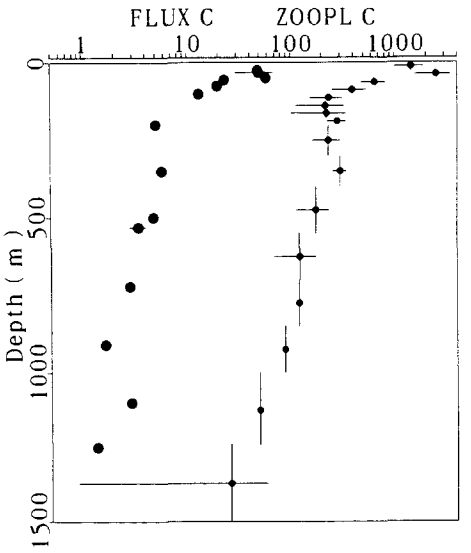

FIG.17. Organic carbon flux (●; mmol $m^{-2}d^{-1}$) Zooplankton biomass (●; nmol C kg^{-1}) distributions in July-August 1979. The horizontal lines where shown denote 1 standard deviation of the data. Vertical lines denote depth interval of MOCNESS samples.

3.9.1 *Organic carbon flux.* Organic carbon flux was obtained by multiplying the mass flux for each sample by the fraction of organic matter in the >53μm fraction (Table 2) and dividing by 2.5 to convert to organic carbon mass units (BISHOP *et al.*1980). Molar fluxes were calculated by dividing the carbon mass flux by 12, the atomic weight of carbon. The organic carbon flux during July-August decreased from 80mmol $m^{-2}d^{-1}$ in near surface waters to approximately 20mmol $m^{-2}d^{-1}$ at 70m, the base of the euphotic zone. The carbon flux continued to decline to 5mmol C_{org} $m^{-2}d^{-1}$ at 200m, but remained nearly constant to 500m before decreasing again to approximately 2mmol C_{org} $m^{-2}d^{-1}$ below 1000m. In the comaprative data for carbon fluxes in November-December there was a decrease from 7mmol C_{org} $m^{-2}d^{-1}$ at 25m, to approximately 3mmol C_{org} $m^{-2}d^{-1}$ at the bottom of the euphotic zone which was still at 70m. Fluxes decreased to approximately 1mmol C_{org} $m^{-2}d^{-1}$ by 300m and dropped to 0.8mmol C_{org} $m^{-2}d^{-1}$ by 1000m.

3.9.1.1 *LVFS carbon flux and zooplankton.* The nighttime zooplankton biomass profile and the carbon flux profile in July-August were highly correlated (Fig.17; ZOOPL = 0.04 ($FLUX^{0.94}$), R^2 = 0.929, n = 14) suggesting a close link between particle flux and the distributions of particle consumers in the water column. The greatest gradient in flux was observed in the upper 100m where all zooplankton groups were most abundant. Within the 200-500m depth interval flux showed little decrease, and here it is speculated that migratory zooplankton feeding at the surface and then defecating within the 200-500m zone contribute to the deep fecal pellet pool, thus compensating any decrease in fecal matter flux resulting from grazing or disintegration. Below 500m, the lower limit of this pellet recharge zone, fluxes decreased in proportion to the zooplankton biomass distribution.

We have derived a zooplankton biomass - particle removal function in two ways. Firstly, carbon flux data from 25m and deeper were regressed against depth using a function of the form: $FLUX = A \cdot DEPTH^B$ which yielded values of 1032 and -0.904 for the A and B coefficients respectively ($R^2 = 0.94$, $n = 14$). The depth derivative of this function yields a smoothed estimate of flux gradient as a function of depth. The results were regressed against night-time zooplankton biomass, since near surface flux estimates were made at night-time using a function of the form: $dFLUX/dz = C \cdot ZOOPL^D$ (Fig.18), to yield values of 6×10^{-7} and 1.92 for C and D respectively ($R^2 = 0.94$, $n = 14$).

The second method involved averaging pairs of carbon flux estimates at successive depths to provide a smoothed flux profile and then calculating flux gradients by finite difference methods. The regression of flux gradient (ignoring 2 negative values) on night-time zooplankton biomass resulted in values of 0.6×10^{-7} and 2.33 for the constants C and D respectively ($R^2 = 0.93$, $n = 10$). Statistically, the results from either method are not significantly different, but since more deep data were used in the first regression, we prefer the results of the first method.

3.9.1.2 *LVFS carbon flux and new production.* Calculated carbon fluxes showed good agreement with estimates of euphotic zone new production for both cruises. New production measurements during July-August (Table 9) indicated that an average of 11.5mmol C_{org} $m^{-2}d^{-1}$ passed through the base of the euphotic zone at 70m. The night-time doubling of the LVFS organic carbon flux at 70m is consistent with the nocturnal increase zooplankton and nekton populations in the euphotic zone. It would be expected that fluxes out of the upper 70m would be lower during the day-time. BISHOP and MARRA (1984) estimated the average particulate carbon flux through the base of the euphotic zone during the November-December cruise to be 5mmol C_{org} $m^{-2}d^{-1}$, but LVFS fluxes were 40% lower. Euphotic zone sampling by LVFS, however, was conducted during midday when lower than average fluxes of fecal material would be expected.

3.9.1.3 *LVFS carbon fluxes and sediment trap carbon fluxes .* A further comparison of shallow carbon fluxes is possible with the shallow drifting sediment trap data of GARDNER, HINGA and MARRA (1983) who found that an unpoisoned sediment trap deployed at 30m for 24 hrs on July 30-31 collected 2mmol C_{org} $m^{-2}d^{-1}$ whereas a trap deployed at 100m at night on July 31 - August 1 collected 1mmol C_{org} $m^{-2}d^{-1}$. These fluxes were 10-20 times lower than fluxes estimated from LVFS data at a similar depth several days later. If anything, the results of BÉ *et al.* (1985) suggest that the trap organic carbon fluxes should have been higher since the mixed layer showed higher nutrient content in late July than during LVFS sampling in early August. Drifting trap carbon fluxes at 300m averaged 2mmol C_{org} $m^{-2}d^{-1}$, roughly 40% of those estimated by LVFS at similar depths. There were no shallow drifting trap data for comparison of carbon fluxes during the November-December cruise.

The most likely cause of disagreement between LVFS and drifting trap carbon data is feeding activities of the numerous zooplankton and fish present at the depth of sampling. Evidence to support this hypothesis comes from the comparison of differences between LVFS and drifting

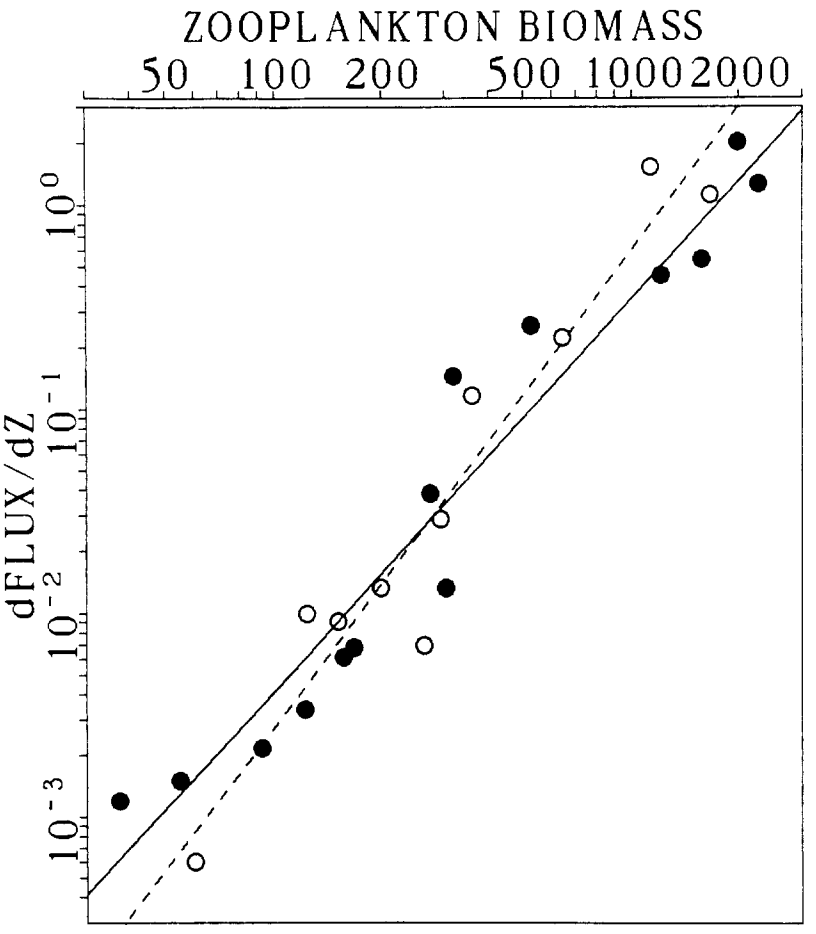

FIG.18. Regressions of carbon flux gradient (mmol $m^{-3}d^{-1}$) versus zooplankton biomass (nmol C kg^{-1}). In order to calculate carbon flux gradient, carbon flux data smoothed by fitting a function of the form FLUX = $A.Z^{B}$ (●; line) or by successive two point averaging (O ; dashed line). Zooplankton biomass data were interpolated to the depth at which the flux gradient was evaluated. Data are fit by a function of the form: log (dFLUX/dZ) = C' + D•log(ZOOPL). At 95% confidence limits C' = 6.221±0.64 and D = 1.92±0.25, n = 14, for the solid line, and C' = 7.2±1.06 and D = 2.33±0.42, n = 10 for the broken line.

trap flux estimates which showed worst agreement in the region of the water column where zooplankton biomass was highest. One drifting trap deployed during the November cruise contained a school of fish on recovery, so biota entering the traps to feed on its contents could result in serious underestimates of the fluxes. On the other hand, there is no evidence to support any upward bias of LVFS results caused by organism congregation near the instrument since swimming organisms like copepods avoid capture by the LVFS (Section 2.3).

Time series sediment trap observations of organic carbon flux at 1268m were made over two week periods for 125 days by LEE, WAKEHAM and FARRINGTON (1983). Degradation of the samples occurred since they were not poisoned (LEE *et al.* 1983). Their carbon flux for the time interval July 28 - August 10 was 1mmol C $m^{-2}d^{-1}$. Such degradation is unlikely to seriously influence LVFS flux estimates because the LVFS samples were only several hours old when preserved. So the increase, by a factor of two, in the LVFS flux estimates is not unexpected.

The last reliable time series trap sample at 1268m corresponded to the period October 20 - November 2 when fluxes of 0.4mmol C_{org} $m^{-2}d^{-1}$ were recorded. Based on the temporal trends of primary production and particulate carbon flux from the euphotic zone (BISHOP and MARRA, 1984) we would expect lower carbon fluxes to have been recorded by traps at 1268m had they been operating during the November-December sampling period. Again LVFS fluxes indicated a factor of two higher carbon flux.

In spite of the large difference in time over which trap and LVFS samples were collected (weeks versus 4 hours) and the problem of trap sample degradation, the agreement of the two methods was remarkably good in waters below the euphotic zone.

3.9.2 *Phosphorus.* Phosphorus showed much greater flux gradients in the water column during both cruises compared to the other measured biogenic elements. During the July-August period, the P flux decreased from 0.5mmol $m^{-2}d^{-1}$ at 12m to an order of magnitude less by 100m, thereafter it decreased at a slower rate to less than 0.003mmol P $m^{-2}d^{-1}$ by 1300m. In November-December phosphorus fluxes were lower throughout the water column, declining from 0.07mmol P $m^{-2}d^{-1}$ at 25m to <0.0005mmol P $m^{-2}d^{-1}$ at 1000m. The rapid loss of phosphorus from the large fraction is not unexpected knowing the higher lability of this element relative to carbon (BISHOP *et al.*1980; COLLIER and EDMOND, 1984).

3.9.3 *Calcium.* The dominant source of calcium in fecal material and in the 1-53µm fraction in the water column is coccoliths composed of calcium carbonate (BISHOP *et al.* 1977, 1978). Coccoliths have on occasion formed the dominant fraction of carbonate collected by deep sediment traps in this basin (HONJO, 1982). In July-August calcium carbonate fluxes carried by fecal material declined with depth very much like organic carbon fluxes, and the unvarying C_{org}/Ca content of the >53µm material indicated no preferential fractionation of these two elements. Calcium fluxes decreased by an order of magnitude from close to 4mmol Ca $m^{-2}d^{-1}$ at 12m to 0.4mmol Ca $m^{-2}d^{-1}$ at 100m, and then more slowly to less than 0.1mmol $m^{-2}d^{-1}$ below 1000m. As for phosphorus, the calcium fluxes in November-December

were lower than July-August values throughout the whole water column, and decreased from 0.5mmol Ca $m^{-2}d^{-1}$ at 25m to less than 0.02mmol Ca $m^{-2}d^{-1}$ by 1000m.

3.9.3.1 *LVFS calcium fluxes and sediment traps* . Total Ca fluxes in July-August were determined by shallow trap deployments (BÉ *et al.* 1985) and were 0.7mmol Ca $m^{-2}d^{-1}$ at 30m and 70m and 1.2mmol $m^{-2}d^{-1}$ at 300m. Foraminifera >149μm accounted for approximately 25% of the carbonate flux in the trap samples. Smaller Foraminifera and migrating pteropods may have contributed a further 25% to the carbonate in the traps. Thus most of the trap carbonate flux was not due to fecal material, and hence the LVFS calcium fluxes being lower at 100m and 300m than determined by the traps can be explained. But why the 30m trap samples had a factor of 4 lower fluxes than predicted by LVFS sampling, needs an alternate explanation such as feeding activities of zooplankton in the trap or by the poor performance of the trap in the conditions of strong currents and turbulence present at the depth of deployment (strong currents and turbulence were experienced on a number of occasions in July-August during MOCNESS tows, and were the cause of strong temperature gradients and temperature inversions; cf Fig.6).

Foraminiferan fluxes, calculated for the six LVFS samples from 530m, averaged 0.30mmol $m^{-2}d^{-1}$ (range 0.16-0.46mmol Ca $m^{-2}d^{-1}$; Fig.15). If we assume these fluxes to be representative of the water column below 500m, and if we sum the foraminiferan flux with the fecal material flux for the samples below 1000m, then reasonable agreement is found with the 0.32mmol Ca $m^{-2}d^{-1}$ flux recorded by the time series trap at 1268m during the July-August period.

Besides dissolution, an alternate explanation for the decrease in fecal material calcium flux would be that coccoliths were lost from the large particles into the small fraction due to fragmentation processes. However, this would have resulted in an accumulation of Ca in the 1-53μm fraction in deeper wamples which was not observed. Therefore it must be concluded that carbonate dissolution occurs in the shallow waters of the Panama Basin. In contrast, HONJO (1982) reported a minimal effect of dissolution on samples collected deeper than 890m.

BISHOP *et al.*(1980) first described carbonate dissolution in the shallow waters of the Panama Basin and concluded that the process had to be biologically mediated because the upper 1500m were at, or exceeded, calcite saturation, and herein further evidence is provided in support of this conclusion. Firstly, the calculated Ca flux shows a strong decrease through the upper 1300m. Secondly, small fecal pellets devoid of coccoliths were found in the water column during both STIE/C-FATE cruises. Thirdly, calcium concentrations in the 1-53μm fraction in deep samples was the lowest ever observed in spite of high surface concentrations. Additional evidence for shallow carbonate dissolution has been found in Atlantic thermocline waters (TAKAHASHI, BROECKER and LANGER, 1985).

3.9.4 *Biogenic silica*. Calculated silica fluxes during the July-August period decreased from 10mmol Si $m^{-2}d^{-1}$ above 25m to less than 0.2mmol Si $m^{-2}d^{-1}$ below 1000m. Once again in November-December Si fluxes were generally an order of magnitude lower and decreased

from a maximum of 0.7mmol Si $m^{-2}d^{-1}$ within the euphotic zone at 50m to <0.02mmol Si $m^{-2}d^{-1}$ below 800m.

The dissolution of silica at shallow depths within the water column is a well known phenomenon (NELSON and GOERING, 1977) and so it is not surprising to find it occurring in the shallow waters of the Panama Basin. No shallow silica flux data are available from the traps and so the time series from the 1268m trap provides the only comparable data set. Biogenic silica was not determined in these samples, so the analyses of total silicate and aluminium have to be used for this estimate. During July-August the 1268m trap flux of silicate and aluminium was 38.6 and 3.5mg $m^{-2}d^{-1}$, respectively (ANDERSON and BACON, 1981). Unfortunately, the Al/Si ratio of the silicate minerals in the Panama Basin is too poorly known for an accurate estimation of biogenic silica. However clay particles are aluminium rich at low latitudes (BISHOP and BISCAYE, 1982) and so the alumino-silicate component is roughly estimated here by multiplying aluminium flux by 8 rather than the more commonly used factor of 10 (LAMBERT, BISHOP, BISCAYE and CHESSELET, 1984). Hence an estimated 70% of the collected "silicates" was alumino-silicate and therefore the remaining 10mg $m^{-2}d^{-1}$ was in biogenic opal. By dividing the resultant weight by 60 to convert to mole units we calculate a biogenic Si flux of 0.17mmol Si $m^{-2}d^{-1}$, which is in remarkably good agreement with calculated LVFS fluxes. The dominance of alumino-silicates in the 1268m trap was consistent with the resuspension of sediments from nearby topography as indicated in the nephelometer data (Fig.4).

4. SUMMARY AND CONCLUSIONS

This study has characterised the particle cycle in the biologically active upper kilometre of the eastern equatorial Pacific ocean. Our interdisciplinary approach is unique in that components of the particle cycle governing both the production and the destruction of particulate matter have been simultaneously determined and related to particle profiles in the upper 1000m.

It has already been demonstrated that rates of primary production and particulate carbon flux through the base of the euphotic zone (calculated based on new production estimates) at the STIE/C-FATE area are closely controlled by the nutrient and light fields of the euphotic zone; these in turn, may be inferred from a knowledge of surface marine conditions and mixed layer depth (BISHOP and MARRA, 1984). Highest primary production and particulate carbon flux through the base of the euphotic zone occurred at times when the nutrient-depleted mixed layer was shallowest (18m in July-August versus 35m in November-December) or after nutrients had been entrained from below into the mixed layer (during several one week periods between the two cruises; BISHOP and MARRA, 1984). The findings of this paper are the following:

1. Samples of particulate matter collected by the Large Volume *in-situ* Filtration System (LVFS) were not positively biased by the presence of organisms near the sampling

equipment during deployment. In fact, we estimate that >60% of the copepods present in the upper 100m avoided capture by the LVFS during sampling.

2. Particles beginning their downward journey from the euphotic zone to the sediments pass through a series of zones of biological activity in the water column prior to reaching the sediments (KARL and KNAUER, 1984). Our zooplankton biomass and taxonomic group data from the Panama Basin show that the water column was divided into several layers: the layer shallower than 100m contained most zooplankton biomass and was coincident with the zone of primary production; the layer between 100-600m was dominated by migrating zooplankton and fish which swam into the upper layer at night to feed; and the layer below 600m contained organisms which did not migrate. This zonation has a significant impact on the particle distributions in the upper 1000m.

3. Investigations of carbon partitioning between zooplankton and particulate pools during the July-August cruise showed that the carbon biomass of >333μm zooplankton (representing particle consumers) exceeded carbon concentrations in the >53μm particulate fraction (representing the sinking fraction of particulate matter) everywhere shallower than 1000m. The fact that the ratio of zooplankton carbon to >53μm particulate carbon was as great as 10, underscores the rapidity with which the >53μm fraction may be processed by the zooplankton consumers present in the upper 1000m.

4. Cruise to cruise differences in zooplankton abundance and vertical distributions permitted an examination of which organisms were important in controlling the particle distributions in the water column. No single zooplankton group could be identified as the source of the large irregular macroscopic aggregates termed fecal matter, although inter- and intra-cruise variations in this class of particle were related to changes in gross zooplankton abundance in the water column. We identified some zooplankton groups which were likely sources of some classes of fecal pellets. Elliptical fecal pellet abundances matched the inter-cruise variations in copepod abundances, and the abundances of the long (1-4mm) tubular fecal pellets in near surface waters in July-August coincided with the presence of dense patches of organisms (most likely schools of fish) which scattered 12kHz sound. Thus in this season, most long tubular fecal pellets found in near surface waters were produced by highly mobile species which were not sampled by nets. Later in November-December euphausiids were probably major contributors to the long tubular fecal pellet class.

5. In July-August the data on long tubular fecal pellet abundances and flux provided direct evidence for feeding activity by coprophagous organisms. Given the fast settling rates of these particles (30m hr^{-1}), the five hundred fold decrease between surface waters and 200m cannot be explained without consumption by coprophagous zooplankton and nekton. The secondary maximum and a diel cycle of abundance and flux of these particles near 500m also suggested the abundances of this pellet class below 200m was controlled by migratory organisms.

6. Microzooplankton increased between July-August and November-December, contrasting with decreases observed for macrozooplankton, fish and 12kHz scatterers. We conclude that

predation by macrozooplankton and fish may have suppressed microzooplankton populations during July-August.

7. We examined bulk properties of the >53μm and 1-53μm particle size classes to understand how particle distributions reflected biological processes in the upper 1000m. Mass and chemical distributions of >53μm particulate matter showed lower concentrations throughout the water column during November-December compared with July-August, following decreases in primary production, new production, and macrozooplankton group abundances.

All elements in the >53μm particle size fraction sampled on both cruises showed greater vertical concentration gradients in the upper 100m compared with the 1-53μm fraction which is explainable if there is enhanced consumption of large particles by the macrozooplankton which had its greatest biomass in this depth interval.

For most 1-53μm elements the vertical concentration gradients in the upper 200m were reduced during November-December compared to during July-August. The cause of this reduction in the concentration gradients was probably a decrease in macrozooplankton abundance and hence grazing, leading to less efficient particle export via fecal material sinking from the upper 200m during the later period.

8. Organic carbon to phosphorus ratios in both 1-53μm and >53μm fractions were similar in value in the euphotic zone (126:1 in July-August; 138:1 in November-December). But the ratios diverged strongly in deeper waters, for the >53μm fraction the ratio rose as high as 1000:1 in waters between 100 and 1300m, whereas for the 1-53μm fraction it remained at an average of 160:1 below 100m during both cruises. These differences are taken to reflect greater lability of phosphorus relative to organic carbon in the >53μm fraction and the possible presence of a refractory phosphorus phase in the 1-53μm fraction, and differences in the processes affecting the two particle size fractions below the euphotic zone.

9. We examined particulate carbon fluxes through the base of the euphotic zone calculated from LVFS data and how they compared to carbon fluxes through the same depth based on new production (BISHOP and MARRA, 1984). LVFS carbon fluxes, based on night-time samples, during July-August were twice the particulate carbon flux based on new production estimates whereas November-December LVFS carbon fluxes, based on midday measurements, were 40% lower than carbon flux estimates based on new production. Diurnal variability of particle flux was assumed to be the major cause of the differences between the two sets of data. But we conclude that on the time scale of days new production is in balance with particulate carbon flux.

10. Calculated organic carbon fluxes based on both LVFS data and new production estimates were an order of magnitude higher than fluxes determined by surface-tethered, unpoisoned sediment traps deployed in the upper 100m during the July-August cruise. We attribute the difference to a combination of the feeding activities of zooplankton in the traps during their deployment and to poor performance of the traps in the conditions of high

current shear and turbulence prevailing in the upper 100m.

11. Organic carbon fluxes through 1260m based on LVFS data were twice those determined by unpoisoned time-series traps deployed at 1268m for a two week period during July-August. It is thought that the traps underestimated the fluxes because the organic material in the traps had undergone degradation during the four month period between sample isolation and recovery, but differences in the time scales of sampling (days versus weeks) could have accounted for some of the disparity between the two methods in deeper waters.

12. The profiles of >333μm zooplankton biomass and of particle flux in the upper 1300m were strongly similar during July-August. Because of this similarity, we were able to calculate a relationship between vertical carbon flux gradient and zooplankton biomass:

$$dFLUX/dz = 6x10^{-7} \cdot ZOOPL^{1.92}_{mmol\ C\ m^{-3}d^{-1}}$$

where zooplankton biomass in in nmol C kg^{-1}.

13. Calculated fluxes of dry weight, organic carbon, phosphorus, calcium carbonate, and biogenic silica carried in fecal material all indicated strong regeneration in the upper 100m. This pattern matched the strong gradients of dissolved phosphate and silica down through the euphotic zone and was consistent with the vertical distribution of zooplankton biomass in the same depth interval. Flux data showed that substantial dissolution of particulate calcium carbonate (mostly produced by coccolithophores) occurs in the upper water column of the Panama Basin. Foraminifera were implicated as major contributors to deep carbonate flux since their shells have substantially higher sinking rates than fecal material.

To conclude, we have demonstrated that particulate matter distributions, chemistry and fluxes in the upper 1000m are related to rates of primary production and new production in the euphotic zone and to the instantaneous distributions and activities of zooplankton and fish over the upper 1000m. These results support the hypothesis that particle distributions and fluxes in the upper 1000m are linked to the physical and biological environments of the euphotic zone and deeper layer on the time scale of days.

ACKNOWLEDGEMENTS

We would like to thank the crews and scientific parties of the Knorr and Gilliss for their assistance in carrying out this experiment. Special thanks are due to Derek Spencer, chief scientist on RV Knorr, who provided the oxygen and salinity data described in this paper. The able help of Craig Hunter (Moss Landing Laboratories) and Jean Ruff (Oregon State University) during LVFS stations is gratefully acknowledged. Al Morton, Joe Poirier and Jerry Cotter, all of Woods Hole Oceanographic Institution, provided valuable help with LVFS and MOCNESS systems. Dorothy Kintas, Robert Sherrell and Norman Van Broekhoven performed

microscopic and chemical analysis of LVFS samples at LDGO. Dr Bishop was supported by ONR grant N000014-80-C-0098 and by NSF grants OCE 80-17468 and OCE 85-13420 and by funds from Lamong Doherty Geological Observatory and Dr Wiebe was supported by NSF grants OCE 80-17248 and OCE 85-08350. Drs A. Alldredge, P. Biscaye, I. Fung and J. Marra are thanked for their comments on the manuscript. We also thank Dr M. Angel and one anonymous reviewer for their contributions to the final form of this paper. This is contribution no.4083 from Lamont Doherty Geological Observatory; contribution no.6296 from Woods Hole Oceanographic Institution.

REFERENCES

ALLDREDGE, A.L. (1984) The quantitative significance of gelatinous zooplankton as pelagic consumers. In: *Flows of Energy and Material in Marine Ecosystems* , editor M.J.R. FASHAM, Plenum Press, New York, 407-433.

ALLDREDGE, A.L., AND M.J. YOUNGBLUTH (1985) The significance of macroscopic aggregates (marine snow) as sites for heterotrophic bacterial production in the mesopelagic zone of the subtropical Atlantic. *Deep-Sea Research*, **32**, 1445-1456.

ANDERSON, R.F. and M.P. BACON (1981) Sediment trap intercomparison experiment, Woods Hole Oceanographic Institution Technical Memorandum, WHOI-1-81, 120 pp.

ANGEL, M.V. (1984) Detrital organic fluxes through pelagic ecosystems. In: *Flows of Energy and Material in Marine Ecosystems*, editor M.J.R. FASHAM, Plenum Press, New York, 475-516.

BÉ, A.W.H., J.K.B. BISHOP, M.S. SVERDLOVE and W.D. GARDNER (1985) Standing stock, vertical distribution and flux of planktonic *foraminifera* in the Panama Basin. *Marine Micropaleontology*, **9**, 307-333.

BETZER, P.R., W.J. SHOWERS, E.A. LAWS, C.D. WINN, G.R. DITULLIO and P.M. KROOPNICK (1984) Primary Productivity and particle fluxes on a transect of the equator at 153°W in the Pacific Ocean. *Deep-Sea Research*, **31**, 1-12.

BISCAYE, P.E. and S.L. EITTREIM (1977) Suspended particulate loads and transports in the nepheloid layer of the abyssal Atlantic Ocean. *Marine Geology*, **23**, 155-172.

BISHOP, J.K.B. (1982) The effects of filtration speed on large particle catch during large volume *in situ* filtration. *EOS, Transactions of the American Geophysical Union*, **63**. 46.

BISHOP, J.K.B. and P.E. BISCAYE (1982) Chemical characterisation of individual particles from the nepheloid layer in the Atlantic Ocean, *Earth and Planetary Science Letters*, **58**, 265-275.

BISHOP, J.K.B. and J.M. EDMOND (1976) A new large volume *in situ* filtration system for sampling oceanic particulate matter. *Journal of Marine Research*, **34**, 181-198.

BISHOP, J.K.B. and J. MARRA (1984) Variations in primary production and particulate carbon flux through the base of the euphotic zone at the site of the sediment trap intercomparison experiment (Panama Basin). *Journal of Marine Research*, **42**, 189-206.

BISHOP, J.K.B., R.W. COLLIER, D.R. KETTEN and J.M. EDMOND (1980) The chemistry, biology and vertical flux of particulate matter from the upper 1500m of the Panama Basin. *Deep-Sea Research*, **27**, 615-640.

BISHOP, J.K.B., J.M. EDMOND, D.R. KETTEN, M.P. BACON and W.B. SILKER (1977) The chemistry, biology and vertical flux of particulate matter from the upper 400m of the Equatorial Atlantic Ocean. *Deep-Sea Research*, **24**, 511-548.

BISHOP, J.K.B., D.R. KETTEN and J.M. EDMOND (1978) The chemistry, biology and vertical flux of particulate matter from the upper 400m of the Cape Basin in the southeast Atlantic. *Deep-Sea Research*, **25**, 1121-1161.

BISHOP, J.K.B., D. SCHUPACK, R.M. SHERRELL and M. CONTE (1985) A Multiple Unit Large Volume *in situ* Filtration System (MULVFS) for sampling Oceanic particulate matter in mesoscale environments. In: *Mapping Strategies in Chemical Oceanography* , Editor A. ZIRINO, American Chemical Society, Washington DC, Advances in Chemistry Series, **209**, 155-175.

BLACKBURN, M., R.M. LAUERS, R.W. OWEN and B. ZEITSCHEL (1970) Seasonal and areal changes in standing stocks of phytoplankton, zooplankton and micronekton in the eastern tropical Pacific. *Marine Biology*, **7**, 14-31.

BRULAND, K.W. and M. SILVER (1981) Sinking rates of fecal pellets from gelatinous zooplankton (salps, pteropods, doliolids). *Marine Biology*, **63**, 295-300.

COLLIER, R.W. and J.M. EDMOND (1984) The trace element geochemistry of marine biogenic particulate matter. *Progress in Oceanography*, **13**, 113-199.

DEUSER, W.G. and E.H. ROSS (1980) Seasonal changes in the flux of organic carbon to the deep Sargasso Sea. *Nature*, **283**, 364-365.

DEUSER, W.G. (1986) Seasonal and interannual variations in deep-water particle fluxes in the Sargasso Sea and their relation to surface hydrography. *Deep-Sea Research*, **33** 225-246.

DUGDALE, R.C. and J.J. GOERING (1967) Uptake of new and regenerated forms of nitrogen in primary productivity. *Limnology and Oceanography* **12**, 196-206.

FAIRBANKS, R.C., M. SVERDLOVE, R. FREE, P.H. WIEBE and A.W.H. BÉ (1982) Vertical distributions and isotopic fractionation of living planktonic Foraminifera from the Panama Basin. *Nature*, **298**, 841-844.

FELLOWS, D.A., D.M. KARL and G.A. KNAUER (1981) Large particle fluxes and vertical transport of living carbon in the upper 1500m of the northeast Pacific Ocean. *Deep-Sea Research*, **28A**, 921-936.

FORSBERGH, E.D. (1969) On the climatology, oceanography and fisheries of the Panama Bight. *Inter-American Tropical Tuna Commission Bulletin*, **14**, 386 pp.

FOWLER, S.W. and L.F. SMALL (1972) Sinking rates of euphausiid fecal pellets. *Limnology and Oceanography*, **17**, 293-296.

FOWLER, S.W. and G.A. KNAUER (1986) Role of large particles in the transport of elements and organic compounds through the oceanic water column. *Progress in Oceanography* , **16**, 147-194.

GARDNER, W.D., K.R. HINGA and J. MARRA (1983) Observations on the degradation of biogenic material in the deep ocean with implications on the accuracy of sediment trap fluxes. *Journal of Marine Research*, **41**, 195-214.

GARDNER, W.D., J.K.B. BISHOP and P.E. BISCAYE (1984) Nephelometer and current observations at the STIE site, Panama Basin. *Journal of Marine Research*, **42**, 207-219.

GOWING, M.M. and M.W. SILVER (1985) Minipellets: A new and abundant size class of marine fecal pellets. *Journal of Marine Research*, **43**, 395-418.

HONJO, S. (1982) Seasonality and interaction of biogenic and lithogenic particulate flux at the Panama Basin. *Science* , **218**, 882-883.

HONJO, S. (1984) Study of ocean fluxes in time and space by bottom-tethered sediment trap arrays: a Recommendation. In: *Global Ocean Flux Study* . National Academy Press, Washington DC, 306-324.

HONJO, S., K.W. DOHERTY, Y.C. AGRAWAL and V.L. ASPER (1984) Direct optical assessment of large amorphous aggregates (marine snow) in the deep ocean. *Deep-Sea Research*, 32 67-76.

ITTEKKOT, V., E.T. DEGENS, and S. HONJO (1984) Seasonality in the fluxes of sugars, amino acids, and amino sugars to the deep ocean: Panama Basin. *Deep-Sea Research* , **31**, 1071-1083.

KARL, D.M. and G.A. KNAUER (1984) Vertical distributions, transport, and exchange of carbon in the northeast Pacific Ocean: evidence for multiple zones of biological activity. *Deep-Sea Research*, **31**, 221-243.

KNAUER, G.A., J.H. MARTIN and K.W. BRULAND (1979) Fluxes of particulate carbon, nitrogen, and phosphorus in the upper water column of the northeast Pacific. *Deep-Sea Research*, **26**, 97-108.

KNAUER, G.A., J.H. MARTIN and D.M. KARL (1984) The flux of particulate matter out of the euphotic zone. In: *Global Ocean Flux Study* . National Academy Press, Washington DC, 137-150.

KOMAR, P.D., A.P. MORSE, L.F. SMALL and S.W. FOWLER (1981) An analysis of the sinking rates of natural copepod and euphausiid fecal pellets. *Limnology and Oceanography* , **26**, 172-180.

LAMBERT, C.E., J.K.B. BISHOP, P.E. BISCAYE and R. CHESSELET (1984) Particulate aluminium, iron and manganese chemistry at the deep Atlantic boundary layer. *Earth and Planetary Science Letters*, **70**, 237-248.

LEE, C., S.G. WAKEHAM and J.W. FARRINGTON (1983) Variations in the composition of particulate organic matter in a time-series sediment trap. *Marine Chemistry*, **13**, 181-194

MADIN, L.P. and G.R. HARBISON (1977) The associations of Amphipoda Hyperiidea with gelatinous zooplankton-I. Associations with Salpidae. *Deep-Sea Research*. **24**, 449-463.

MARRA, J., P.H. WIEBE and J.K.B. BISHOP (in press) Primary production and grazing in the plankton of the Panama Bight. *Bulletin of Marine Science*

MARTIN, J.H. and G.A. KNAUER (1983) VERTEX: Manganese transport with $CaCO_3$. *Deep-Sea Research*, **30**, 411-425.

McCAVE, I.N. (1975) Vertical flux of particles in the ocean. *Deep-Sea Research* , **22**, 491-502

NELSON, D.M. and J.J. GOERING (1977) Near-surface silica dissolution in the upwelling region off northwest Africa. *Deep-Sea Research*, **24**, 31-36.

ROBINSON, M.K. (1973) Atlas of monthly mean sea surface and subsurface temperature and depth of the top of the thermocline Gulf of Mexico and the Caribbean Sea. SIO Reference 73-8.

ROBISON, B.H. and T.G. BAILEY (1981) Sinking rates and dissolution of midwater fish fecal matter. *Marine Biology* **65**, 135-142.

SHELDON, R.W., A. PRAKASH and W.H. SUTCLIFFE, JR (1972) The size distribution of particles in the Ocean. *Limnology and Oceanography*, **17**, 327-340.

SILVER, M. and ALLDREDGE, A.L. (1981) Bathypelagic marine snow: deep-sea algal and detrital community. *Journal of Marine Research*, **39**, 501-530.

SMALL, L.F., S.W. FOWLER and M.Y. UNLU (1979) Sinking rates of natural copepod fecal pellets. *Marine Biology* , **51**, 233-241.

SMETACEK, V.S. (1985) Role of sinking diatom life-history cycles: ecological, evolutionary and geological significance. *Marine Biology* , **84**, 239-251.

STEVENSON, M.R. and B.A. TAFT (1971) New evidence of equatorial undercurrent east of the Galapagos Islands. *Journal of Marine Research*, **29**, 103-115.

SVERDRUP, H.U., M.W. JOHNSON and R.H. FLEMING (1942) The Oceans. Their Physics, Chemistry and General Biology. Prentice Hall, NJ, 1078 pp.

TAKAHASHI, T., W.S. BROECKER and S. LANGER (1985) Redfield ratio based on chemical data from isopycnal surfaces. *Journal of Geophysical Research*, **90**, 6907-6924.

TSUCHIYA, M. (1981) The origin of the Pacific equatorial 13°C water. *Journal of Physical Oceanography*, **11**, 794-812.

WELSCHMEYER, N.A. and C.J. LORENZEN (1985) Chlorophyll budgets: zooplankton grazing and phytoplankton growth in a temperate fjord and the central Pacific gyres. *Limnology and Oceanography*, **30**, 1-21.

WIEBE, P.H., S. BOYD and J.L. COX (1975) Relationships between zooplankton displacement volume, wet weight, dry weight, and carbon. *Fishery Bulletin*, **73**, 777-786.

WIEBE, P.H., K.H. BURT, S.H. BOYD and A.W. MORTON (1976) A multiple opening/closing net and environmental sensing system for sampling zooplankton. *Journal of Marine Research*, **34**. 313-326.

WYRTKI, K. (1966) Oceanography of the eastern Pacific Ocean. *Oceanography and Marine Biology Annual Review*, **4**, 33-68.

WYRTKI, K. and G. ELDIN (1982) Equatorial upwelling events in the central Pacific. *Journal of Physical Oceanography*, **12**, 984-988.